RAINFALL-RUNOFF MODELING IN HUMID SHALLOW WATER TABLE ENVIRONMENTS

Tatiana X. Hernandez

Thesis submitted on the Faculty of the
University of South Florida
in partial fulfillment of the requirements for the degree of

Master of Science

In

Civil Engineering

Mahmood H. Nachabe, Ph.D., P.E.
Mark A. Ross, Ph.D., P.E.
Jayantha Obeysekera, Ph.D., P.E.

May 5, 2001
Tampa, Florida

Keywords: Variable Source Areas, rainfall variability, hydrologic modeling

DEDICATION

This work is dedicated to my family, Oscar, Blanca, Kelly, and Mauricio for their love, support and patience. To all of them for encouraging me each step along the way.

Los quiero mucho

ACKNOWLEDGMENTS

I like to thank Professor Rudolf Henning for providing the rainfall data, which is part of a study being conducted at the University of South Florida, Electrical Engineering Department and NASA. I want to acknowledge the South Florida Water Management District for providing funds to support this research. I also want to thank Jeff Vomacka for providing field measurement data. His assistance is gratefully acknowledged. I wish to thank Dr. Mahmood Nachabe, Dr. Jayantha Obeysekera and Dr. Mark Ross, the members of my committee for taking the time and effort to ensure my work was of quality. I would particularly like to thank Dr. Nachabe for his continuous guidance, and encouragement. His support and wise counsel were invaluable. Finally, I want to thank my family and friends for being always there for me. Thank you all.

TABLE OF CONTENTS

LIST OF FIGURES

LIST OF TABLES

RAINFALL-RUNOFF MODELING IN HUMID SHALLOW WATER TABLE ENVIRONMENTS

Tatiana X. Hernandez

(ABSTRACT)

Simulating the processes of rainfall and runoff are at the core of hydrologic modeling. Geomorphologic features, rainfall variability, soil types, and water table depths strongly influence hydrological process in Florida ecosystems. Topographic characteristics of the terrain define the stream paths and landscape. Alteration of these characteristics as a result of urban and/or agricultural developments, for example, can highly influence wetlands and river basin response. There are two predominant landforms in Florida: wetlands, where Variable Saturated Areas form near streams causing saturation excess runoff, and uplands where runoff is mainly generated by infiltration excess. The objective of this work is to analyze the impacts of geomorphologic and hydrologic characteristics on runoff mechanisms in humid environments such as Florida. In general, most research at the hillslope scale use hypothetical values of rainfall, sometimes non-realistic values, and single slope forms to explain the geomorphic and hydrologic process on Variable Saturated Areas. In this thesis, the complexity of hillslope processes on actual Florida topography is assessed by coupling a Digital Elevation Model with a two-dimensional variable saturated-unsaturated flow model called HYDRUS-2D. Actual rainfall records and soil parameters from the Characterization Data for Selected Florida Soils, Soil Survey were used to evaluate hydrologic impacts. A commercial software package, River Tools was used to display and extract topographic information from the Digital Elevation Models.

Results show that when infiltration excess runoff is dominant, infiltration and runoff are very sensitive to time resolution, especially for convective storms. When saturation excess occurs, runoff is not affected by rainfall intensity. However, saturated hydraulic conductivity, depth to the water table, slope and curvature highly influence the extent of Variable Saturated Areas. Results indicate runoff in shallow water table environments is produced mainly by subsurface storm runoff, running below the surface, except in hillslopes with concave curvature and mild slopes. The extent of Variable Saturated Areas on mild slope topographies is larger than for steep slopes. Additionally, concave hillslopes generate more saturation excess runoff than straight and convex hillslopes.

CHAPTER 1. INTRODUCTION

1.1. Background

Simulating the processes of rainfall, infiltration, and runoff is a primary objective of hydrologic modeling. These processes are influenced by the temporal and spatial variability of rainfall, geomorphologic features of the terrain, soil properties, and depth to the water table. Adequate prediction of runoff is essential for hydrologic modeling required for flood forecasting, storm water management plans, reservoir management, development, and permitting.

In the last decades infiltration excess overland flow, also called "Hortonian Runoff", was the traditional concept applied for analysis of runoff response. Later studies showed that Hortonian runoff mechanism was not applicable to all watersheds (Dunne and Black, 1970a). In south and central Florida, runoff or overland flow can be generated by two mechanisms: infiltration excess and saturation excess runoff. Infiltration excess occurs when the rainfall intensity exceeds the infiltration capacity of the soil. This type of runoff usually occurs in deep water table environments and is influenced by the temporal variability of actual rainfall. In contrast, saturation excess runoff occurs when the total infiltration depth exceeds the soil water storage capacity above the water table. This mechanism is more likely to develop in a shallow water table environment, where infiltration depth fills the storage capacity of the soil, and excess saturation spills into the surface as runoff.

Figure 1a) depicts the infiltration excess runoff mechanism for a vertical profile with depth against water content. During rainfall, water infiltrates into the soil increasing the water content at the surface. From Figure 1a), the moisture content profiles increase with time. Downward movement of the water into the soil takes place until saturation at the surface is reached. At this time, ponding at the surface occurs. For a time t, less than the ponding time, tp, the infiltration rate is equal to the rainfall rate and greater than the infiltration capacity of the soil.

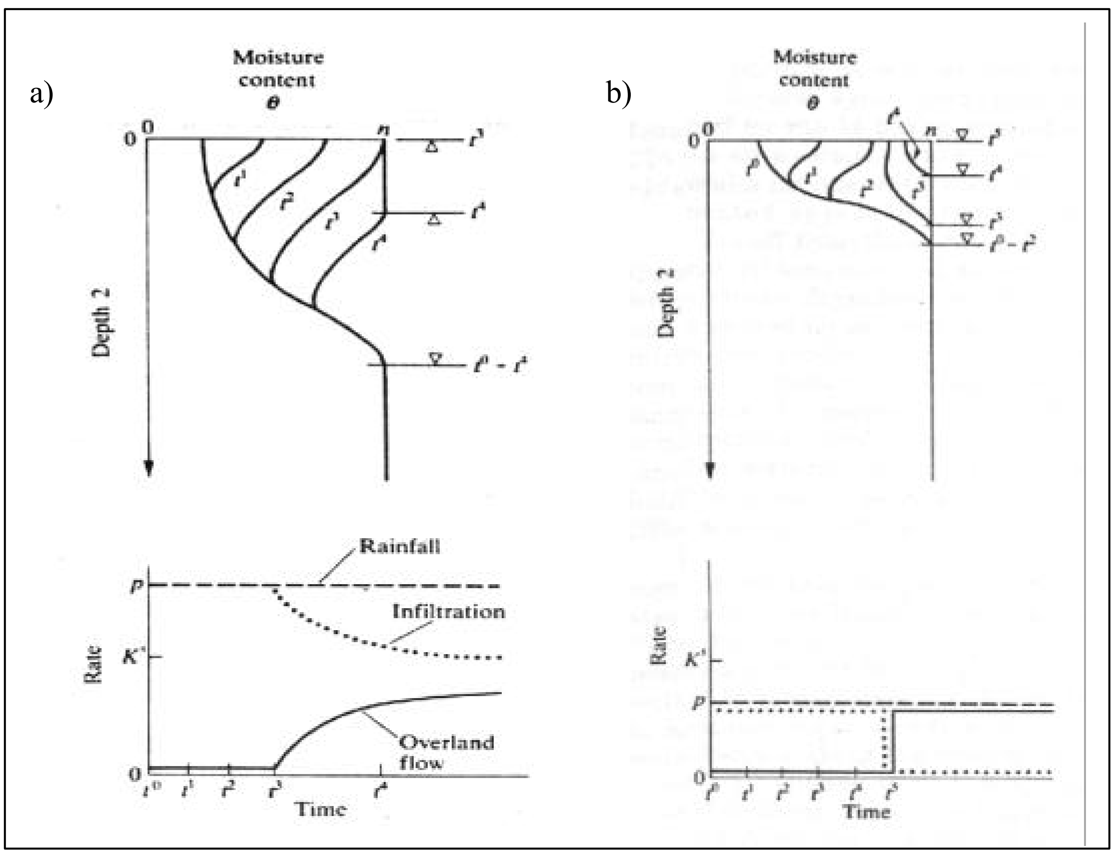

Figure 1. Mechanisms of infiltration and runoff. Source: R. A. Freeze, “A Stochastic Conceptual Analysis of Rainfall-Runoff Process on a Hillslope”, Water Resources Research. 16(2): 395, 1980.

After ponding takes place, infiltration rate decreases, overland flow or runoff increases and can be estimated as the difference between infiltration rate and infiltration capacity. Notice that the water table level in this case is deep and is not affected by rainfall or infiltration processes.

Saturation excess runoff is explained in Figure 1b). The profile of depth against moisture content shows how the moisture content in the soil increases with time. Since the water table is shallow, the storage capacity of the soil is small. Therefore, water going into the soil raises the water table levels filling the porous media and reaching surface saturation from below. For a time t, less than the time for surface saturation, the infiltration rate is equal to the rainfall rate and there is not runoff. For a time t, equal or greater than the time for surface saturation, the storage capacity of the soil is full and infiltration stops. Thus, all the rain runs off. During infiltration, some of the water may also run laterally below the ground surface. This flow is called subsurface flow and it is a faster flow that runs in the vadose zone until it enters a stream.

1.2. Objective and Scope

The purpose of this thesis is to analyze these two mechanisms of runoff and determine how geomorphologic characteristics and hydrologic processes impact these shallow water table environments. This work is divided into six chapters. The first chapter is the introduction and contains a background of the runoff mechanisms including infiltration excess and saturation excess runoff. It explains the need to go into fine time resolution of rainfall when infiltration excess runoff is prevalent and the importance of topographic changes of the landscape in variable saturated areas dominated by saturation excess runoff. Chapter 2 contains the analysis of rainfall data. It explains what type of rainfall data is used and how it is aggregated. A statistical analysis of rainfall and how variability is lost when coarse time resolution of rainfall is used are comprised in this chapter as well. Chapter 3 describes HYDRUS 1D, a variable saturated model for 1-dimensional water movement in the soil. This chapter includes simulations with HYDRUS 1D to analyze the impacts in runoff as a result of temporal variability in rainfall and depth to the water table. Chapter 4 contains a description of Digital Elevation Models (DEM) and how their features can be utilized in variable-saturated water movement models to describe topographic features of actual terrains. Chapter 5 of this thesis explains the saturation excess runoff process and the sensitivity analysis of geomorphologic and hydrologic characteristics that have an effect on Variable Saturated Areas (VSA). The complexity of hillslope processes on realistic non-simple slopes is analyzed here. The development of techniques for the identification, description, or extent of variable saturated areas is also included. And last of all, Chapter 6 summarizes the conclusions of this work.

1.3. Rainfall Variability

The estimation of infiltration excess runoff is highly dependent on rainfall variability. Often hydrologic models such as SWMM and HSPF used to simulate the hydrologic processes at the large scale —watershed scale— and use large time resolution of rainfall time series. Therefore, the effects introduced by the internal structure of rainfall are ignored. Gammeter and Fankhauser (1998) have expressed the necessity of finer resolution to capture the temporal variability of rain. In their work, they developed a program that disaggregates 10-minute observed rainfall data into 1-minute time step. Due to the lack of natural, fine time resolution rainfall data, hydrologists have been forced to create stochastic models to simulate the temporal structure of rainfall.

Arnold and Williams (1989) developed a stochastic model to generate 0.5 hr rainfall intensities from daily rainfall series. The temporal distribution of rainfall generated in this study is exponentially distributed within the storm. Woolhiser and Goodrich (1988) developed a stochastic model to disaggregate daily rainfall into short-period rainfall intensity. They showed that the disaggregation method is superior to the constant and isosceles method. The constant intensity rainfall pattern was not recommended in their study. Flanagan et al. (1988) used a programmable rainfall simulator to reproduce several storm intensity patterns. This study showed that runoff is greatly affected by rainfall intensity patterns. Rodriguez-Iturbe and Eagleson (1987) created a precipitation model to reproduce rainfall fields. These models in general simulate rainfall variability under limited conditions, and cannot be used for all types of rainfall patterns due to the complex variability of rainfall in time.

Some studies of rainfall-runoff have been done using actual rainfall data. Agnese and Bagarello (1997) studied the temporal resolution of natural storms on the infiltration predicted by the Chu model (Agnese and Bagarello, 1997) on both peak and time to peak intensity. Results of their study showed that the influence of the temporal resolution of rainfall on infiltration prediction was highly dependent on soil type, especially for soils with intermediate hydraulic conductivity. For these soils, an increase in the temporal resolution of rainfall led to a decrease of runoff prediction. When coarser resolution was used, predicted variability was underestimated. In general, variable rainfall intensities generate greater peak discharge than constant rainfall intensities (Singh, 1997).

Currently, most rainfall data used for storm water modeling is collected daily or hourly by rainfall gauges distributed around Florida. Recently, rainfall data from NEXRAD images having a resolution of 15-minutes are becoming available for modeling. Figure 2 and 3 depict radar images of total daily rainfall depth for two storms in Florida. The first graph shows a frontal storm that occurred on January 10, 1999. This storm is uniformly distributed over a large domain with an average intensity of 7 dba (0.4 inches).

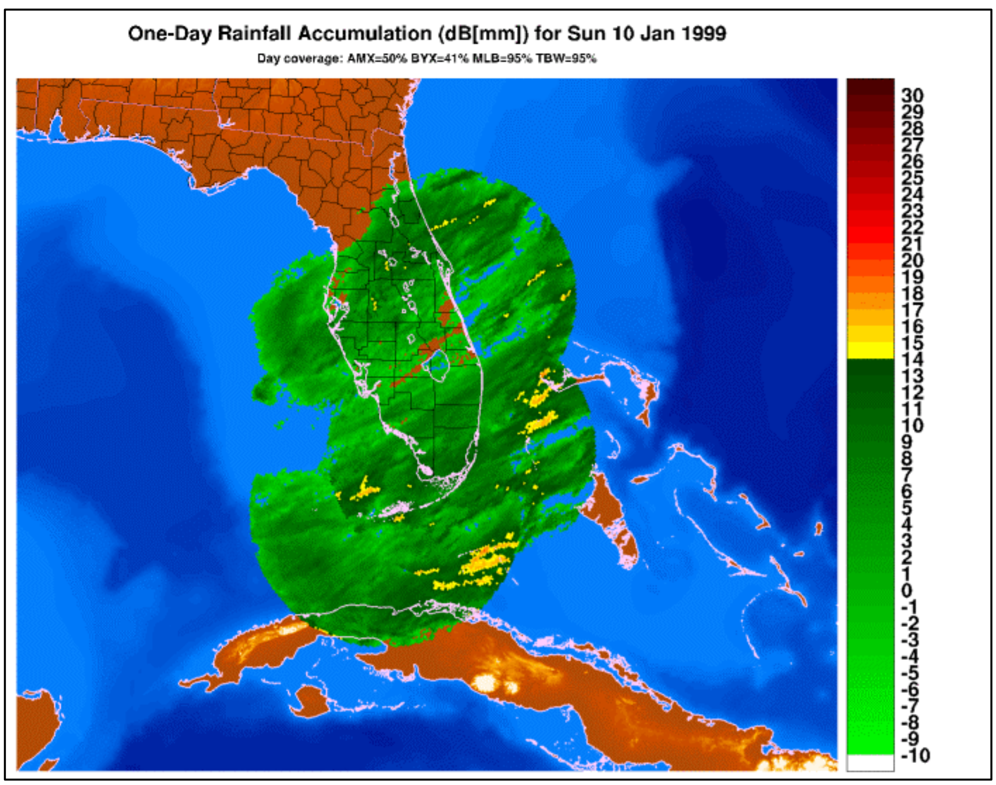

Figure 2. Radar image for a frontal storm in Florida. Note: values are in dBA

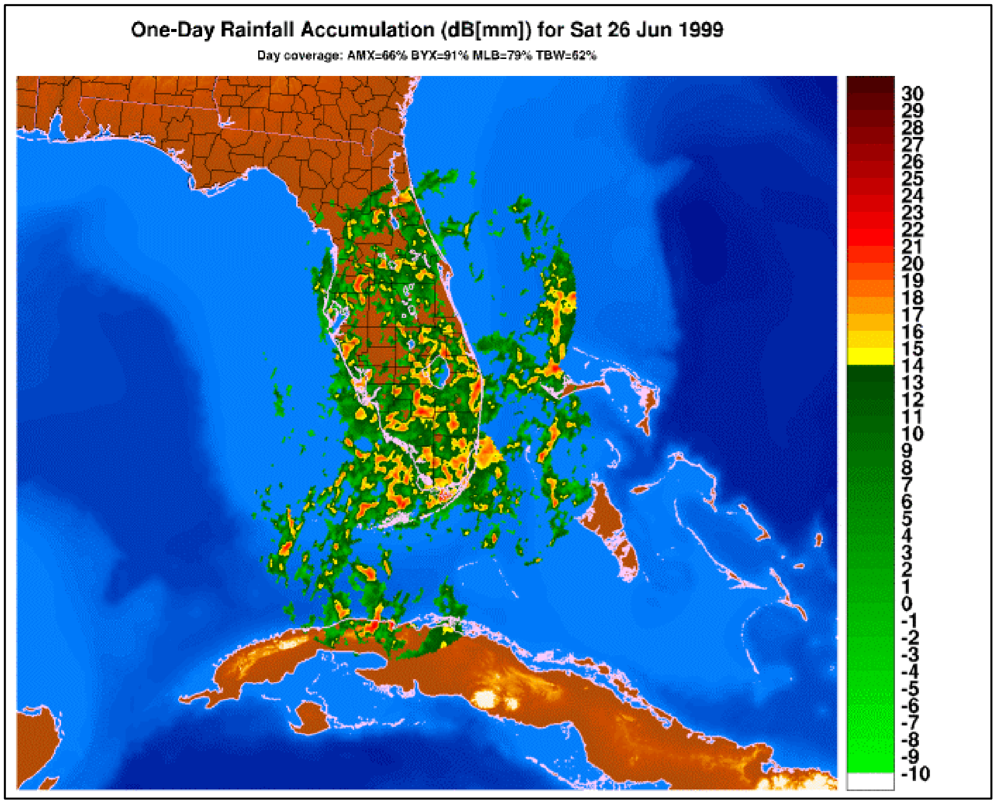

Figure 3. Radar image for a convective storm in Florida. Note: values are in dBA

Figure 3, on the other hand, shows a convective storm that occurred on June 26, 1999. Total rainfall depth for this storm is scattered over the domain coverage area. The storm has spots where total daily rainfall was about 15 dba (1.2 inches). Rainfall data at a finer resolution is rarely collected, and if collected, it is not distributed over a large domain.

Several studies have been conducted to determine the effect of rainfall variability on runoff (Lamb, 1999; Loague, 1988; Sepulveda, 1997; Milly and Eagleson, 1988). The complex structure of rainfall has been found to exhibit a large degree of temporal variability under natural conditions, which substantially affects the downward water movement in the vadose zone. Other studies have shown that accuracy of hydrologic models can be improved by using fine time step resolution of rainfall data in the determination of infiltration excess runoff (Finnerty et. al., 1997). In order to determine infiltration and runoff, it is necessary to know how much water infiltrates in the soil. Ground water movement in the soil is governed by Richards equation. Assuming vertical downward ground water movement on a homogeneous soil, the infiltration process can be simulated with the one dimensional Richards equation. Because estimates of Hortonian runoff depends on rainfall intensity, hyetographs with a fine time resolution are usually required to capture rainfall variability.

1.4. Variable Saturated Areas

The other mechanism of runoff, which develops in shallow water table depths, is saturation excess runoff. Dunne and Black (1970a) studied the runoff generation mechanisms on the Sleepers River Experimental Watershed near Danville, Vermont. Dunne and Black (1970a) noticed that surface runoff was produced on hillside by saturation from below. This led to the concept of saturation-excess overland flow (Kirkby and Chorley 1967; Dunne, 1978) which take place when water fills up the storage capacity of the soil with the water table reaching the surface, and producing runoff. This type of overland flow is likely to occur close to the stream banks where water table is shallow and a seepage face develops. Along with the concept of saturation-excess overland flow are "Variable Saturated Areas" (VSA).

Several authors studied Variable Saturated Areas since the 60's and observed that VSA were the major contributor of overland flow especially in humid environments

(Hewlett, 1961; Hewlett and Hibbert, 1963; Dunne and Black, 1970a,b; Freeze, 1972a,b; and Kirkby, 1978). Hewlett (1961) first described the concept of variable source areas as saturation excess runoff production. Then, Hewlett and Hibbert (1963) studied the contribution of runoff by extension of variable source areas. According to Dunne and Black (1970a,b), the variable saturated areas were controlled by topography, antecedent water content, soil moisture storage capacity, and rainfall intensity. A detail study about the impacts of these controlling characteristics was not included in his work. Dunne and Black (1970a,b) used a real watershed of steep slopes and poorly drained downslope. Here, variable saturated areas were produced by overland flow due to precipitation and return flow, or the subsurface flow that seeps through the surface and becomes overland flow. In thin soils, gentle concave downslopes with wide valley bottoms, runoff is dominated by direct precipitation and return flow (Kirkby, 1978). On an investigation of runoff generation at the hillslope scale, Freeze (1972a,b) used a small range of possible combinations of soils, slopes, and rainfall patterns and noticed that the most sensitive factor influencing runoff was the saturated hydraulic conductivity. In his study, rainfall intensity, duration, soil thickness, and slope did not have a major effect on runoff.

Numerous researchers have also developed and used hydrologic models to generate overland flow. Some of these models simulate the hydrologic processes at the watershed scale (O'Loughlin, 1986; Stagnitti et al., 1992, Wigmosta et al., 1994; Steenhuis, 1995; Evans et al., 1999) and some others at the hillslope scale (Loague, 1988; Govindaraju and Kavvas, 1991; Salvucci and Entekhabi, 1995; Ogden and Watts, 2000).

O'Loughlin (1986) used a 3 dimensional topographic model as a function of hillslope height to predict growth and contraction of VSA. His analyses assume runoff saturation caused by subsurface flow. This model does not account for transient changes in saturated boundaries because steady state conditions were part of the assumptions. Stagnitti et al. (1992) developed a mathematical model to predict hillslope and watershed discharge in a real basin with shallow water table depths and average slope. In their work, rapid subsurface flow traveling along the granite ledge produced runoff. Overland flow was not significant. Wigmosta et al. (1994) developed a spatially distributed hydrology-vegetated model that generates runoff by saturation excess on the snowmelt-dominated mountain basin. Digital Elevation Model (DEM) data is used here to model topographic characteristics. The extent of VSA was not discussed in this study. Steenhuis (1995) used the SCS approach to calculate runoff produced merely by VSA. This simplistic method do not account for temporal variation, rainfall intensity or landscape formations.

New attempts to describe Variable Saturated Areas have been done at the hillslope scale. For example, Loague (1988) used the Freeze stochastic rainfall simulator model SCRRS to create different rainfall intensities and soil hydraulic properties and to produce overland flow. He observed that saturated hydraulic conductivity was more important than rainfall intensity for convex topography. Govindaraju and Kavvas (1991) developed a physics-based deterministic distributed model by coupling overland flow, stream flow, and subsurface flow to study the saturated areas near streams. They analyzed the effect of hydraulic conductivity, rainfall intensity, antecedent moisture content, and slope. Landscape convergence and divergence, as well as concave and convex hillslopes were not considered in their work.

Salvucci and Entekhabi (1995) described an example application of a statistical-dynamical approach that coupled saturated and unsaturated flow to illustrate the sensitivity of hydrologic process to variations in topographic and climatic conditions. They used a non-real hillslope on a semi-humid climate of certain length, soil depth, and slope with no curvature. Some variations of these parameters were analyzed for an equilibrium steady state condition. Results of this study showed that a decrease in soil depth (shallow water tables) increased evaporation, decreased baseflow, and produced more runoff. An increase in soil depth increased recharge and produced no surface runoff. Convergence and divergence hillslopes were analyzed here as defined by the convergence ratio of the contour length at the water divide to the length at the stream.

Ogden and Watts (2000) used a 2-dimensional variable saturated subsurface model (VS2D) under uniform rainfall rate. They analyzed the importance of hillslope properties and rainfall on the temporal evolution of variable saturated areas. In their study, Ogden and Watts (2000) simulated the response of a non-convergent, constant-slope hillslope. They showed that hillslopes with shallow water tables, constant rainfall intensity, smaller slope angles, longer hillslope lengths, and smaller saturated hydraulic conductivity are more susceptible to variable saturated area formations. Neither hillslope curvature, nor landscape convergence was included in this investigation.

Rainfall variability seems to have an impact in the infiltration-runoff process near streams with shallow water tables. VSA expand and contract as a result of temporal variation in rainfall. During rainfall events the VSA expand. Then, when rainfall stops water is taken by evapotranspiration, redistribute in the soil, and seeps as subsurface drainage. As a consequence, the variable saturated areas shrink. When rainfall intensity increases, the variable saturated areas increase (Govindaraju and Kavvas, 1991).

Topographic attributes such as slope and curvature are important factors in defining the extent of VSA. Mild slope topographies have larger VSA than steep slopes. Therefore, more water infiltrates in the soil raising the water table levels and saturating the ground surface. Two types of hillslope curvature are studied in this work: concave and convex hillslope. Concave hillslopes curve upward whereas convex hillslopes curve downward. Freeze (1972b) found out that on convex hillslopes with deeply incised channels and high-saturated hydraulic conductivity subsurface flow is very significant. On the other hand, for concave hillslopes with low saturated hydraulic conductivity runoff generation comes from direct precipitation rather than from subsurface flow. He also pointed out that saturated hydraulic conductivity has major effects on runoff. Kirkby (1978) observed that topography with concave slopes have a larger contributing area.

Convergence and divergence is another landscape characteristic that affects variable saturated areas. On convergent hillslopes, the flow area reduces downstream and a larger source area sustains a smaller discharge area at the stream. In contrast, the flow area on divergent hillslopes increases downhill approaching the stream with a larger discharge area. Topographic settings like convergence and divergence are important in Florida because VSA are controlled by their surrounding upland landscapes. There has not been relevant research on convergence topography and how it affects the runoff response. Recently, Salvucci and Entekhabi (1995) studied the hillslope fluxes as a result of landscape convergence for long time response. They defined convergence as the ratio of contour length at the water divide to contour length at the stream. Their findings demonstrated that VSA increase for convergent landscape and tend to generate more runoff. Philip (1996) looked at the convergence and divergence perturbations on infiltration at the hillslope. He found these perturbations to be negligible small.

Initial conditions of the soil also affect the extent of variable saturated areas because they are highly influenced by the initial position of the water table. For shallow water tables, the initial moisture content of the soil is high, the storage capacity of the soil decreases and saturation excess occurs faster. As a result, the VSA extend more rapidly. This does not happen during the dry season. During winter, the water table position is usually deeper. Therefore, the antecedent moisture content of the soil is lower and the soil has more storage capacity. Under these conditions the soil takes longer to be fully saturated.

Stream shape and incision depth also affect VSA. Large incision depth increases the area of the subsurface in contact with the stream. Therefore, the contribution of subsurface water to the stream increases (Govindaraju and Kavvas, 1991).

In general, most research at the hillslope scale has only studied single slope forms to explain the hydrologic process on variable saturated areas. This work analyzes natural topography in Florida and the impacts in saturation excess runoff due to changes in geomorphologic properties. Flat slopes usually with shallow water table depths and numerous wetlands, some of them isolated, characterize Florida landscapes. Wetlands are saturated areas that shrink during the dry season and expand in the wet season as part of their hydro-periods. Wetlands are considered important and valuable ecosystems because they maintain biodiversity and wildlife habitat, provide flood protection, stream-flow maintenance, and recharge control. Furthermore, wetland ecosystems are very important for hydrologic modeling, flood forecasting, reservoir management, wetlands conservation plans, soil pollution, etc. In forested wetlands near streams, Variable Saturated Areas form due to saturation excess runoff mechanism. Alteration of topographic characteristics of the terrain can highly influence wetlands and the river basin response. The extent of these variable saturated areas is controlled by several factors such as landscape changes, rainfall variability, topography, landscape convergence, initial moisture conditions, and stream sinuosity and incision depth. Therefore, impacts of geomorphologic and hydrologic features on runoff in humid shallow water tables should be studied.

CHAPTER 2. RAINFALL ANALYSIS

Rainfall directly influences surface and subsurface runoff, streamflow, and groundwater recharge. Two types of mechanisms characterize Florida rainfall: frontal and convective. Frontal precipitation usually occurs when a cold front from the north results in lifting of air masses. Frontal precipitation generates longer periods of rain and small intensities usually during the dry season, November through March. In contrast, convective rainfall during the wet season (May through September) is characterized by short storm duration with fairly high rainfall intensities. The months of April and October excluded above are transition periods that can be either convective, frontal or both. Two thirds of the rainfall in Central Florida are due to convective thunderstorms originating inland during the summer. Figure 4 and Figure 5 shows a typical rainfall hyetograph for a convective and a frontal storm, respectively, obtained from a gauge station in the Tampa area.

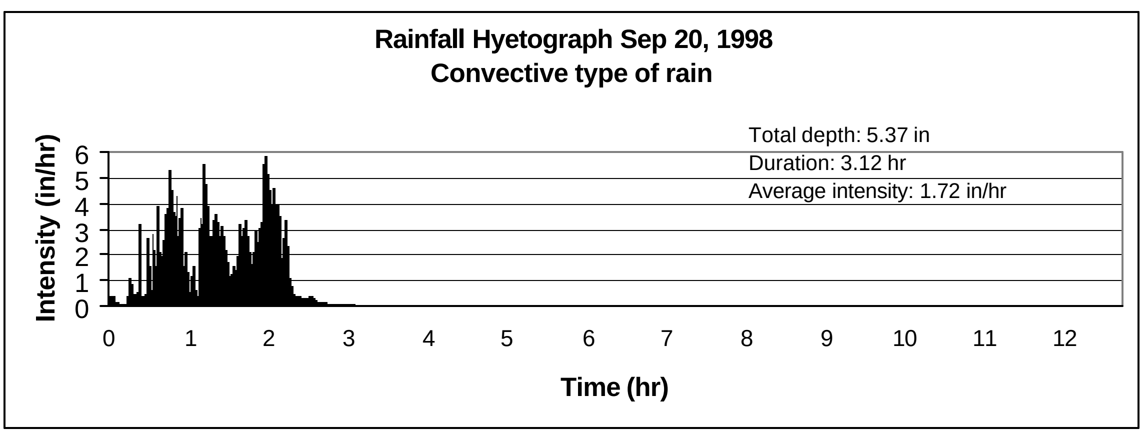

Figure 4. Convective storms from a rainfall gauge located at the University of South Florida, Tampa campus

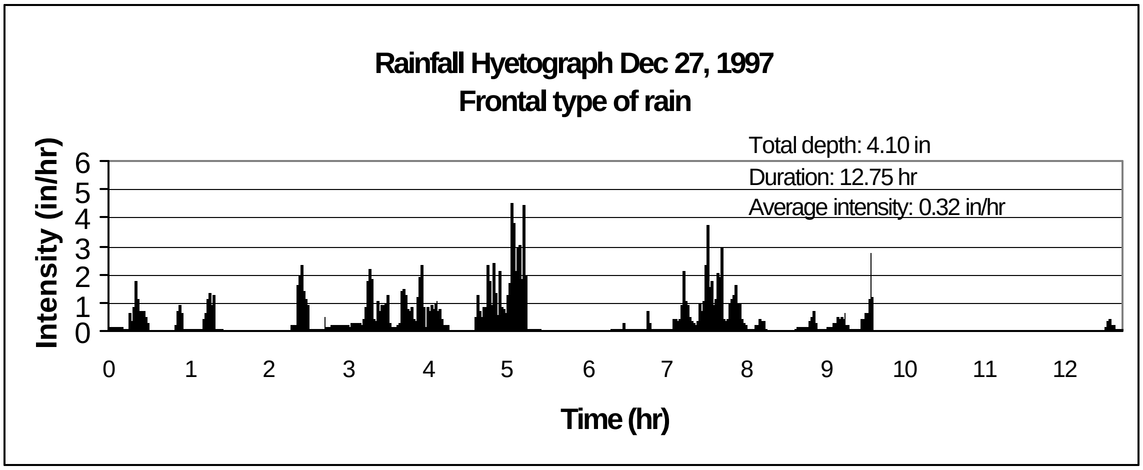

Figure 5. Frontal storms from a rainfall gauge located at the University of South Florida, Tampa campus

The complex structure of these rainfall events cannot be captured when rainfall data is collected at large-time resolution intervals such as daily and hourly time steps. In order to study the temporal variability of rainfall, actual precipitation has been used and converted to a 1-minute time series. A statistical analysis of intensity of rain, total duration, and depth of rainfall storm is carried out here and is explained below.

2.1. Rainfall Data

Collecting data at a small time resolution or if possible continuous data is crucial in this research. Currently, data is collected at 15-minute or greater time steps. Rainfall data at a fine resolution is rarely collected or is not collected over a large domain. Moreover, the data have to be collected over a long period of time in order to perform a statistic analysis of the data. Fine time resolution data is required to analyze the temporal variability of rainfall in Florida. Accordingly, a suitable source for this research is a local rainfall gauge placed in Tampa. The rainfall data employed was collected from the roof of the Engineering Building II at the University of South Florida. Data is obtained from a tipping bucket gauge, which records time to tip with a depth resolution of 0.01 inches per tip. Water flows directly and without time delay from the funnel to the bucket. Time intervals between consecutive tips are recorded. The rainfall records used dated from March 1995 to September 1998, which is about four years of continuous rainfall data. Long-term time series of rainfall at this resolution are not recorded. Furthermore, they are not needed because of the scale of this research. The tipping bucket gauge is part of a study being conducted at the University of South Florida, Electrical Engineering Department and NASA.

2.2. Rainfall Model Description

A model to disaggregate the continuous rainfall data was developed. This is a model created with Visual Basic code and is divided in 2 subroutines: *Rainfall_minute* and *Event_minute.* The model creates 1-minute time series, separate storms, and calculates total rainfall depths and durations for each storms.

Rainfall_minute is a subroutine that converts the actual data in 1-minute time resolution. The purpose of this subroutine is to create a time series of 1-minute time resolution from continuous rainfall data files. The program reads date, time, and time to tip in seconds from a text file and calculates the intensity of rain and cumulative depth of rain every minute. 1-minute intervals are linearly interpolated to find the intensity and cumulative rainfall depth up to that period. The source code for this subroutine can be found in Appendix A. The steps used by the 1-minute time step rainfall program include:

* Input file: it is a comma separated ASCII file (.csv) with three columns including date, time and time to tip in seconds. The program reads and accumulates time to tip. If time to tip is less than 5 minutes, then it starts accumulating the time and depth of rain. If time to tip for a single tip is greater than 5 minutes (no rain within 5 minutes or more), then it assigns to that period the same time to tip as the next period that tips in less than 5 minutes. As a result, intensities generated by the rainfall model are not small than 0.002 in/min (0.01 inches / 5 minutes). Long periods with no tips have intensities equal to zero.

* Linear Interpolation: Once the file is read and values are cumulated, the subroutine interpolates linearly every minute and calculates the cumulative rainfall depth in inches as well as the intensity for each minute. When the time to tip is less than 1 minute the program averages intensities by distributing rainfall depth over the minute.

* Output file: this is a comma separated ASCII file with a text extension suffix (.txt) and contains the following columns: Date and time, time in minutes, intensity in in/hr every minute, and cumulative depth of rainfall in inches.

Event_minute is the subroutine that separates storms. The 1-minute time step rainfall data were previously separated into convective and frontal activity. Convective storms are storms during the months of May through September. Frontal storms are the storms during the months of November through March. The months of April and October were separated manually by looking at their rainfall intensities and duration. Once the rainfall data are divided into convective and frontal activity, they are entered into the model in order to separate storms events. Convective storms are separated using 1-hour inter-event period of no rain (Bosch and Davis, 1999). That is, every time there is a period greater than 1 hour with no rain there is a new convective storm. There are no criteria established to separate frontal storms. However, experience with actual data shows that frontal storms have long durations and occur about every 8 hours or more. Therefore, 8-hour inter-event period is used for frontal storms. The source code for the Event_minute subroutine can be found in Appendix B. The steps used for the subroutine to separate storms include

* Input file: it is a comma separated ASCII file (.txt) generated previously by the Rainfall_minute subroutine. This file contains four columns including date and time, time every minute, intensity in in/hr, and cumulative depth of rainfall in inches. The subroutine distinguishes between frontal or convective activity. Therefore, only one of these criteria can be used at a time.

* Calculations: Once the file is read, cumulative depth of rain and duration for each storm are calculated. Rainfall depth is cumulated each minute until there is a period of 1 hour or more with no rainfall. In that case, the program records an event or storm and print to file the cumulative depth and duration up to that time.

Then, a new storm begins and these variables are reinitiated and start cumulating depth of rain and duration again all the way to the end of the file.

* Output file: this is a comma separated ASCII file with a text extension suffix (.txt) that contains the following output columns: date and time, time every minute, intensity in in/hr, cumulative depth of rain in inches, total duration for each storm in hours, and total rainfall depth for each storm in inches. Appendix C includes a sample of the output file generated by this subroutine.

The actual rainfall data were converted to 1-minute time series. Then, the time series were separated in convective and frontal storms. It was observed that some of the convective activity occurred during the dry months were frontal type of storms were expected. Therefore, these storms were separated manually to avoid errors.

2.3. Statistical Analysis

From the four years of actual record data with 1-min time resolution, 409 storms were generated. 316 storms were convective and 93 were considered frontal. Statistical analysis for these data was done. Basic statistics such as mean, standard deviation, coefficient of variation, median, kurtosis, and skewness were calculated for the 1-minute time series. The basic statistics for the rainfall data are shown in Table 1. Rainfall statistics shown in Table 1 have been computed for depth of rainfall and duration of storms. From Table 1, it can be concluded that mean total rainfall depth and duration for frontal storms are greater than for convective storms. The mean rainfall depth for frontal storms is 0.94 inches compared to 0.31 inches for convective storms.

Table 1. Basic statistics for 1-minute total rainfall depth and duration in Tampa.

All storms 1 minute Total Depth (in)	*Values*
Mean	0.457
Standard Error	0.040
Median	0.160
Mode	0.020
Standard Deviation	0.799
Sample Variance	0.638
Kurtosis	24.792
Skewness	4.186
Range	7.800
Minimum	0.010
Maximum	7.810
Sum	187.040
Count	409

All storms 1 minute Total Duration (hr)	*Values*
Mean	2.269
Standard Error	0.222
Median	0.739
Mode	0.050
Standard Deviation	4.497
Sample Variance	20.226
Kurtosis	18.574
Skewness	3.891
Range	35.204
Minimum	0.033
Maximum	35.237
Sum	928.161
Count	409

Frontal 1 minute Total Depth (in)	*Values*
Mean	0.943
Standard Error	0.128
Median	0.500
Mode	0.350
Standard Deviation	1.236
Sample Variance	1.529
Kurtosis	9.991
Skewness	2.688
Range	7.790
Minimum	0.020
Maximum	7.810
Sum	87.680
Count	93

Convective 1 minute Total Depth (in)	*Values*
Mean	0.314
Standard Error	0.030
Median	0.130
Mode	0.020
Standard Deviation	0.539
Sample Variance	0.290
Kurtosis	33.431
Skewness	4.783
Range	5.380
Minimum	0.010
Maximum	5.390
Sum	99.360
Count	316

Frontal 1 minute Total Duration (hr)	*Values*
Mean	7.243
Standard Error	0.764
Median	4.454
Mode	1.351
Standard Deviation	7.365
Sample Variance	54.236
Kurtosis	3.092
Skewness	1.650
Range	35.170
Minimum	0.067
Maximum	35.237
Sum	673.564
Count	93

Convective 1 minute Total Duration (hr)	*Values*
Mean	0.806
Standard Error	0.054
Median	0.488
Mode	0.050
Standard Deviation	0.952
Sample Variance	0.906
Kurtosis	10.212
Skewness	2.653
Range	7.168
Minimum	0.033
Maximum	7.201
Sum	254.597
Count	316

Table 2. Basic statistics for actual and 1-minute rainfall intensities in Tampa, Fl.

1 minute Intensities (in/hr) for 4 years	
Mean	0.527
Standard Error	0.005
Median	0.239
Mode	0.122
Standard Deviation	0.734
Sample Variance	0.538
Kurtosis	12.516
Skewness	3.186
Range	8.119
Minimum	0.000
Maximum	8.119
Sum	11222.398
Count	21307

Actual data intensities (in/hr) for 4 years	
Mean	1.572
Standard Error	0.011
Median	1.100
Mode	4.105
Standard Deviation	1.570
Sample Variance	2.466
Kurtosis	5.611
Skewness	1.675
Range	17.734
Minimum	0.000
Maximum	17.734
Sum	30141.103
Count	19176

Frontal 95-98 actual data intensity (in/hr)	
Mean	1.250
Standard Error	0.014
Median	0.752
Mode	2.875
Standard Deviation	1.371
Sample Variance	1.879
Kurtosis	5.062
Skewness	1.802
Range	16.216
Minimum	0.000
Maximum	16.216
Sum	11176.852
Count	8944

Convective 95-98 actual data intensity (in/hr)	
Mean	1.853
Standard Error	0.017
Median	1.478
Mode	2.963
Standard Deviation	1.676
Sample Variance	2.809
Kurtosis	5.603
Skewness	1.555
Range	17.734
Minimum	0.000
Maximum	17.734
Sum	18964.252
Count	10232

Frontal 95-98 1-minute data intensity (in/hr)	
Mean	0.431
Standard Error	0.005
Median	0.219
Mode	0.122
Standard Deviation	0.586
Sample Variance	0.344
Kurtosis	18.315
Skewness	3.748
Range	6.643
Minimum	0.001
Maximum	6.644
Sum	5260.799
Count	12220

Convective 95-98 1-minute data intensity (in/hr)	
Mean	0.656
Standard Error	0.009
Median	0.272
Mode	0.011
Standard Deviation	0.878
Sample Variance	0.771
Kurtosis	7.992
Skewness	2.613
Range	8.119
Minimum	0.000
Maximum	8.119
Sum	5961.600
Count	9087

Table 1 also confirms that frontal storms have longer durations than convective storms. Frontal storm mean duration for this rainfall record is 7.24 hr whereas the mean duration for convective storms is 0.8 hr. Rainfall intensities were also compared with the actual intensities for the 4 years of records and are shown in Table 2. From this table, it can be noticed that the rainfall intensities calculated from the 1-minute time series are considerably small than the actual rainfall intensities. This is because there were a lot of small intensities created when the rainfall data were aggregated into 1-minute time steps. These small non-realistic intensities created a bias on the time series that makes the averages smaller.

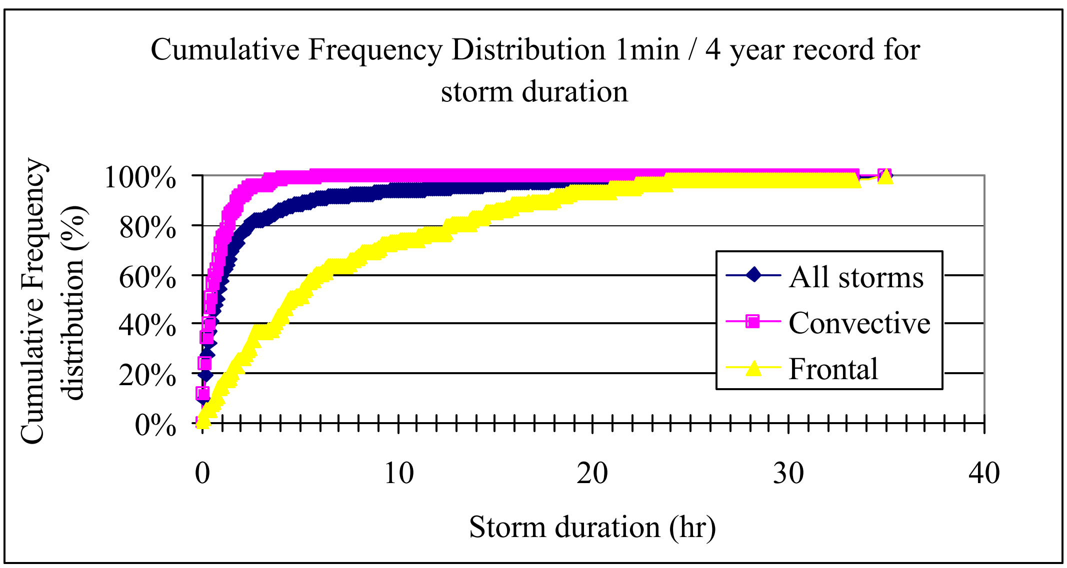

Figure 6. Cumulative frequency distribution for storm duration

Figure 6 and Figure 7 depict the cumulative frequency distributions for total duration and depth of storms respectively. It is clear that convective storms have smaller storm duration with 90% of the storms having durations less than 2 hours. In contrast, 90% of the frontal storms have durations of about 17 hours or less. Storm rainfall depth on the other hand, is more similar for convective and frontal storms, being greater for frontal storms. Looking at 90% of the storms, the rainfall depth for convective storms is 1 inch or less and the rainfall depth for frontal storms is approximately 2.5 inches.

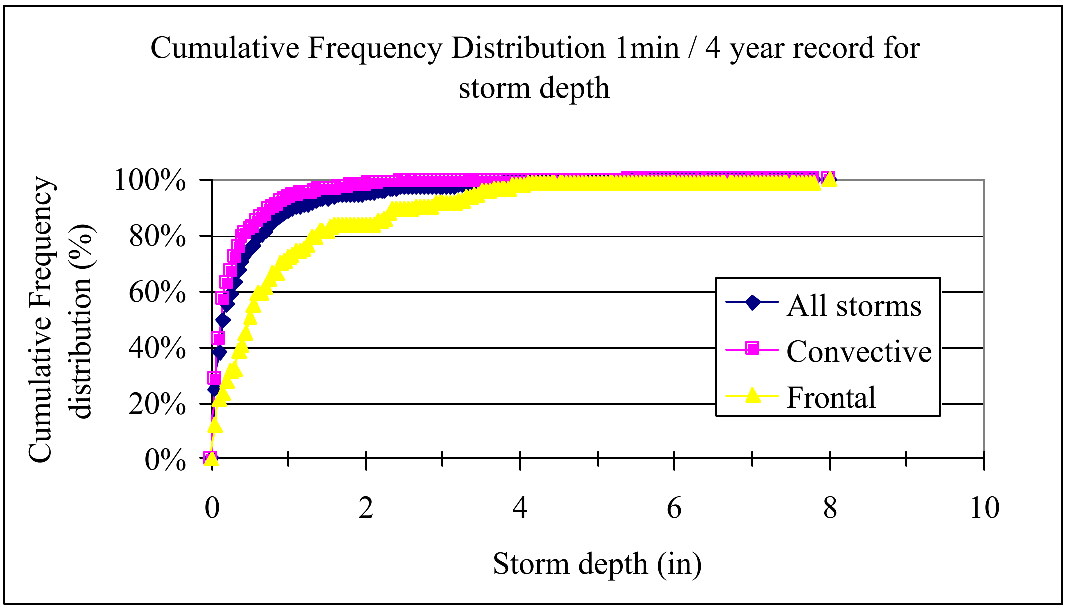

Figure 7. Cumulative frequency distribution for storm depth

For each storm, total rainfall depth, storm duration, maximum and average intensity are determined. In conclusion, statistics showed that convective storms have more variability, shorter duration and lower total rainfall depth than frontal storms. On the other hand, frontal storms are more uniform distributed, have longer duration and larger total rainfall depth.

Figure 8 shows the cumulative frequency distribution of intensities for the four years of data. The graph illustrates different cumulative frequency distributions of 1-minute time series for all 4 years of rainfall intensities. With the purpose of reducing the bias in the intensities when the 1-minute time series where created, intensities less than 0.25 in/hr were deleted from the record and frequency distributions where calculated again. The mean rainfall intensity for all record is 0.53 in/hr. After ignoring rainfall intensities less that 0.25 in/hr, the mean intensity is 0.93 in/hr. The same was done but now ignoring rainfall intensities less than 0.50 in/hr. As a result, the mean intensity increased to 1.41 in/hr, which compared better with the mean intensity for the actual record of 1.57 in/hr. From Figure 8, after ignoring all intensities less than 0.50 in/hr, this graph matches closer the graph for the actual (raw) rainfall intensities. All small intensities were not necessary created by the rainfall model. Some of these intensities could have been captured by the rainfall gauge as part of a moving storm that was either approaching or moving away from the gauge.

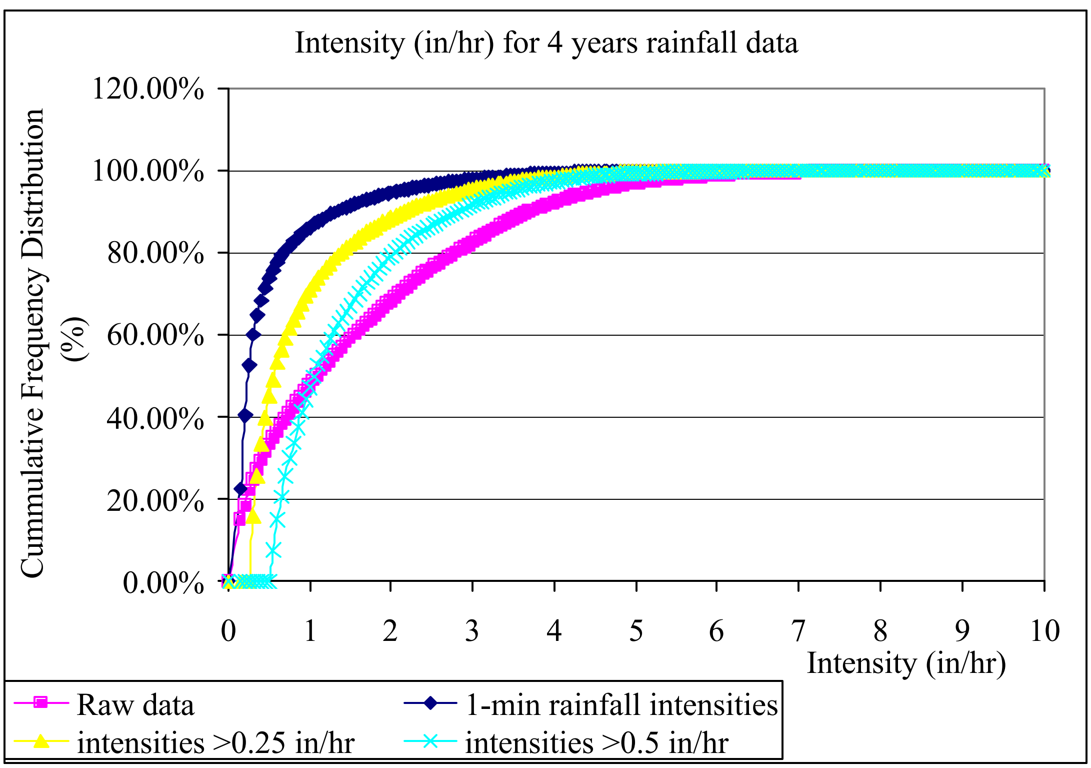

Figure 8. Cumulative frequency distribution for rainfall intensity

2.4. Temporal Variability of Rainfall

Trying to describe the temporal and spatial variability of actual precipitation is one of the objectives of hydrologist. Several authors have demonstrated that runoff is sensitive to this variability.

From the four years of records, two rainfall storms, one convective and one frontal were selected to analyze the temporal variability of these storms and how details are lost when coarse time resolution of rainfall data is used. The 1-minute time step hyetographs for the storms are illustrated on Figure 4 and Figure 5. These hyetographs were aggregated in different time steps including 3, 5, 10, 15, 30 minutes and 1 hour. Hyetographs of the convective storm were created for these time resolutions and are shown in the figures below. The convective storm selected had a total duration of 3.12 hours and rainfall depth of 5.37 inches. The frontal storm had a total duration of 12.75 hours and rainfall depth of 4.1 inches. Basic statistics such as mean, standard deviation, and variance were calculated for the aggregated hyetographs.

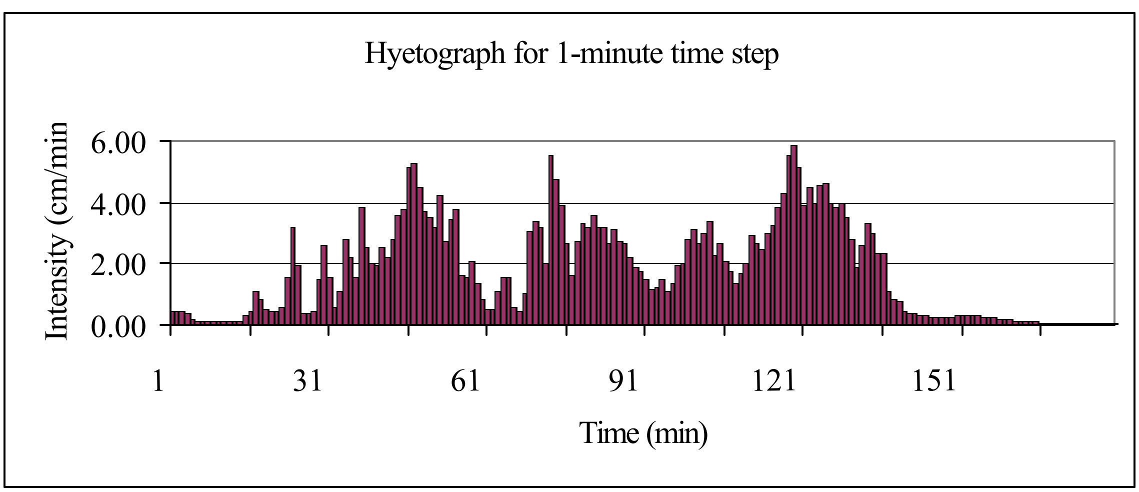

Figure 9. Hyetograph for 1-minute time resolution of rainfall

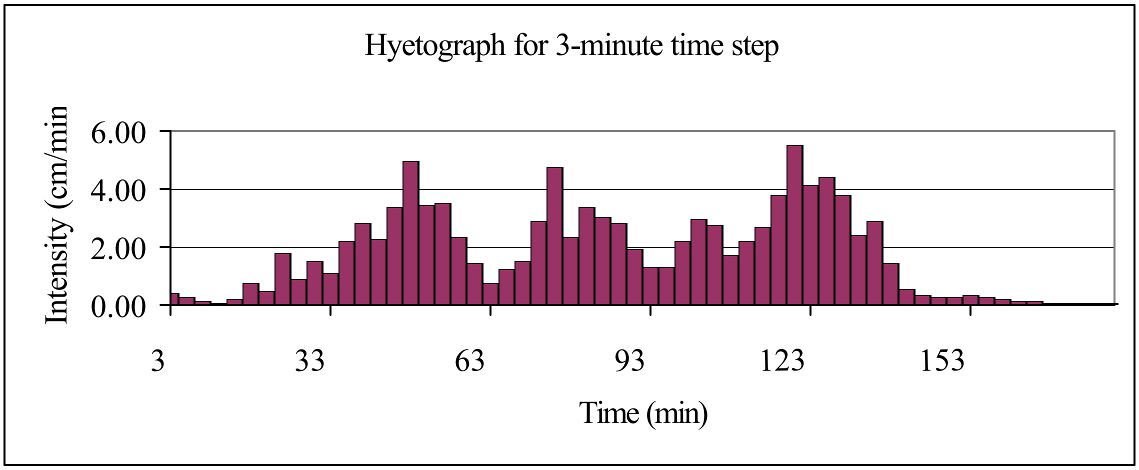

Figure 10. Hyetograph for 3-minute time resolution of rainfall

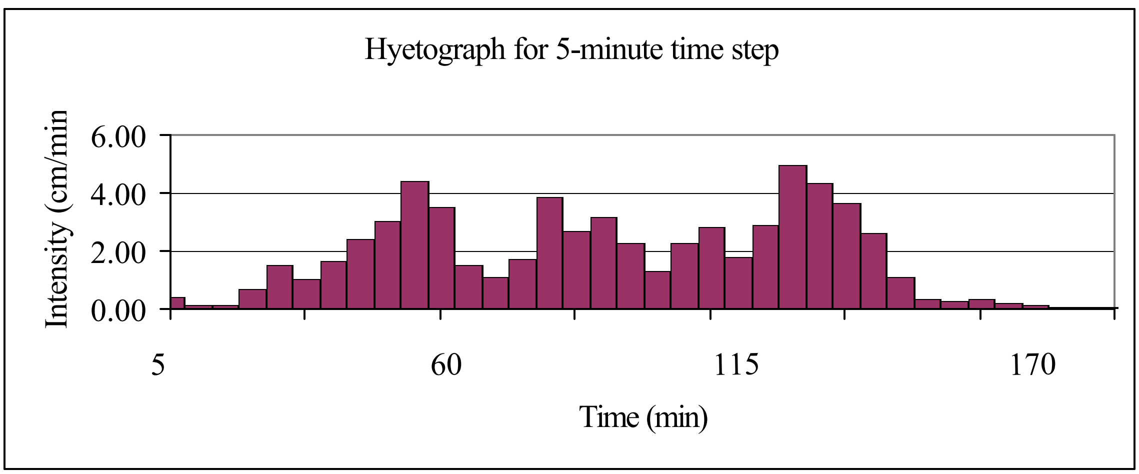

Figure 11. Hyetograph for 5-minute time resolution of rainfall

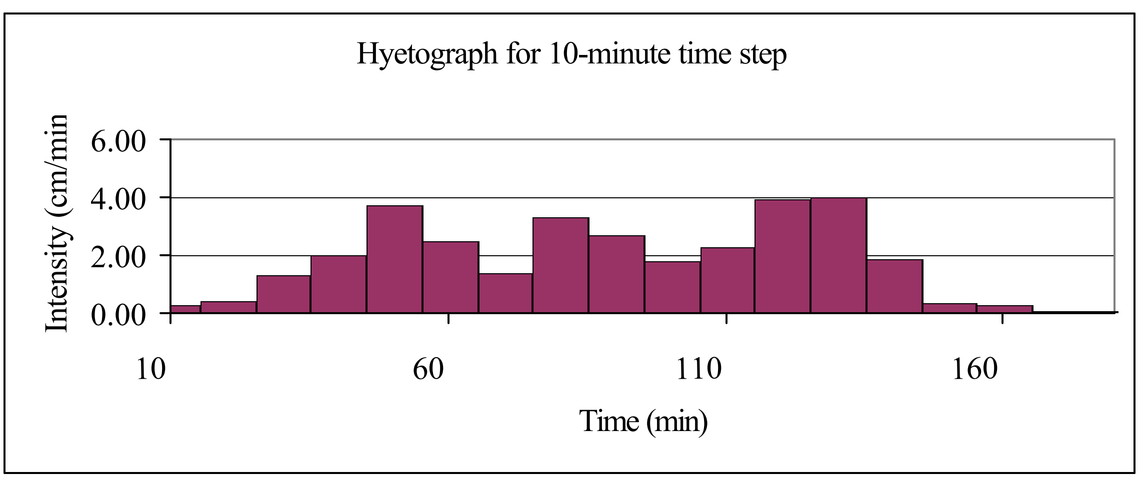

Figure 12. Hyetograph for 10-minute time resolution of rainfall

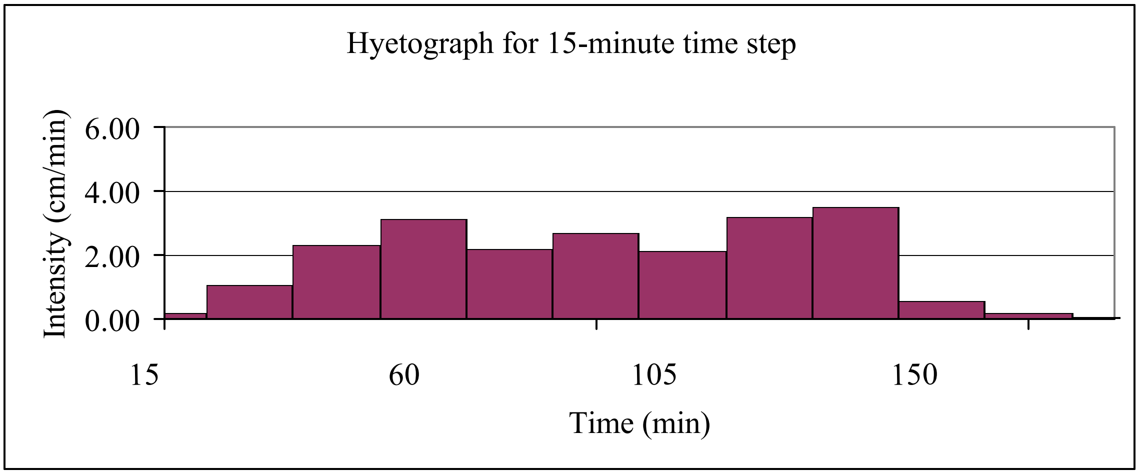

Figure 13. Hyetograph for 15-minute time resolution of rainfall

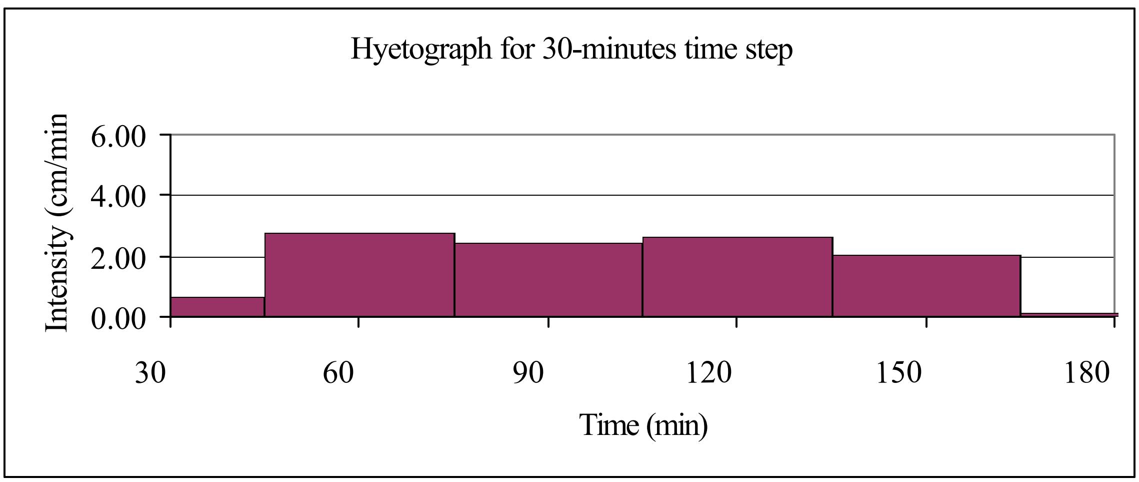

Figure 14. Hyetograph for 30-minute time resolution of rainfall

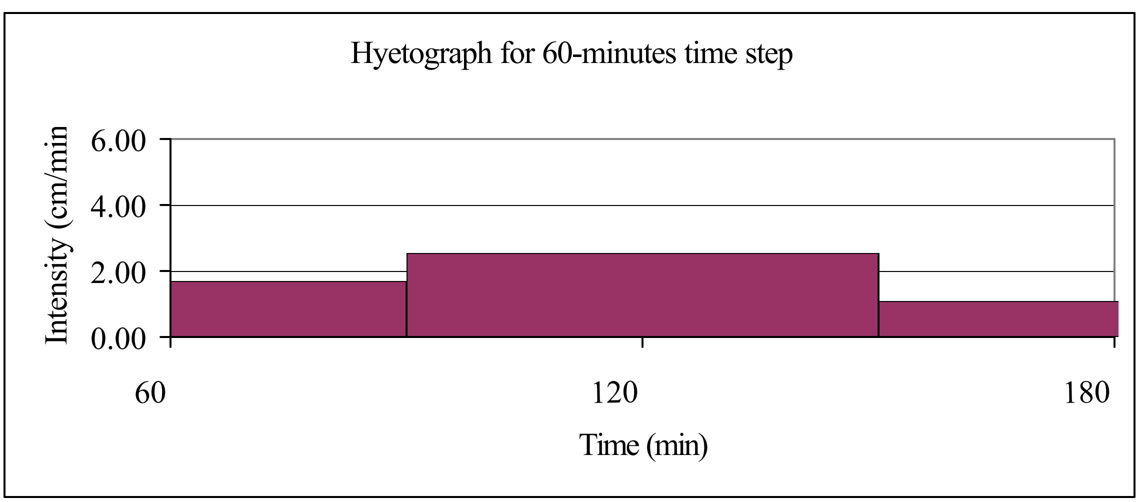

Figure 15. Hyetograph for 60-minute time resolution of rainfall

From these hyetographs, it is clear how temporal variability in the intensities for convective storms is lost. The hyetograph at 1-min time resolution shows the rainfall variability during the 3-hour rainfall storm. The average intensity is 0.08 cm/min but there is considerable difference with respect to the mean. Table 3 and Table 4 show the mean, standard deviation, and variance for the convective and frontal storms respectively. This variability is being lost when the time resolution increases from 1-min to 60-min. When intensities are aggregated in coarser time steps, they are smoothed out and the intensities become more uniform distributed over time. For comparison, the intensities for the 1-minute time resolution hyetograph shows intensities as high as 6 cm/min, whereas the intensities for the 1 hour time resolution are less that 3 cm/min. As we move to coarser time resolution, the details in rainfall distribution are lost. The hyetograph at 60-min time resolution doesn't show the real distribution of rainfall on time; it shows a uniform storm with an average intensity of 0.08 cm/min. The mean does not change when the time resolution changes. It is constant whereas the standard deviation and variance decrease when the time resolution increases. Therefore, large time resolution (60min, 30 min, 15 min) has less variation with respect to the mean.

Table 3. Main statistics for aggregated hyetographs of a convective storm

Time step (minutes)	*Mean*	*Standard deviation*	*Variance*
1	0.0757	0.0648	0.0042
3	0.0757	0.0627	0.0039
5	0.0757	0.0613	0.0038
10	0.0757	0.0581	0.0034
15	0.0757	0.0545	0.0030
30	0.0757	0.0472	0.0022
60	0.0757	0.0312	0.0010

Table 4. Main statistics for aggregated hyetographs of a frontal storm

Time step (minutes)	*Mean*	*Standard deviation*	*Variance*
1	0.0133	0.0256	0.0007
3	0.0133	0.0243	0.0006
5	0.0133	0.0228	0.0005
10	0.0133	0.0209	0.0004
15	0.0133	0.0211	0.0004
30	0.0133	0.0163	0.0003
60	0.0133	0.0131	0.0002

The variance vs time resolution graphs below illustrate how much details are being lost when the time resolution of the rainfall time series is coarse. For example, looking at the graph below for convective storms, the variance when small time steps are used is larger than the variance for coarser time resolution. As a result, more details in the temporal variability of rainfall can be captured using small or fine time steps. Plots for variance and log variance against time resolution are shown in Figures 16 and 17.

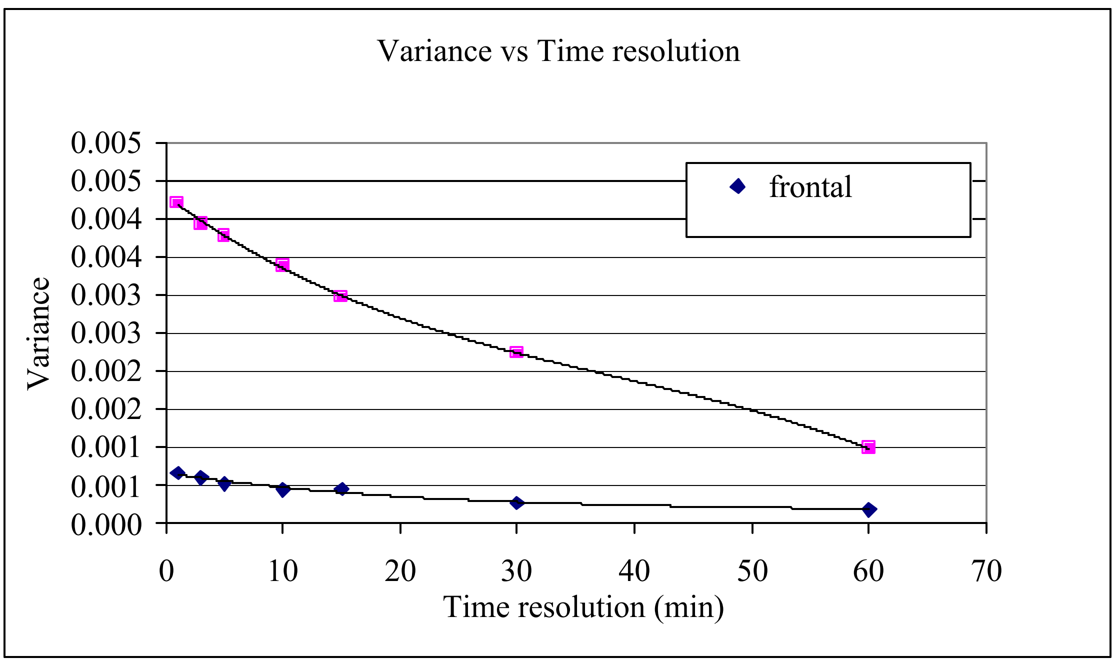

Figure 16. Variance vs time resolution (minutes) in natural scale

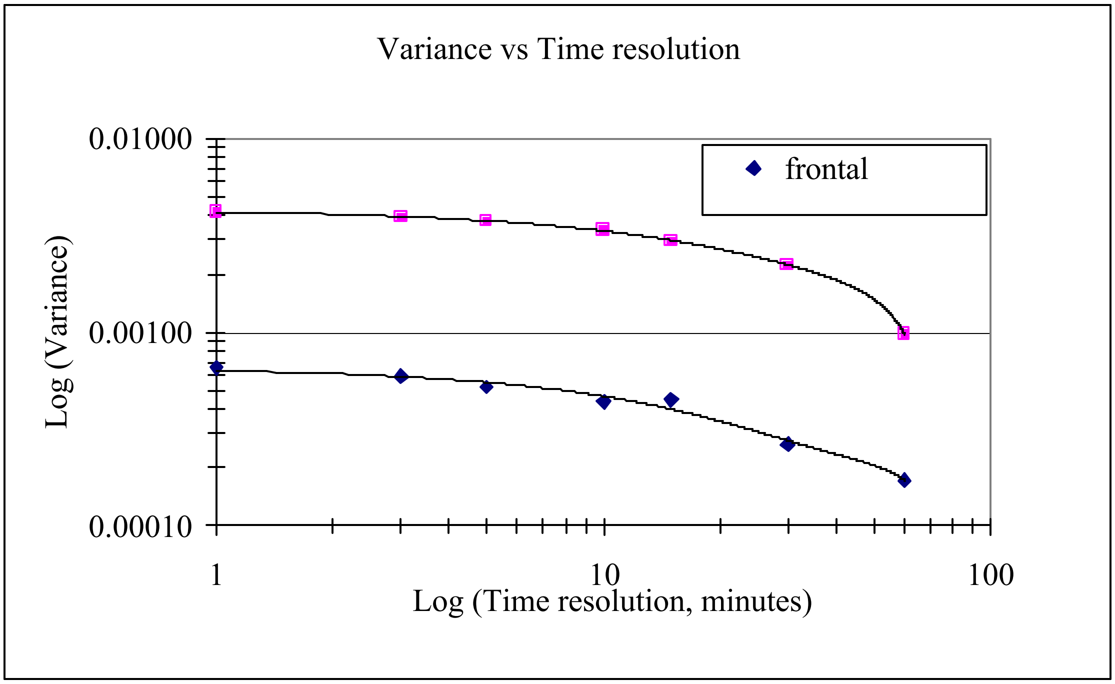

Figure 17. Variance vs time resolution (minutes) in Log scale

Comparing the variance for frontal storms with the variance for convective storms, it can be concluded that frontal storms are more uniform and their variability is smaller. From the graph in natural scale, the variance for convective storms is about 4 times larger than the variance for frontal storms. Figure 17 demonstrates, in logarithmic scale, how many details are captured in the temporal variability of rainfall. Notice that the pattern of the curves in this graph shows a rapid decrease in the variance for time resolutions larger than 10 minutes. It explains the loss in details for large time resolution rainfall series.

CHAPTER 3. INFILTRATION EXCESS RUNOFF

Infiltration excess runoff or 'Hortonian Runoff' depends on generation of surface runoff by rainfall excess. Infiltration excess runoff occurs when the rainfall intensity exceeds the infiltration capacity of the soil. Runoff is calculated as the difference between rainfall intensity and infiltration capacity. This type of runoff occurs especially in soils with deep water table levels. After ponding, the time at which ground surface reaches saturation, water starts running off while part of it may still infiltrate.

Due to the temporal variability of rainfall, there are periods when the rainfall intensity is less than the saturated hydraulic conductivity or periods of no rain at all. These periods are called hiatus (Ogden and Sagharian, 1997) and can be of any duration. During hiatus, water infiltrating into the soil moves downward due to gravity and capillary drive. When the hiatus periods are long (3 hours or more), water redistribute in the soil and the moisture content decreases with time. The model used here accounts for redistribution of the water content in the soil.

The infiltration-runoff process for deep water table environments can be impacted by temporal variability of rainfall, as well as depth to the water table. For instance, convective storms having short bursts of high rainfall intensities can generate more infiltration excess runoff when fine time resolution of rainfall is used. Frontal storms on the other hand, lasting longer periods with low intensities, have a slower response.

3.1. HYDRUS 1D

A commercial software package, HYDRUS 1D, for simulating the one-dimensional movement of water in variably-saturated media was utilized to study the impacts of temporal variability of rainfall on runoff. This program was developed by U.S. Salinity Laboratory, U.S. Department of Agriculture, Agriculture Research Service (Simunek and van Genuchten, 1998).

HYDRUS-1D is an interactive graphics-based user interface developed in support of the computer model HYDRUS (FORTRAN source code). HYDRUS-1D may be used to simulate one-dimensional water flow, heat, and solute transport in variably saturated soils. For this, HYDRUS uses the Richards equation to predict water movement between the soil surface and the groundwater table.

The user interface includes data pre-processing and graphical presentation of the output results in Microsoft Windows environment. Data pre-processing involves specification of all necessary parameters to successfully run the FORTRAN source code, discretization of the soil profile into finite elements, and definition of the vertical distribution of hydraulic and other parameters characterizing the soil profile (Simunek and van Genuchten, 1998)

HYDRUS 1D module contains the main program unit and the overall computational environment of the system. This module controls execution of the program and determines which other optional modules are necessary for a particular application. The module contains both the pre-processing and post-processing units. The pre-processing unit includes specification of all parameters for the FORTRAN code. At first, the processes to be simulated are selected (water flow, chemical transport, heat transport, root growth, and/or root water uptake). Length unit, depth and inclination of the soil profile to be analyzed, and the number of materials to be used are specified. The time and space scales are selected, and boundary conditions are entered among many other operations. A small catalog of soil hydraulic parameters based on soil texture is part of the pre-processing unit. The user can choose between direct simulation and inverse solution, where parameter optimization can be carried out.

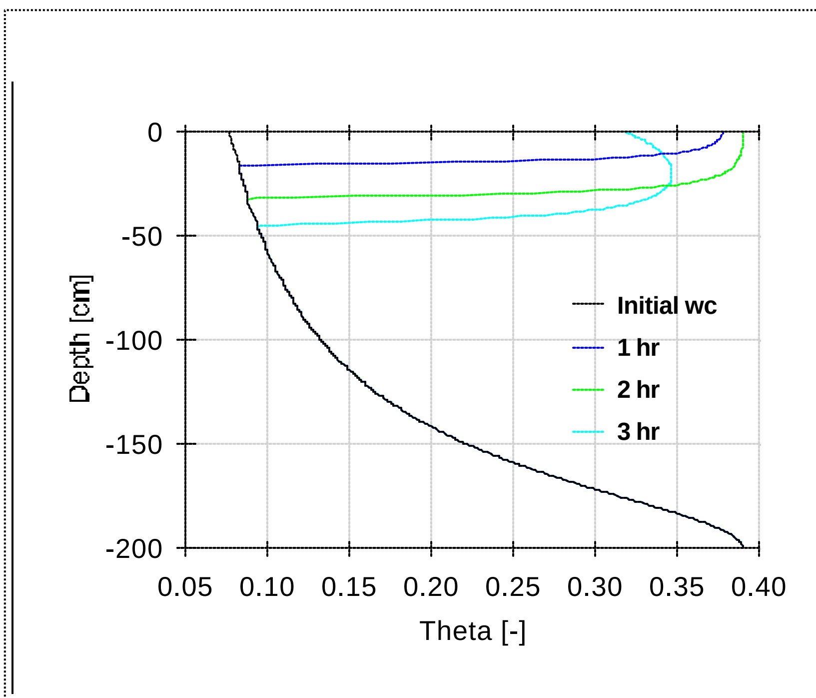

Figure 18. Static initial water content profile for a convective storm

The post-processing unit consists of simple x-y graphics for graphical presentation of the soil hydraulic properties, time changes of a particular variable at selected observation points in the profile, and actual or cumulative water fluxes across the upper and lower boundaries. Water content and pressure head profiles can be obtained. Examples of these profiles are shown in Figures 18 and 19 where variable rainfall rate was used. Figure 18 explains the redistribution process of water content in the soil for a storm that lasted about 3 hours. The soil depth for this example is 200 meters. Initial static water content was assumed for this simulation (black solid line). Notice that water redistributes in the soil during 2 and 3 hours. The water content profile for 3 hours has smaller water content at the surface and moved downward with time. This process takes place when there is no rainfall or when the rainfall is smaller than the saturated hydraulic conductivity.

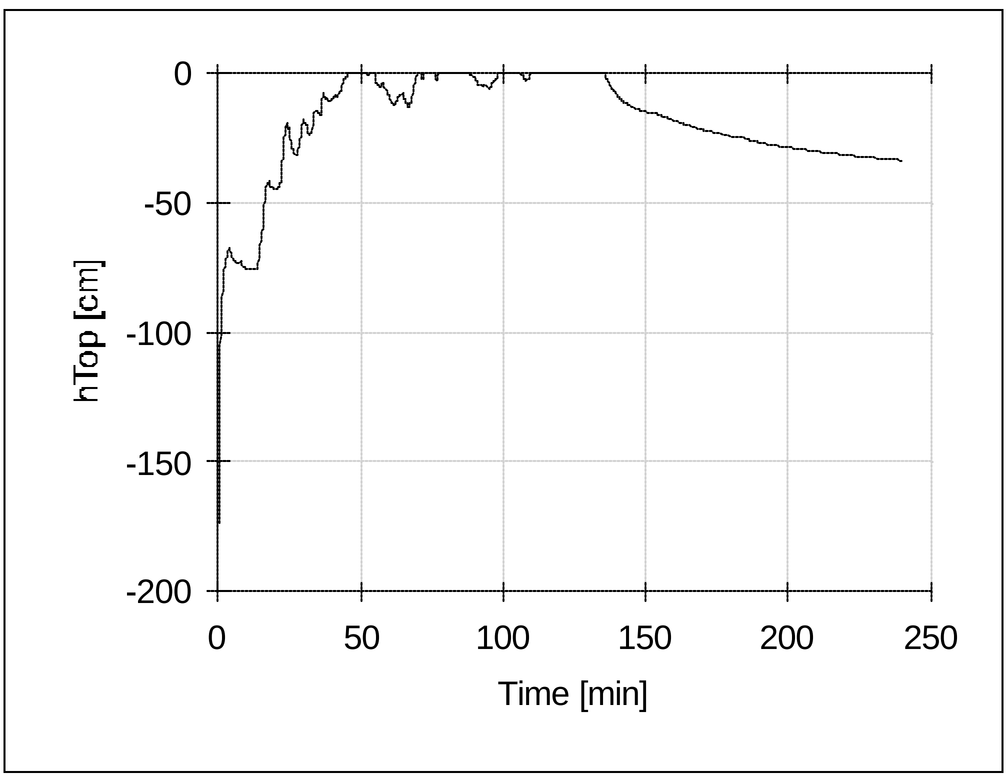

Figure 19. Pressure head at the surface for convective storm

Distribution of the pressure head with time for infiltration excess runoff can be explained in Figure 19. The simulation parameters for this graph are the same as in Figure 18. In this graph, when the pressure head is zero, saturation at the surface occurs. This might have been caused by a burst of high rainfall intensity, saturating the surface. Therefore, the infiltration rate decreases, water infiltrates into the soil, and pressure head decreases. When another burst of high intensity comes or when the soil saturates due to accumulation of water at the surface, the pressure head increases until zero value, which is saturation. After 140 minutes approximately, rainfall stops, water drains and pressure head decreases.

The profile module is conformed by the discretization of the flow domain in a graphical mode and specification of domain properties. It is an external module which may be used to discretize a one-dimensional soil profile into finite difference cells. The module also helps a user to specify the initial conditions in the pressure head and the water content, as well as the spatial distribution of other parameters characterizing the soil profile (e.g., spatial distribution of soil materials and root water uptake parameter) and/or observation nodes. All parameters in this module are specified in a graphical environment.

HYDRUS 1D solves numerically the Richards equation for variably saturated water flow in one dimension (Simunek and van Genuchten, 1998). The flow equation incorporates a sink term to account for water uptake by plant roots. Richards equation for one-dimensional vertical flow with one dependent variable is

$$\frac{\delta\theta(z,t)}{\delta t} = \frac{\delta}{\delta z}\left(K(\theta) \left(\frac{\delta h(\theta)}{\delta z} - 1\right)\right)$$

Where,

$\theta(z,t)$ is the water content of the soil (cm^3 of water/cm^3 of soil)

* $h(\theta)$ is the matric potential head
* z is the depth of the soil
* $K(\theta)$ is the unsaturated hydraulic conductivity.
* t is the time

The program considers prescribed head and flux boundaries, boundaries controlled by atmospheric conditions such as rate of application at the surface or evapotranspiration, and free and deep drainage boundary conditions assuming transient flow. It has three different models to calculate the hydraulic conductivity: van Genuchten (1980), Brooks and Corey (1964), and van Genuchten modified. Hysteresis in the soil hydraulic properties can be specified as well.

3.2. Impacts to Depth to the Water Table

To analyze the effect of depth to the water table on runoff and infiltration, the infiltration process was simulated utilizing HYDRUS 1D. The assumptions used for this simulation follow.

A convective storm selected from the actual rainfall record with 3.1-hour duration and total depth of 13.6 cm was used. The time resolution of the storm is 1-minute time step. This storm is a representative observed storm in this region. Soil properties of a representative soil in Florida (Mulat fine sand) obtained from the soil survey was used.

Initial static water content distribution was assumed. Van Genuchten (1980) parameters were applied to estimate the soil hydraulic properties. The residual water content for this soil was 0.02, saturated water content of 0.39, alpha parameter of 0.03 1/cm and *n* equal to 2.041 (n= 1/(1-m)). The upper boundary condition was variable rainfall rate at the surface, and the lower boundary condition was zero flux at the bottom.

Five simulations were made using different depth to the water table. They include 5, 2, 1, 0.5, and 0.1 meters below the ground surface. Time to ponding and time to start of saturation were calculated as well.

Table 5. Total runoff for different depths to the water table using HYDRUS 1D

Depth to the water table	*Time to ponding*	*Time to excess saturation*	*Total infiltration*	*Total runoff*
5 meters	45.13 min	--	10.7 cm	2.9 cm
2 meters	45.1 min	--	10.5 cm	3.1 cm
1 meter	44.4 min	--	9.96 cm	3.64 cm
50 centimeters	43 min	68.5 min	3.81 cm	9.79 cm
10 centimeters		2.8 min	0.052 cm	13.55 cm

The results show that when the depth to the water table increases, the total depth of infiltration increases and the total depth of runoff decreases (Figure 20). Thus, for shallow water table there was more runoff and less infiltration in the soil. This happens in shallow water table where the type of runoff dominating is excess saturation runoff. So the soil pores fill up quickly, and more rainfall becomes runoff. In contrast, for deep water table, the amount of water that infiltrate was greater, and there was less runoff. In these water table environments, infiltration excess runoff occurs. Therefore, the soil reaches ponding and infiltration occurs at a smaller rate than the rainfall rate. See Figure 20.

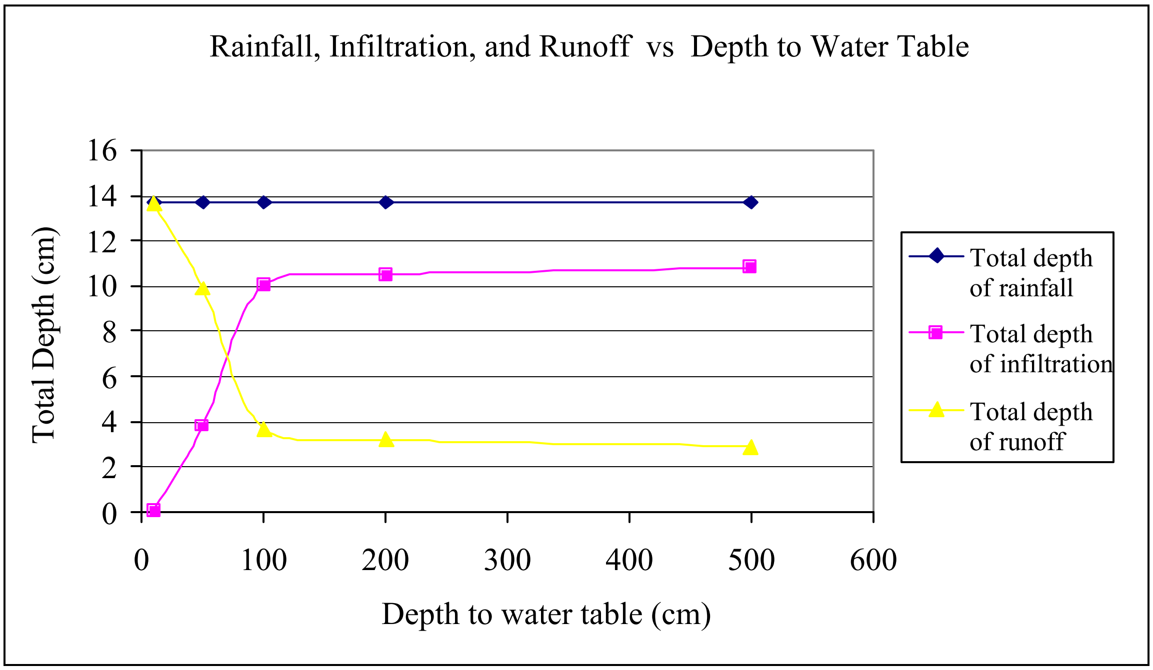

Figure 20. Rainfall, infiltration and runoff vs depth to water table

According to these simulations, some of the impacts of runoff as a result of convective or frontal type of rain are described below.

* Convective rainfall storms tend to have short bursts of high intensity especially at the beginning of the storm. As a result, in shallow water tables, this type of rain can cause the soil to reach the storage capacity of the soil faster thus potentially producing saturation excess runoff. For soils with deeper water table, runoff due to convective storms can only be produced by infiltration excess. When coarser

time resolution is used, the intensities are smoothed out, surface saturation takes longer, and runoff is underestimated.

* Frontal storms have longer periods of time usually with low rainfall intensities. Rainfall variability for these storms is small and does not significantly impact runoff response. Precipitation is more distributed and uniform over the duration of the storm. When the water table is shallow, a long duration storm might end up filling the storage capacity of the soil resulting in excess saturation runoff. The same can occur for deep water table levels, although it is not very common.

3.3. Impacts to Temporal Variability of Rainfall

Under natural conditions, the complex structure of rainfall exhibits a large degree of temporal variability. This variability substantially affects the downward water movement in the vadose zone. Many studies have shown that accuracy of hydrologic models can be improved by using finer time resolution of rainfall data in the determination of infiltration excess (Finnerty et al., 1997). Again, HYDRUS 1D, a model that simulates water movement in the soil, was used to model the process of infiltration and excess rainfall. HYDRUS 1D solves Richards equation in one dimension, assuming vertical downward water movement on a homogeneous soil.

To analyze the impacts of temporal variability of rainfall, a convective and a frontal storm were selected (See Figure 4 and Figure 5 for hyetographs of the storms). The frontal storm with duration of 12.75 hours was used in the numerical simulation with

HYDRUS 1D. Parameters utilized in the simulation included initial static water content distribution, boundary conditions at the surface accounted for variable rainfall rate, and no flux boundary condition was assumed at the water table, or lower boundary. Van Genuchten parameters were used to model the hydraulic properties of the soil. Three scenarios including 1m, 2m, and 5m depths to the water table were tested with simulations lasting 12.75 hours, the duration of the frontal storm.

The following table compares the runoff obtained from previous simulations using the convective storm shown in Figure 4 with the runoff obtained from the simulations of this frontal storm using 1-minute time steps. The total storm depth for the convective storm was 13.64 cm and for the frontal storm was 10.41 cm.

Table 6. Runoff for convective and frontal storm using HYDRUS 1D

Depth to the water table	*Total runoff Convective storm*	*Total runoff Frontal storm*	*% Runoff Convective*	*% Runoff Frontal*
5 meters	2.9	0.2	21.3	1.9
2 meters	3.1	0.2	22.7	1.9
1 meter	3.64	0.3	26.7	2.9

The percentage of runoff was obtained by dividing the total runoff by the total depth of rain for each storm. From the table, the percentage of runoff depth to total storm depth generated from convective storms was much greater than the runoff percentage of frontal storms. This can be explained by the high intensities during the convective storm. Furthermore, when the water table is deeper, there is no percentage difference in runoff for frontal storms (5 and 2 meters with % runoff equal to 1.9). Results indicated that convective storms generate more runoff than frontal storms, and the runoff response is more sensitive to temporal variability of rainfall. Appendix E contains the Hydrus 1D graphs for the convective and frontal simulations with depth to the water table of 5 m, 2 m, and 1 m.

The temporal variability of rainfall, especially for convective storms, cannot be captured if coarser time resolution (e.g. hourly rainfall) is used. Runoff response for simulations of 6 aggregated convective rainfall hyetographs are shown on Table 7. The hyetographs are depicted in Figures 9 to 15. HYDRUS 1D simulations also included four depths to the water table: 0.5, 1, 2, and 5 meters. For Hortonian type of runoff, the time resolution greatly affects runoff response. The error in runoff depth increases when the time resolution increases. For example, for 5 meters depth to the water table, the error in runoff depth is 65.5% using 60-min time steps. In contrast, for a time resolution of 5 minutes, the error is only 6.9%. The next section discusses in more detail how this error also increases when the depth to the water table increases.

In Table 7, for a time resolution of 30 minutes, the error in runoff with a depth to the water table of 1 meter is 36.8% whereas for 5 meters the error is 51.7%. Notice that there are no runoff depth errors for the simulation using shallow soil depths of 0.5 meters. For shallow soil depths, infiltration-runoff modeling is not sensitive to the time resolution of rainfall data because runoff is generated by saturation excess and not by infiltration excess.

Table 7. Error in runoff depth for different time steps

Time (min)	*INFILTRATION DEPTH (centimeters)*			
	5 meters	*2 meters*	*1 meter*	*50 centimeters*
1	10.7	10.5	9.96	3.81
3	10.8	10.6	10.1	3.81
5	10.9	10.6	10.1	3.81
10	11.2	11.0	10.5	3.81
15	11.3	11.1	10.5	3.81
30	12.2	11.9	11.3	3.81
60	12.6	12.4	12.0	3.81

Time (min)	*RUNOFF DEPTH (centimeters)*			
	5 meters	*2 meters*	*1 meter*	*50 centimeters*
1	2.9	3.1	3.64	9.79
3	2.8	3.0	3.5	9.79
5	2.7	3.0	3.5	9.79
10	2.4	2.6	3.1	9.79
15	2.3	2.5	3.1	9.79
30	1.4	1.7	2.3	9.79
60	1.0	1.2	1.6	9.79

Time (min)	*ERROR IN RUNOFF DEPTH (%)*			
	5 meters	*2 meters*	*1 meter*	*50 centimeters*
1	0.0	0.0	0.0	0.0
3	3.4	3.2	3.8	0.0
5	6.9	3.2	3.8	0.0
10	17.2	16.1	14.8	0.0
15	20.7	19.4	14.8	0.0
30	51.7	45.2	36.8	0.0
60	65.5	61.3	56.0	0.0

It can be concluded that for fine sand soils with deep water table levels, where Hortonian runoff dominates, the time resolution suitable for infiltration-runoff modeling seems to be less than 15 minutes. However, the rainfall time step used should be 5 minutes or less leading to errors of around 10%. Figure 21 depicts the percentage of error in runoff depth estimated by the model against time resolution of the rainfall data. The curves for three different water table depths are shown. These curves are very close which confirms that depth to the water table is not significant when Hortonian runoff is the dominant runoff process. From this graph, the error in runoff estimated increases when time resolution of rainfall increases.

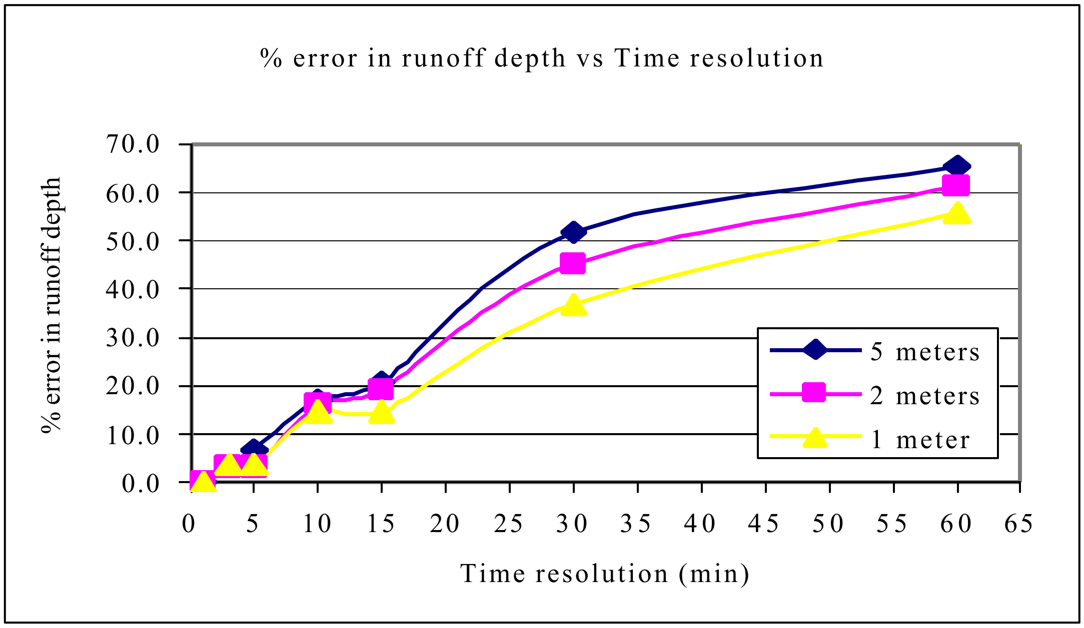

Figure 21. Percentage error in runoff depth against time resolution of rainfall

Lastly, in hydrologic modeling, high rainfall intensities generated especially by convective storms are smoothed when using large time resolution rainfall data. In consequence, runoff is underestimated. Results show that, where Hortonian runoff is dominant, infiltration and runoff are very sensitive to time resolution. For finer time resolution of rainfall, runoff generated by the model increased.

CHAPTER 4. DIGITAL ELEVATION MODELS (DEM)

Digital Elevation Models or DEMs are digital records of terrain elevations in a raster form for ground positions at regularly spaced horizontal intervals. DEMs produce accurate topographic maps and surface models with grids and contours. They are used in a number of applications in the earth, environmental and engineering sciences, and have proved to be an important method for modeling and analysis of spatial-topographic information. There are many application domains where DEMs are utilized. Some of these applications include civil engineering, earth sciences analysis, planning and resource management, surveying and photogrammetry, global topography data, and military applications.

The use of DEMs to extract the geomorphologic attributes of the terrain to develop parameters for hydrologic models has not being widely used. DEMs with both high horizontal and vertical resolution are required to detect and measure critical geomorphic features, such as hillslope angles, slopes, stream channels, etc. The DEMs used here are derived from United States Geological Survey (USGS). The U.S. Geological Survey produces three primary types of digital elevation model data for the United States. They are:

* 7.5-minute DEM data are produced in 7.5-minute units, which correspond to 1:24,000 and 1:25,000 scale topographic quadrangle map series for all of the United States and its territories. 7.5-minute DEM data consist of a regular array of elevations referenced horizontally on the Universal Transverse Mercator (UTM) coordinate system of the North American Datum of 1927 (NAD 27). These data are stored as profiles with 30-meter spacing along and between each profile. The vertical accuracy of 7.5-minute DEMs is equal to or better than 15 meters.

* 30-minute (2 Arcsecond) DEM data which correspond to the east half or west half of the USGS 30- by 60-minute topographic quadrangle map series for the conterminous United States and Hawaii. It covers 30-minute by 30-minute areas where each 30-minute unit is produced and distributed as four 15- by 15-minute cells representing one half of a 1:100,000-scale map. 30-minute DEM data have the same characteristics as the 15-minute DEM data (available for Alaska) except that the spacing of elevations along and between each profile is 2 arc seconds.

* 1-degree DEM data are produced by the Defense Mapping Agency in 1-degree by 1-degree units, which correspond to the east half or west half of USGS 1- by 2-degree topographic quadrangle maps series, for all the United States and its territories. 1-degree DEM data consist of a regular array of elevations referenced horizontally using the geographic (latitude/longitude) coordinate system of the World Geodetic System 1972 Datum. Spacing of the elevations along and between each profile are 3 arc seconds (approximately 90 meters) with 1,201

elevations per profile. The 1-degree DEMs are also referred to as 3-arc-second or 1:250,000 scale DEM data.

The accuracy of a DEM is dependent upon the level of detail of the source and the spatial resolution, that is the grid spacing used to sample that source. The primary limiting factor for the level of detail of the source is the scale of the source materials. The proper selection of grid spacing determines the level of content that may be extracted from a given source during digitization. The source material for 7.5 minute DEM are 5 feet contour quadrangle maps. This vertical scale is not appropriate to capture the topographic details needed at the hillslope scale. Therefore, aerial photography with 1-foot contours of the area studied here was used to create the DEM. To accurately describe topographic characteristics at the hillslope scale, DEMs with good spatial resolution are needed.

4.1. DEM Data

DEMs have proved useful in different areas. Therefore, they are used in this work to develop actual geomorphologic parameters for hydrologic modeling including slope, curvature, landscape convergence, and other topographic attributes. The study area is located Southeast of Tampa at a proposed reservoir site in Hillsborough County, Florida. Doe Creek, one of the tributaries of the Alafia River basin crosses the study area. Currently, there are no USGS DEMs for the Alafia River basin with a vertical resolution better than 7.5 minute. Hence, a DEM was created for this area.

The Digital Elevation Model was built using a 1-foot aerial photography map from the Southwest Florida Water Management District. DEMs based on 1-foot contours in South Florida can be found for small areas. Usually, they are 30 meters horizontal resolution. The aerial sheet number corresponds to section 2, township 31 S, and range 21 E with a scale of 1" = 200'. The 1-foot contours for this map were digitized using AutoCAD and imported into Arcview to create the grid file needed for River Tools. The AutoCAD drawing included contour lines, elevation points, and breaklines or lines that represent a sharp break in slope. This drawing was imported into Arview GIS to create the grid file. A Triangular Irregular Network (TIN) was created to represent the surface of the map. A TIN partitions a surface into a set of small, contiguous, non-overlapping triangles. An elevation value is recorded for each triangle node. Elevations between triangles can also be interpolated.

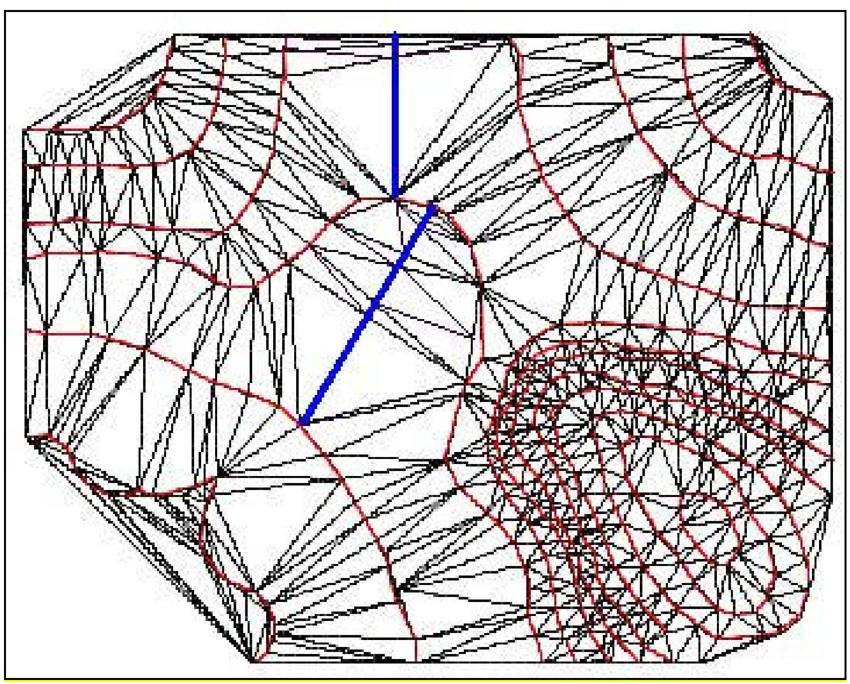

Figure 22. TIN and contour lines

Figure 22 depicts a surface built using the TIN method. The red lines are the contours and the blue lines are breaklines. The last ones were added to improve accuracy when the TIN was being created, so the triangles were not interpolated within the same contour lines as if it were a flat area. The grid for the map was then produced using the TIN and specifying the cell size. 5 meters by 5 meters cells were used for the grid. Data files containing the grid were imported into River Tools to visualize and analyze the domain. The AutoCAD drawing with 1-foot contour lines is displayed in Figure 23. Breaklines and elevation points are also shown. The colors in the figure indicate different elevations. Light pink represents the uplands or higher elevations and dark red represents lower elevations (streams).

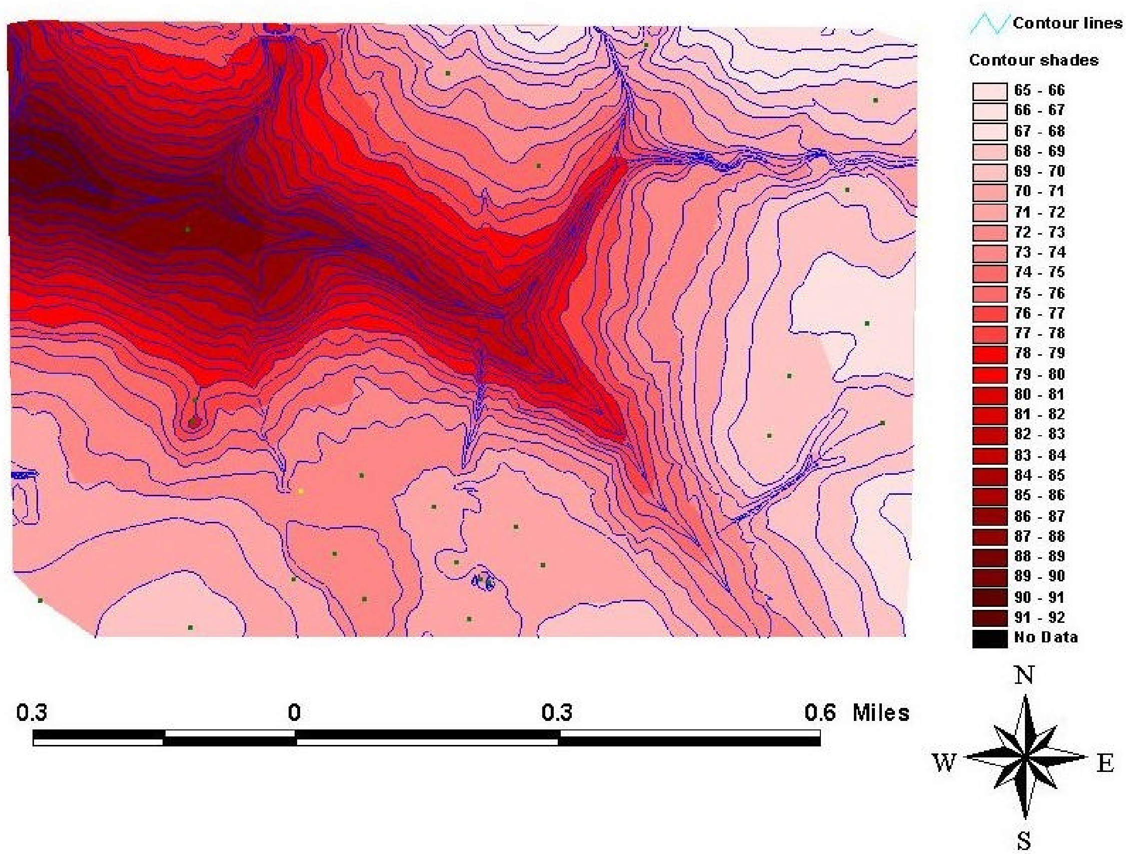

Figure 23. 1-foot contour map for Lithia near the Tampa Bay Regional Reservoir

4.2. River Tools 2.0

RiverTools 2.0 (Research Systems, 1999), an application for DEMs and river network analysis is used to import, display, analyze, and extract information from DEMs data. RiverTools uses an Interactive Data Language for data analysis and visualization that runs on Windows. Shaded relief graphs of the DEMs can be displayed by RiverTools as raster images where every pixel in a DEM is assigned a color that depends on its elevation and brightness. Other information such as profiles and corresponding flow paths, stream order, contributing area to the stream, basin delineation, slope and curvature, flow distance, etc., can be extracted from RiverTools.

River Tools allows you to import and prepare the input data from different sources. Information such as measurements can be extracted from the input data. Flow grid and river network can be extracted to display and analyze flow paths. Visualization of the DEM and display of the spatial properties of the objects contained in the DEM are some of the main tools of this program. Shaded relief of the study areas can be displayed a long with profiles, flow paths, and river channel properties. Statistical analysis of the many measurements is also available. Elevation values are typically gridded in one of two pixel geometries, fixed-length or fixed-angle. In the first way, the x-size and y-size of each grid cell or pixel has some fixed length. For example, the pixels for the DEM used in this work measure 5 meters on a side. In the second way, the x-size and y-size of each grid cell or pixel has a fixed, angular measure. For example, the pixels in a USGS 1-Degree DEM measure 3 arcseconds on a side. A shaded relief of the DEM used in this study is shown in Figure 24.

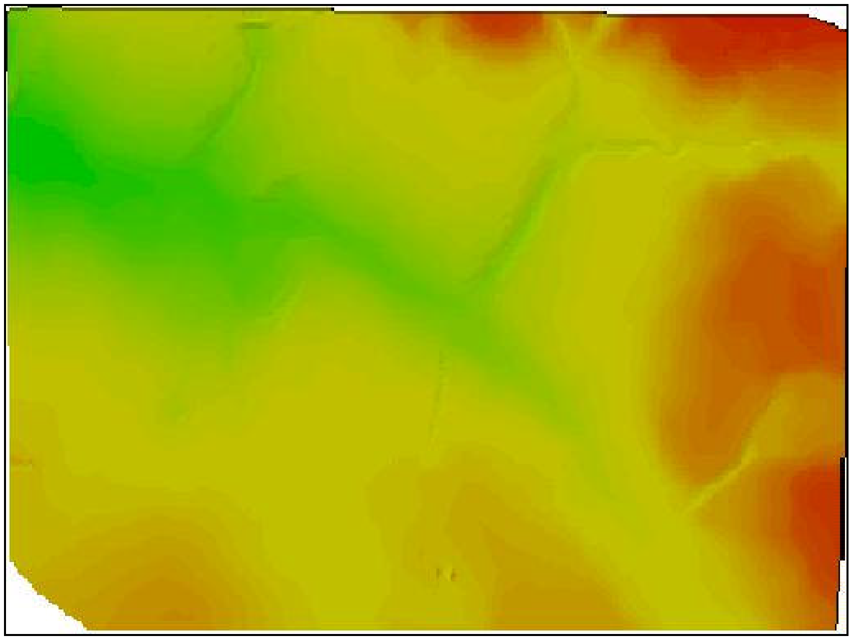

Figure 24. Shaded relief of the DEM at Doe Creek near a proposed Reservoir

Flow grid was extracted from the DEM study in this work. Upstream areas, downstream slope, and downstream curvature were pulled out from the grid. These features are necessary to display the line profiles, flow paths, and reach information so geomorphologic characteristics like slope, curvature, and divergence can be obtained.

The coupling of a Digital Elevation Model with a variable saturated model has not been done before and it has several advantages. Topographic features like slope, curvature, convergence, and divergence can be specified more accurately. Flow paths and their respective profiles can be easily obtained. These geomorphologic features of the terrain are very important in the extent of variable saturated areas near streams and need to be study in more detail. At the small scale–hillslope scale-, coupling DEMs with rainfall-runoff models takes into account the variations of saturated areas due to changes in geomorphologic and hydrologic features.

CHAPTER 5. SATURATION EXCESS RUNOFF

Saturation excess runoff occurs when soil saturation from below causes runoff at the surface. During this process, water infiltrates in the soil and fills the water storage capacity of the soil. Then, the soil gets saturated and all rainfall runs off. This scenario occurs especially in soils with high initial water content, shallow water table, or by accumulated volume of infiltrated water during a storm. If saturation excess occurs, the runoff rate is equal to the rainfall rate (Maidment, 1993).

Topographic features such as slope, curvature, and degree of convergence have an impact on the extent of variable saturated areas that form by saturation excess mechanisms. Most research at the hillslope scale use hypothetical values, and sometimes non-realistic values, to represent the hillslope properties needed. In order to capture the topographic variations of Florida environments, digital terrain data should be used. To analysis the conditions explained above, River Tools, a Digital Elevation Model (Research Systems, 1999), is coupled with HYDRUS 2D, a two dimensional variable saturated-unsaturated model that simulates water flow in variably saturated soils. River Tools provides analysis of geomorphologic characteristics of the region such as slope, concave and convex curvature, convergence, and divergence. After extracting these landscape attributes from DEMs, they are incorporated into HYDRUS 2D to describe the upper boundary of physical domain. Sensitivity analysis is done on landscape and hydrologic parameters. Actual rainfall data was used in the simulations as well with the purpose of looking at the impacts due to temporal variability of rainfall.

5.1. HYDRUS 2D Model

HYDRUS 2D is an interactive graphics-based user interface that runs in Windows and executes HYDRUS2, which is the Fortran code. It includes SWMS_2D which is a two-dimensional finite element model used for the analysis of water flow and solute transport in variable saturated porous media. The model has the same features of Hydrus 1D plus a mesh generator for unstructured finite element grids, MESHGEN_2D, which has the capability of simulating flow on irregular boundaries. HYDRUS 2D was developed by U.S. Salinity Laboratory, U.S. Department of Agriculture, Agriculture Research Service (Simunek and van Genuchten, 1999).

In HYDRUS 2D, flow and transport can occur in the horizontal plane, vertical plane, or axisymmetrical vertical region (a three-dimensional region exhibiting radial symmetry about the vertical axis). The finite element variable saturated flow model used in this work solves the Richard's equation in two dimensions shown below

$$\frac{\delta\theta(t)}{\delta t} = \frac{\delta}{\delta z}\left(K(\theta)\left(\frac{\delta h(\theta)}{\delta z} - 1\right)\right) - \frac{\delta}{\delta x}\left(K(\theta)\left(\frac{\delta h(\theta)}{\delta}\right)\right)$$

Where $\theta(t)$ is the water content of the soil (cm^3 of water/cm^3 of soil), $h(\theta)$ is the matric potential head, z is the depth of the soil, x is the distance from the stream, $K(\theta)$ is the unsaturated hydraulic conductivity, and t is the time.

A vertical plane was used for most of the simulation except for runs involving convergence and divergence. Analysis of convergence was achieved by using axisymmetrical vertical flow. Several boundary conditions can be described with HYDRUS 2D including prescribed and variable pressure head, prescribed and variable flux, no flux, free drainage, seepage and atmospheric conditions. A combination of polylines, arcs, circles, and splines define the specifications of the flow region. Domain geometry as well as initial conditions can also be imported from files (Simunek and van Genuchten, 1999).

Some of the applications of HYDRUS 2D include irrigation management, seasonal simulation of water flow and plant response, deep percolation, seepage in highway design, lake basin recharge, groundwater aquifer and stream interaction, and environmental impacts of drawdown of shallow water tables.

Input preparation for HYDRUS 2D includes soil hydraulic parameters, initial and boundary conditions, and mesh generation. The code allows users to select three types of models to describe the soil hydraulic properties: van Genuchten, Brooks and Corey, and modified van Genuchten type equations. In this study, soil properties are chosen from the Characterization Data for Selected Florida Soil (Carlisle et al., 1989) and van Genuchten parameters are fitted. Boundary conditions at the surface were defined as "atmospheric boundary" to simulate rainfall falling uniformly over the domain during rainfall, and "seepage face" to allow water to go out of the domain surface as saturation excess after rainfall stops. At the stream, the boundary condition was constant pressure head equal to the level of the water table at the stream. All other boundaries were no flow boundaries. Initial conditions were specified pressure head corresponding to an equilibrium profile. Initial water table depth for the reference simulation was sloping. The water table was assumed curved down to the stream and was almost parallel to the ground surface.

5.2. Reference Simulation

A reference simulation designed with field data was used as the starting point for all simulations and from which the parameters were changed one at a time to analyze their sensitivity. The reference hillslope topography was taken from a DEM created from a 1-foot aerial photography map of Southwest Florida Water Management District. The Digital Elevation Model from Lithia, at Doe Creek is located in the southeastern portion of Hillsborough County, Florida. The reference simulation consisted of a small stream on Doe Creek with an average hillslope of 1.1 %. The ground surface was a mix slope conformed by a concave downslope with a convex upslope. Several profiles were taken from the DEM on that specific site, and one with an average slope and overland flow plane was chosen. The hillslope profile had an overland flow plane of 387 meters (1271 ft). The stage at the stream was 0.6096 meters (2 ft). Incision depth in the stream was 1.07 m (3.5 ft), and the depth of the soil from the streambed was 2.1336 meters (7 ft).

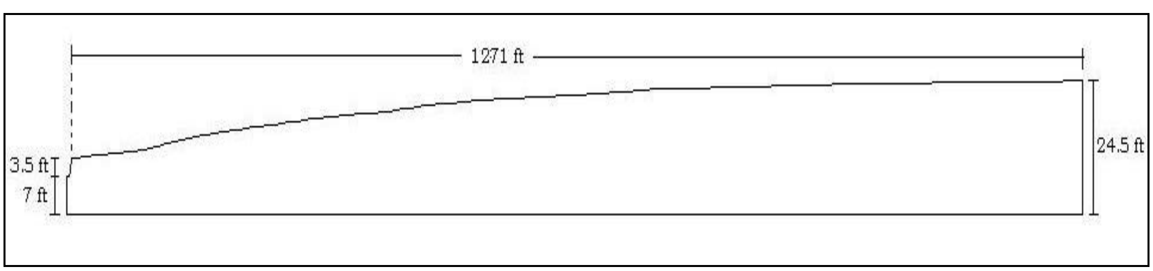

Figure 25. Reference simulation profile at the reservoir site, Doe Creek

Figure 25 shows the profile used for the reference simulation with the domain measurements. This profile is vertically exaggerated for better view and it is not to actual scale.

The actual stream was intermittent and the regular depth of the water level at the stream varied around 2 feet or more during summer. Initial water table depth on the profile was not flat. It curved down to the stream stage, which was 2 ft, and follows a path almost parallel to the ground surface as illustrated in Figure 26. The colors in Figure 26 represent the pressure head distribution in the profiles for the initial conditions. Notice that the line at which the pressure head is zero (line inside profile) corresponds to the water table level.

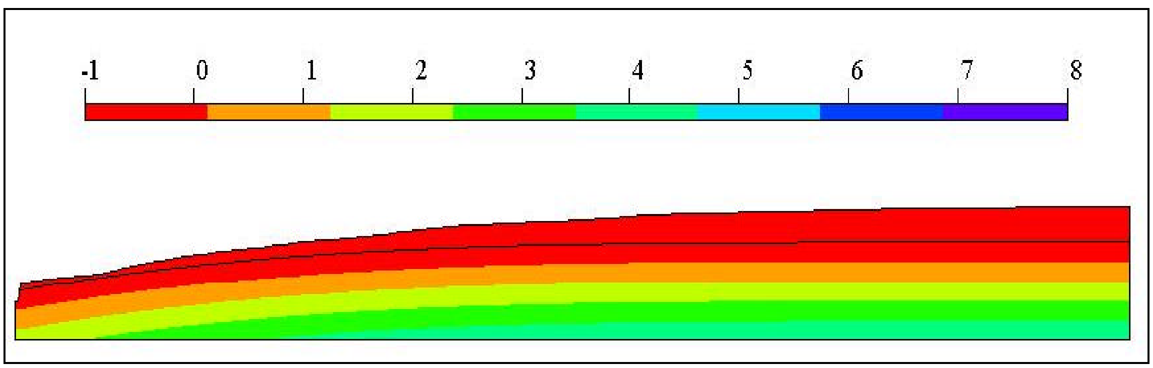

Figure 26. Initial water table level for the cross section

A van Genuchten (1980) soil hydraulic model was utilized with a Myakka fine sand (layer 3) soil type, predominant at the reservoir site (Carlisle, 1989). This hydraulic model was used because it explained the total water retention curve, including water retention characteristic at the air entry pressure. Myakka fine sand soil parameters were obtained from the Characterization Data for Selected Florida Soils, Soil Survey (1989). These parameters included a saturated hydraulic conductivity of 0.128 m/hr. The van

Genuchten parameters alpha (α) and n ($n = 1/ (1-m)$) were fitted to the actual water retention curve of Myakka fine sand to use these parameters in the model. Appendix D shows a copy of these parameters obtained from the Soil Survey. Figure 27 depicts the Myakka fine sand water retention curve and the fitted van Genuchten curve. The saturated water content was 0.479 and the residual water content was 0.020. The van Genuchten curve was fitted using a spreadsheet, and alpha (α) was found equal to 0.105, m equal to 0.205, and n equal to 1.26.

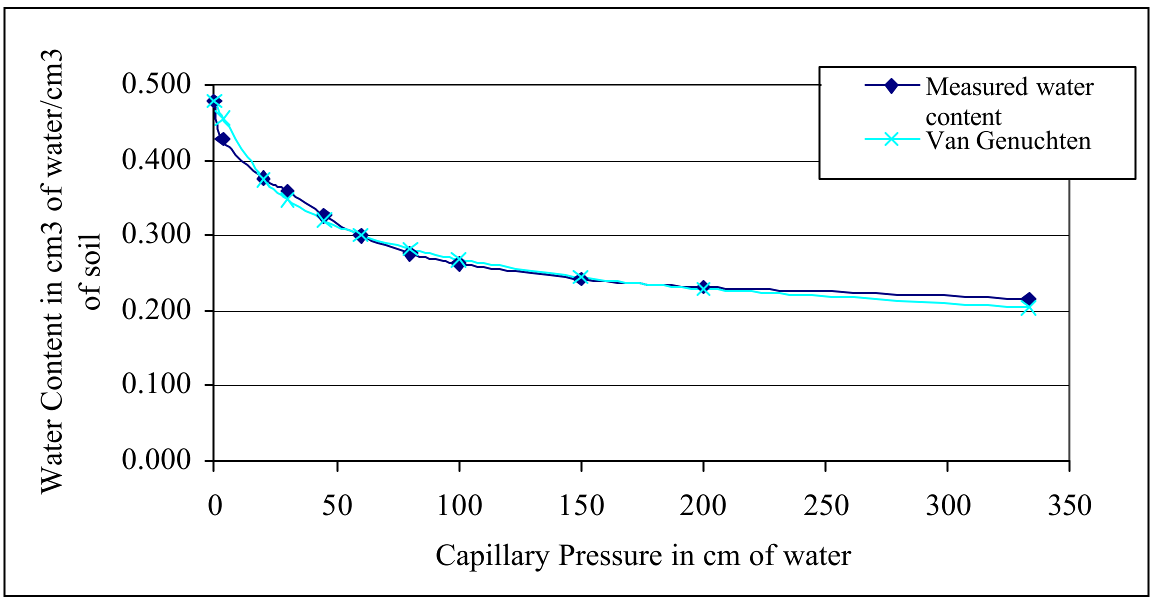

Figure 27. Van Genuchten fitted water retention curve

For comparison, the water retention curve calculated by HYDRUS 2D using the van Genuchten soil hydraulic model for the fitted parameters is illustrated in Figure 28. The water retention characteristic curve describes the ability of the soil to release and store water. It is defined as the relationship between water content and matric potential (Maidment, 1993). Notice that this type of fine sand does not have a capillary fringe or it is very small, which means that the water drains quickly in the soil. For the simulations, homogeneous soil with vertical flow was assumed. Hysteresis was not taken into account.

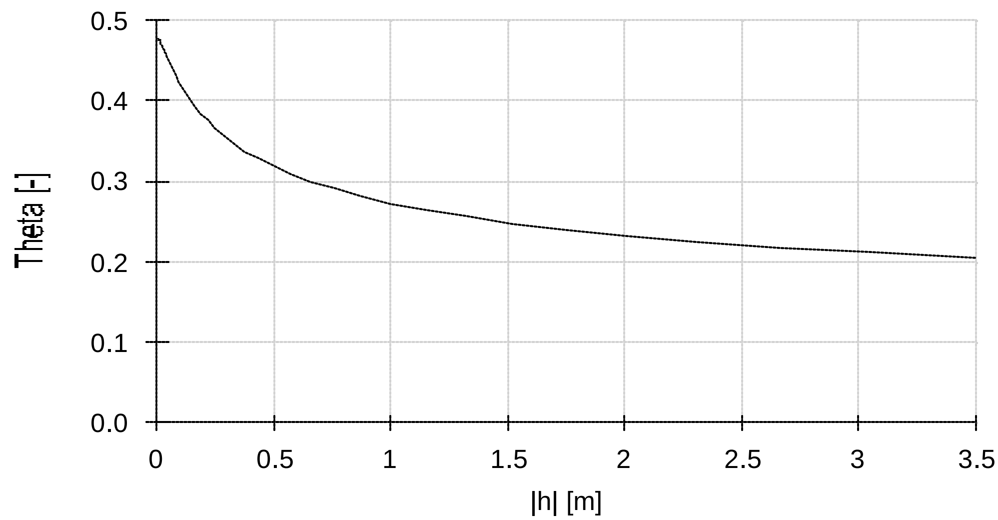

Figure 28. Water content vs head obtained by HYDRUS 2D

The rainfall rate was constant for 2.25 hours with an intensity of 0.013 m/hr. Rainfall intensity and duration were obtained from actual rainfall data taken from the roof of the Engineering Building at the University of South Florida. The analysis was based on convective storms since most of the rainfall in Florida is owing to convective activity. The mean duration for convective storms was 1.16 hours and the mean rainfall depth was 0.51 inches. Small storms created by the rainfall model with total depth less than 0.1 inches were ignored. The standard deviation for storm duration was 1.09 hours and for rainfall depth was 0.64 inches. The standard deviation was added to the mean depth and duration to increase the total rainfall depth and produce some runoff. As a result, the average rainfall depth and duration (mean plus standard deviation) used in this work were

1.15 inches and 2.25 hours respectively. The rainfall rate was considerably small compared to the saturated hydraulic conductivity, thus Hortonian runoff did not occur.

HYDRUS 2D is a finite element model that has the ability to generate a mesh of irregular elements improving discretization for the domain. The model was discretized into a finite element mesh of irregular elements, where boundary conditions, initial conditions, and parameter values discussed previously were assigned. The resolution of the mesh closer to the stream was finer to better approximate the fluxes moving across this area, to capture the irregularities of the ground surface, and to have a more accurate solution (See Figure 29). The mesh was generated using the automatic features of the model. For the reference simulation, the mesh had a total of 3427 mesh points with 6553 mesh triangles, which were created of irregular sizes and shapes.

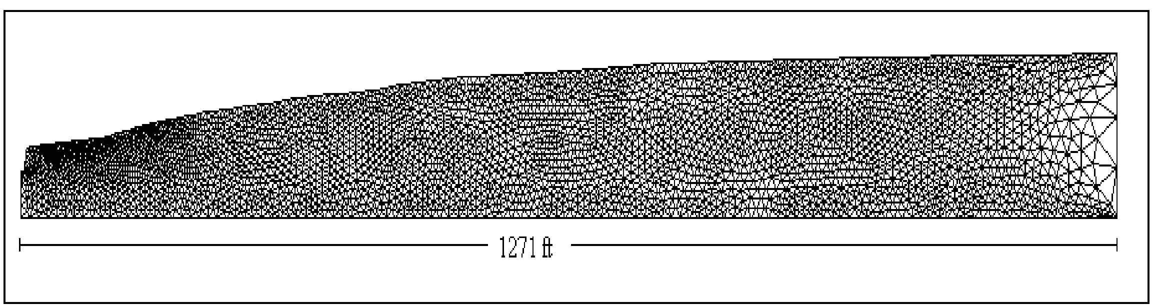

Figure 29. 2-D mesh for cross section at the reservoir site

Boundary conditions on the domain included no flow boundary condition at the bottom of the profile and on the sides of the domain. The left side corresponds to the boundary below the streambed and the right side corresponds to the water divide at the upslope. Therefore the assumption of no flow at these boundaries is applicable. At the stream or water surface, constant pressure head boundary condition was applied with linear distribution in the pressure head. Along the land surface, atmospheric boundary conditions were used during rainfall. Atmospheric boundary conditions account for precipitation, evaporation, transpiration, and drainage fluxes. These fluxes are assumed uniformly distributed along the domain. In this analysis, precipitation was the only flux considered. After rainfall stops, seepage boundary condition at the ground surface was used. Under this condition, water is allowed to exfiltrate (leave) the domain at the surface and run off towards the stream. Figure 30 illustrates the boundary conditions used during rainfall. When saturation at the surface was reached, HYDRUS 2D changed the boundary conditions at the surface domain to prescribed pressure head equal to zero.

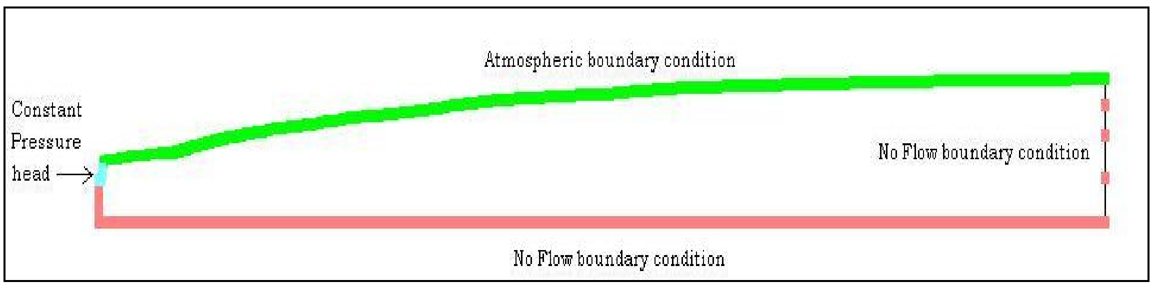

Figure 30. Boundary conditions for the cross section domain

The simulations were divided into two runs. The first run was during the rainfall period with atmospheric boundary conditions at the surface. The second run used the output of the first run as the initial conditions in the pressure head and had a seepage face surface boundary condition, so water came out of the domain as saturation excess proceeded.

HYDRUS 2D graphs including the potential atmospheric, actual atmospheric, subsurface, and seepage fluxes were utilized for the sensitivity analysis. Since runoff can be produced by saturation excess runoff or subsurface storm runoff, different graphs were used to estimate these fluxes. Saturation excess runoff was calculated on the first run of the simulations as the difference between the potential and actual atmospheric fluxes (total rainfall minus infiltration). The subsurface graphs were used to calculate the lateral subsurface flux going to the stream. The seepage graphs helped in calculating the amount of water going into the stream as saturation excess after the storm stops on the second run of the simulations. The 2-dimensional profiles displayed by HYDRUS 2D were used to estimate the extent and shrinkage of variable saturated areas, as well as the water table position with time. HYDRUS 2D graphs for the reference simulation are illustrated in Appendix F. These graphics include subsurface and seepage fluxes during and after rainfall. Extent of VSA is also shown in this appendix.

After defining the reference simulation, some hydrologic properties and geomorphologic features were tested to analyze their sensitivity to saturation excess runoff. Following are the parameters that were modified here and their ranges of variation.

5.3. Hydrologic Characteristics

Hydrologic characteristics that can impact the extent of variable saturated areas are soil parameters, rainfall variability, and initial water table depth. A sensitivity analysis was performed in order to define the effects in VSA as a result of a change in these characteristics.

* Soil parameters: Several types of soil were used: Myakka fine sand, Mulat fine sand, and Millhopper fine sand were taken from the Characterization Data for Selected Florida Soils, Soil Survey (Carlisle, 1989). Other soils used were sand, sandy loam, and loamy sand taken from the HYDRUS 2D soil catalog for the USDA texture soil classification. Saturated hydraulic conductivity, Ks, ranged from 0.044 m/hr to 0.297 m/hr. The van Genuchten parameters ? (alpha) and *n*, along with Ks were varied. Water retention curves with fitted van Genuchten parameters for actual soil data including Myakka fine sand, Mulat fine sand, and Millhopper fine sand can be found in Appendix G.

* Rainfall rate: Constant rainfall rate and variable rainfall rate obtained from actual rainfall records were used in the simulations. Rainfall rate was less than the saturated hydraulic conductivity in order to avoid infiltration excess runoff. A series of storms, three convective and two frontal, were used in the model. The hyetographs for these storms are added to the Appendix H.

* Initial conditions for the water table: Wet and dry soils given by the depth to the water table level were sampled. For these simulations, the initial water table was assumed flat. Dry soils started with a dry stream whereas wet soils were assumed to be fully saturated with the water table at the ground surface on the downslope profile. Shallow water table depths ranging from 1 foot above the streambed to 4 feet above the streambed were analyzed to account for dry and wet season respectively. Appendix I contains the profiles for these water table depths.

5.4. Geomorphologic Characteristics

Natural topography extracted from Digital Elevation Models was coupled with the variable saturated model, HYDRUS 2D, to address the changes in the extent of variable saturated areas due to geomorphologic features including slope, curvature, and divergence. The topographic features analyzed here included flat and steep slopes, convex and concave curvature, and landscape divergence. Flat initial water table at 3.5 feet above the streambed was assumed throughout these simulations. Some of the simulations used average values of curvature in order to see the response when small changes were applied.

* Straight slope: refers to flat and steep slopes with zero curvature. Profiles taken from DEMs showed that hillslopes slopes are less that 2.5% average. Therefore, straight slopes were changed from 0.5% to 2.5%. Figure 31 illustrates the three slopes utilized.

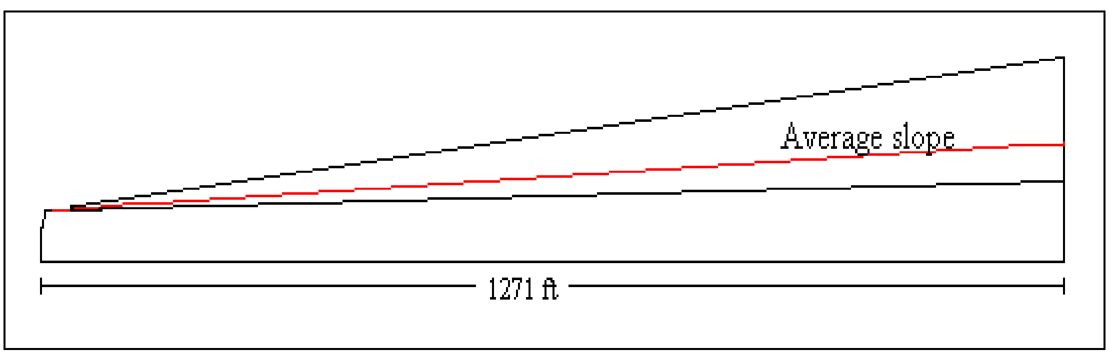

Figure 31. Profile for 0.5%, 1.1%, and 2.5% slopes

* Curvature: refers to the degree of curvature of the ground surface boundary. Curvature can be positive or negative for convex and concave profiles,

respectively. The following graphs show the three different radii evaluated for each curvature (Figure 32 and Figure 33).

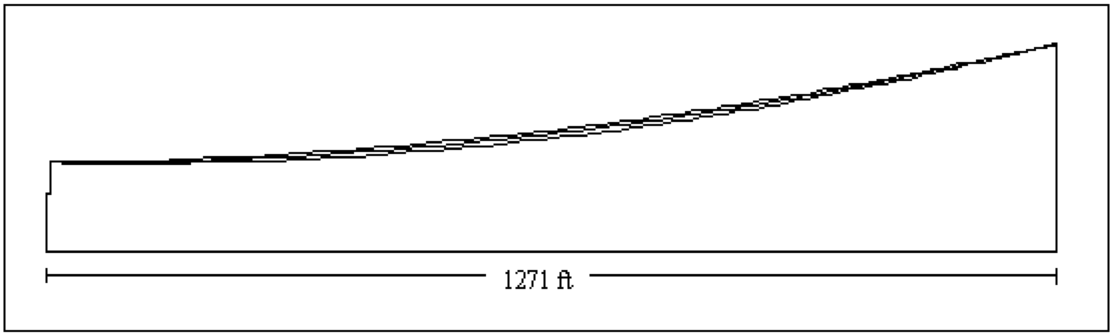

Figure 32. Concave profiles for three negative radius of curvature

The degree of curvature is attained by the radius of curvature. Slightly changes in the radius of curvature for concave slopes were enough to demonstrate its impact in runoff generation. The radii for concave slopes were 14871.1 m, 17148.7 m, and 19474 m. The radiuses for convex slopes were 35349.4 m, 15928.8 m, and 11779.1 m.

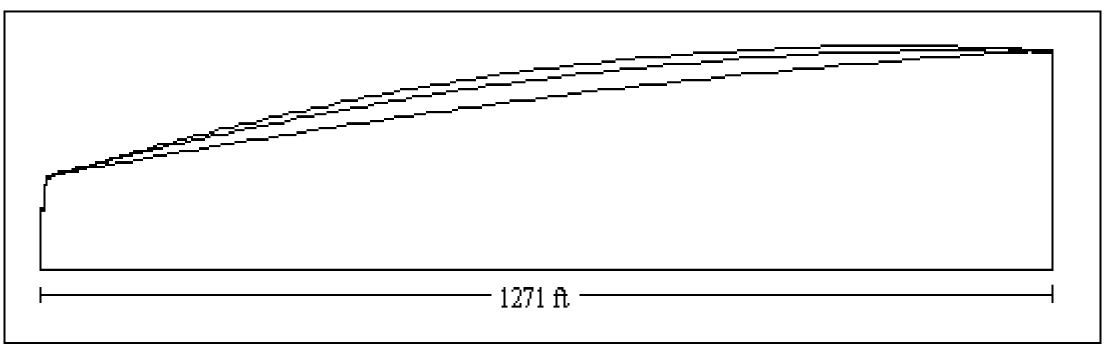

Figure 33. Convex profiles for three negative radius of curvature

* Landscape divergence is described by the ratio of downslope width to upslope width using the axisymmetrical vertical flow option in HYDRUS 2D. Flow through divergent hillslopes was simulated as radial flow going away from the symmetric axis with the axisymmetrical axes coinciding with the left side of the

domain. For these simulations, the domain was reverted to have the stream at the right side. A discharge area with divergent flow is shown in Figure 34.

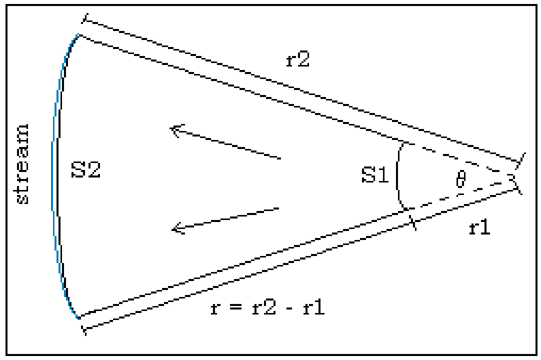

Figure 34. Divergence parameter for HYDRUS 2D

From Figure 34, assuming concentric radius we have

$$r_1\theta = S_1 \quad r_2\theta = S_2 \quad r_1 = \frac{S_1}{S_2} r_2$$

Where r_2 is the radius from the center to the stream, r_1 is the radius from the center to the water divide of the profile, S_2 is the length of the stream (arc length), and S_1 is the length of the water divide. The degree of convergence and divergence is defined as the ratio of r_2/r_1 or S_2/S_1. If this ratio is greater than one, the flow in the discharge area diverges. On the other hand, if the ratio is smaller than one, the flow in the discharge area converges.

5.5. Simulation Results

Different types of soils predominant in the area were used. Figure 35 displays the water retention curve obtained from actual data for the soils used in these simulations. Notice that even for fine sand, the water retention curve differs significantly (Myakka fine sand vs Mulat fine sand). Table 8 shows the extent of VSA and values of the fluxes when soil parameters n, θ, and Ks were changed. All fluxes were compared with the reference simulation for Myakka fine sand (layer 3). From these simulations subsurface runoff and saturation excess were seen to be very sensitive to the van Genuchten paramete n and the saturated hydraulic conductivity, Ks. For the same type of soil, when n increased, saturation excess decreased. In this case, subsurface storm flow also decreased but it was not very significant. On the other hand, when the saturated hydraulic conductivity increased, subsurface storm flow increased considerably whereas saturation excess runoff was not affected.

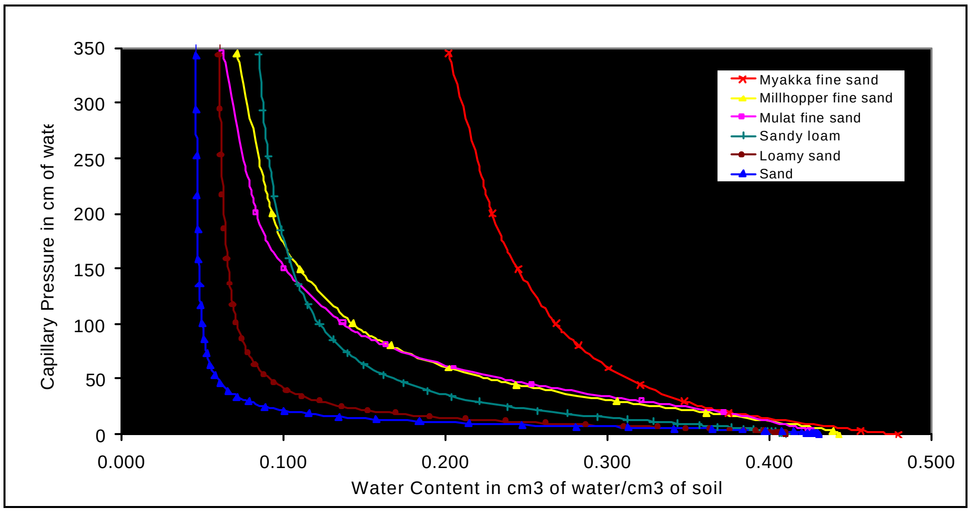

Figure 35. Water retention curves for different soils used in simulations

Sandy loam soils, with very low hydraulic conductivity for example, produced less percentage of total subsurface flux. In Table 8 observe that combinations of these parameters produced saturation excess runoff only when the parameter n was decreased. Thus, VSA extended largely for these cases and seepage was observed. Also, the amount of water running as saturation excess is substantially smaller compared to the amount of subsurface flow. The values highlighted on Table 8 are parameters that were changed for these particular simulations.

Table 8. Soil Parameters changes in a, n, and Ks

Types of soil used	Soil Properties					Extent of VSA (m)	Fluxes (meters^2)					
	θr	θs	α	n	Ks		Qsur1	Qsub1	Qsur2	Qsub2	Tsur (%)	Tsub (%)
Maykka Fine Sand (layer 3). Reference simulation	0.02	0.479	9.5238	1.26	0.128	35.5	0.1	0.0374	0.0356	1.5	1.2	13.605
	0.02	0.479	9.5238	2.28	0.128	0	0	0.0303	0	1.36	0	12.304
Mulat Fine Sand (layer 4)	0.04	0.427	33.33	2.22	0.263	0	0	0.0604	0	2.44	0	22.127
Millhopper Fine Sand (layer 1)	0.04	0.442	26.316	2	0.105	0	0	0.0267	0	1.09	0	9.8823
Sand	0.045	0.43	14.5	2.68	0.297	0	0	0.0675	0.0389	2.87	0.344248	25.996
	0.045	0.43	9.5238	2.68	0.297	0	0	0.0694	0	2.92	0	26.455
	0.045	0.43	14.5	1.26	0.297	33.2	0.1	0.0802	0.0389	3.04	1.229204	27.612
	0.045	0.43	14.5	2.68	0.128	0	0	0.0318	0	1.34	0	12.14
Sandy loam	0.065	0.41	7.5	1.89	0.0442	31.6	0.05	0.0123	0.00384	0.603	0.47646	5.4451
	0.065	0.41	12.4	1.89	0.0442		0.01	0.0119	0.000527	0.577	0.181655	5.2115
	0.065	0.41	7.5	2.28	0.0442		0.01	0.0118	0.00109	0.581	0.186637	5.246
	0.065	0.41	7.5	1.89	0.146		0.01	0.0411	0.00697	1.64	0.238673	14.877
Loamy sand	0.057	0.41	12.4	2.28	0.146	0	0	0.0359	0	1.56	0	14.123
	0.057	0.41	9.5238	2.28	0.146		0.01	0.0365	.000094	0.0159	0.089325	0.4637
	0.057	0.41	12.4	1.26	0.146	36.4	0.12	0.0457	0.151	2.08	2.39823	18.812
	0.057	0.41	12.4	2.28	0.297	0	0	0.0692	0	2.93	0	26.542

θ r	Residual water content
θs	Saturated water content
α	alpha
n	n
Ks	Saturated hydraulic conductivity
Qsur1	Cumulative saturation excess runoff during rainfall
Qsub1	Cumulative subsurface flux during rainfall
Qsur2	Cumulative saturation excess runoff and seepage after rainfall
Qsub2	Cumulative subsurface flux after rainfall
Tsur (%)	Total percetage of flux going as saturation excess
Tsub (%)	Total percetage of flux going as subsurface runoff

Constant rainfall rate was used for the reference simulation. The storm had duration of 2.25 hours and constant intensity of 0.013 m/hr. To analyze the impacts of temporal variability, actual storms with variable rainfall intensities were tested. The storms used here were three convective storms with the same duration and total rainfall depth as the reference simulation, and two frontal storms with the same total depth as the reference simulation but durations of 5.62 and 3.8 hours.

Table 9. Changes in runoff cumulative fluxes because of variable rainfall intensity

Rainfall variability	*Extent of VSA (m)*	*Fluxes (meters^2)*					
		Qsur1	*Qsub1*	*Qsur2*	*Qsub2*	*Tsur (%)*	*Tsub (%)*
Reference simulation, I = 0.013 m/hr, d = 2.25 hr	35.5	0.1	0.037	0.036	1.500	1.200	13.605
Convective storm with high intensities at the beginning	35	0.1	0.043	0.126	2.010	2.000	18.170
Convective storm with high intensities in the middle	37	0.1	0.035	0.043	1.510	1.268	13.675
Convective storm with high intensities at the end	34	0.1	0.036	0.038	1.500	1.219	13.589
Frontal storm, d = 5.62 hr	33	0	0.100	0.040	1.490	0.350	14.070
Frontal storm, d = 3.8 hr	35.2	0.000	0.068	0.036	1.500	0.315	13.879

During rainfall, the VSA expanded. Then, when rainfall stopped the variable saturated areas shrunk. From Table 9, the extent of VSA changed slightly. Frontal storms did not produce saturation excess during rainfall, but there was some seepage after rainfall stopped. Convective storms with high intensity at the beginning of the storm produced more seepage and saturation excess after rainfall stopped. The fluxes for all other storms were relatively similar. At the small scale, temporal variability of rainfall seemed not to impact substantially the infiltration-runoff process near the streams with shallow water tables. Appendix H contains the hyetographs for these storms.

Different depths to the water table were simulated. Water table levels used were 1, 3, 3.5, and 4 feet above the streambed. The reference simulation had an initial flat water table level at 3.5 feet from the streambed. For dry initial conditions, 1-foot water table depth was used. The water table was later increased to 4 feet where part of the soil surface was already saturated. Variable saturated areas expanded when the initial water table depth was closer to the surface. A shallow water table depth of 4 feet above the streambed produced an extent in the VSA of 20.7 m, whereas a deep water table depth of 1 foot above the streambed did not produce saturation excess runoff.

Table 10. Runoff cumulative fluxes due to changes in the initial water table depth

Depth to the water table	*Extent of VSA (m)*	*Fluxes (meters ^{2})*					
		Qsur1	*Qsub1*	*Qsur2*	*Qsub2*	*Tsur (%)*	*Tsub (%)*
Reference simulation, water table at 3.5 feet	19.4	0.200	0.014	0.000	0.261	1.770	2.434
Water table at 1 foot from streambed	0	0.000	0.009	0.000	0.155	0.000	1.449
Water table at 3 feet from streambed	9.5	0.000	0.057	0.000	0.363	0.000	3.719
Water table at 4 feet from streambed	20.7	0.300	0.009	0.002	0.203	2.669	1.874

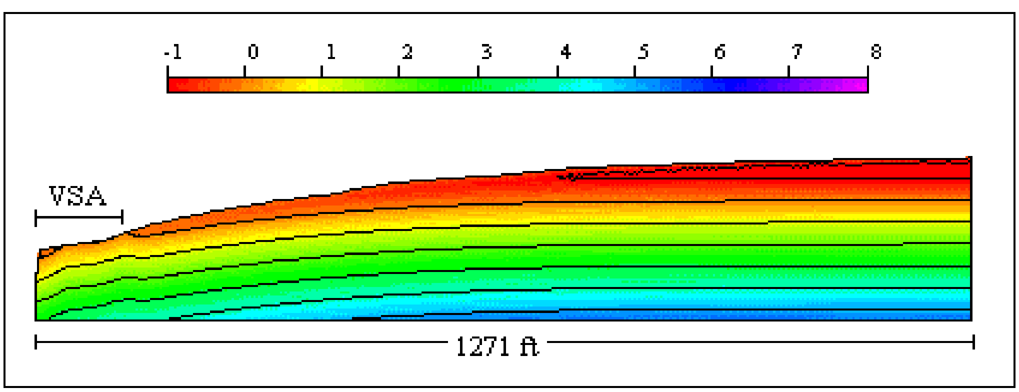

Figure 36. Pressure head distribution for the reference simulation

Figure 36 illustrates the pressure head distribution in the reference simulation right after rainfall stops. The line that intercepts the ground surface near the stream is equal to the zero pressure line, which represents the water table depth at 2.25 hours.

Geomorphologic features like slope, curvature, and divergence were studied here. Profiles with slopes of 0.5%, 1.1%, and 2.5% were simulated. Initial water table level at 3.5 ft from the streambed was used for all simulations. Table 11 shows an increase in the size of VSA when slope of the cross section was increased.

Table 11. Runoff cumulative fluxes for different slopes in the profiles

Slopes with flat initial water table	*Extent of VSA (m)*	*Fluxes (meters ^{2})*					
		Qsur1	*Qsub1*	*Qsur2*	*Qsub2*	*Tsur (%)*	*Tsub (%)*
Reference simulation	19.6	0.2	0.0140	0.00159	0.261	1.784	2.4336
Straight slope of 0.5%	73.7	0.2	0.0052	0.0199	0.154	1.946	1.4086
Straight slope of 1.1%	30.1	0.3	0.0053	0.0133	0.22	2.773	1.9942
Straight slope of 2.5%	12.8	0.1	0.0176	0.00279	0.279	0.910	2.6248

For instance, decreasing the slope of the profile to 0.5% caused a substantially increase of the variable saturated areas which expand up to 73.7 meters. Other fluxes did not have major changes.

The degree of curvature was analyzed by taking different curved profiles representative of real topographic terrains. Three convective profiles and three concave profiles were studied in this work. Flat initial water table level at 3.5 ft feet above the streambed was assumed for the simulations of changes in curvature. Table 12 summarizes the cumulative runoff fluxes obtained after changing the curvature of the profile. Notice that variable saturated areas were greater for concave slope profiles than convex slopes. Small changes in the degree of curvature for concave slopes produced significant extent of VSA and saturation excess runoff during and after rainfall.

Table 12. Runoff cumulative fluxes for different curvatures

Types of curvature	*Extent of VSA (m)*	*Fluxes (meters ^{2})*					
		Qsur1	*Qsub1*	*Qsur2*	*Qsub2*	*Tsur (%)*	*Tsub (%)*
Reference simulation	19.6	0.2	0.014	0.002	0.261	1.784	2.434
Concave slope with r = 14871.1 meters	134.9	1.58	0.001	0.295	0.086	16.593	0.776
Concave slope with r = 19474 meters	94.02	1.25	0.0015	0.106	0.049	11.998	0.437
Concave slope with r = 28631.9 meters	63.89	0.3	0.002	0.076	0.107	2.446	0.966
Convex slope with r = 11779.1 meters	20.7	0.1	0.012	0.006	0.283	0.942	2.610
Convex slope with r = 15928.8 meters	14.5	0.1	0.015	0.005	0.292	0.925	2.720
Convex slope with r = 35349.4 meters	12	0.1	0.018	0.003	0.285	0.911	2.683

Slight changes occurred in the saturation excess runoff generated by the model when convex slopes where changed. On the other hand, subsurface fluxes for convex curvature were higher than subsurface fluxes for concave curvature. From Table 12, it can be observed that the percentage of total saturation excess produced by concave curvature was greater that the percentage of total subsurface flux. Saturation excess runoff dominates in concave curvature profiles. Appendix N shows the extent of VSA on these concave profiles.

Changes in the landscape such as convergence and divergence were also considered in this work. Divergence and convergence were assessed as the relationship between the radii of two concentric circles that represent the left (stream) and right (water divide) boundaries of a cross section taken from a flow path. Figure 37 depicts different flow paths that converge and diverge. This analysis was based on a discharge area bounded by two flow paths that either converge or diverge towards the stream.

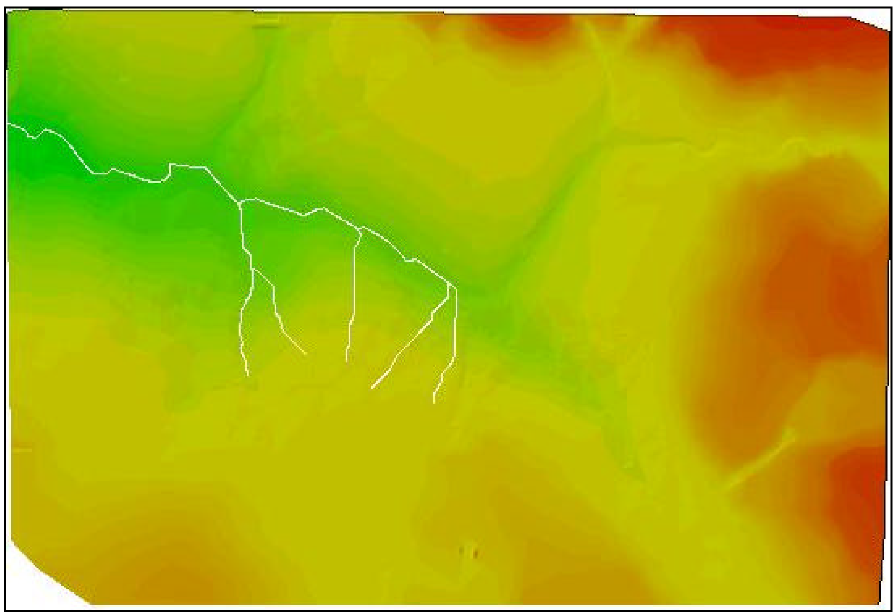

Figure 37. Shaded relief of the Lithia DEM with several flow paths

Simulations using divergence showed that when the radius of divergence increased, the area of possible saturation also increased. Therefore, the VSA extended farther from the stream. For this DEM, most of the flow paths diverged towards the stream. Few flow paths showed convergence, which was not expected for the type of topography predominant in Florida.

CHAPTER 6. CONCLUSIONS

Infiltration excess, also called "Hortonian Runoff", and saturation excess are the runoff mechanisms predominant in Florida. These mechanisms are highly influenced by geomorphologic and hydrologic characteristics. Temporal variability of rainfall has been shown to impact the infiltration excess runoff process whereas hillslope topography, soil parameters, and depth to the water table have a greater impact on runoff generated by saturation excess mechanisms.

When Hortonian runoff is dominant, results showed that infiltration and runoff were very sensitive to time resolution, especially for convective storms. Actual rainfall data with fine time resolution was used. Statistical analysis of rainfall showed that details in rainfall temporal distribution are lost when coarse time resolution was used. Consequently, high rainfall intensities generated by convective storms were smoothed out, and Hortonian runoff was underestimated. The error in runoff response increased when coarser resolution was used. Fine time resolution may, therefore, be used in existing hydrologic models to accurately simulate infiltration excess runoff. The time resolution suitable for infiltration-runoff modeling on this fine sandy soil should be less than 5 minutes leading to manageable errors of around 10%.

Runoff generated by saturation excess is more common in shallow water table environments, especially close to wetlands and streams. Under these conditions, Variable Saturated Areas (VSA) are present. VSA at the hillslope scale were assessed by coupling a Digital Elevation Model (DEM) with the variable saturated water flow model, HYDRUS 2D. Geomorphologic characteristics of the hillslope including slope, curvature, and divergence were extracted from DEMs. Sensitivity of the model to these characteristics was attained with HYDRUS 2D, by running different simulations to generate overland flow. From these simulations, subsurface storm flow was very significant especially for hillslopes with relatively high saturated hydraulic conductivity soils like fine sands. On the other hand, hillslopes with flatter slopes and concave curvature showed more saturation excess runoff. The most important soil hydraulic parameter influencing runoff was found to be the saturated hydraulic conductivity and van Genuchten parameter *n*. Subsurface flux increased when saturated hydraulic conductivity increased, and saturation excess increased when *n* decreased. Rainfall temporal variability did not influence the magnitude of Variable Saturated Areas. Depth to the water table, in contrast, generated more saturation excess than subsurface flux when the water tables were high.

Further verification and especially a field study to observe and measure these "theoretical model" results have not yet been made. There is a need for actual rainfall data with high temporal resolution, digital elevation data with high vertical resolution, and soil data for actual soils to be able to verify these results.

REFERENCES

Agnese, C., and V. Bagarello. 1997. Describing Rate Variability of Storms Events for Infiltration Prediction. Transactions of the ASAE, Volume 40, No. 1, pp 61-70.

Arnold, J. G. and J. R. Williams. 1989. Stochastic Generation of Internal Storm Structure at a Point. Transactions of the ASAE, Volume 32, No. 1, pp 161-167.

Bosch, D. D., and F. M. Davis. 1999. Rainfall Variability and Spatial Patterns for the Southeast. Proceedings of the Fourth International Conference on Precision Agriculture, pp 535-545.

Brooks, R. H., and A. T. Corey. 1964. Hydraulic Properties of Porous Media. Hydrology Paper 3, Colorado State University, Fort Collins, Colorado.

Carlisle, V. W., F. Sodek, M. E. Collins, L. C. Hammond, and W. G. Harris. 1989. Characterization Data for Selected Florida Soils, Soil Survey. U.S. Department of Agriculture, Soil Conservation Service. Soil science research report number 89-1. Florida, pp 307.

Dunne, T. and R. Black. 1970a. An Experimental Investigation of Runoff Production in Permeable Soils. Water Resources Research, Volume 6, No. 2, pp 478-490.

Dunne, T. and R. Black. 1970b. Partial Area Contributions to Storm Runoff in a Small New England Watershed. Water Resources Research, Volume 6, No. 5, pp 1296-1311.

Dunne, T. 1978. Field Studies of Hillslope Flow Processes. *Hillslope Hydrology*, ed. M. J. Kirkby. Wiley-Interscience, New York, pp 227-293.

Evans, M., T. Burt, J. Holden, and J. Adamson. 1999. Runoff Generation and Water Table Fluctuations in Blanket peat: Evidence from UK Data Spanning the Dry Summer of 1995. Journal of Hydrology, Volume 221, pp 141-160.

Finnerty, Bryce, M. B. Smith, D. Seo, V. Koren, and G. E. Moglen. 1997. Space-Time Scale Sensitivity of the Sacramento Model to Radar-Gage Precipitation Inputs. Journal of Hydrology, Volume 203, pp 21-38.

Flanagan, D.C, G. R. Foster, and W.C. modeng. 1988. Storm Pattern Effects on Infiltration, Runoff, and Erosion. Transactions of the ASAE, Volume 31, No. 2, pp 414-420.

Freeze, R. 1972b. Role of Subsurface Flow in Generating Surface Runoff 1. Base Flow Contributions to Channel Flow. Water Resources Research, Volume 8, No. 3, pp 609-623.

Freeze, R. 1972a. Role of Subsurface Flow in Generating Surface Runoff 2. Upstream Source Areas. Water Resources Research, Volume 8, No. 5, pp 1272-1283.

Freeze, R. A. 1980. A Stochastic Conceptual Analysis of Rainfall-Runoff Process on a Hillslope. Water Resources Research, Volume 16, No. 2, pp 395.

Gammeter, S. Burckhardt, and R. Fankhauser. 1998. Analysis of Rainfall Time Series with Regard to Temporal Disaggregation for the Use in Urban Hydrology. Water Science Technology, Volume 37, No. 11, pp 65-72.

Govindaraju, R. and M. Kavvas. 1991. Dynamics of Moving Boundary Overland Flows Over Infiltrating Surfaces at Hillslope. Water Resources Research, Volume 27, No. 8, pp 1885-1898.

Hewlett. 1961. Some Ideas about Storm Runoff and Baseflow. In: Process Studies in Hillslope Hydrology, ed. M. G. Anderson and T.P. Burt. John Wiley & Sons, England, pp 314.

Hewlett, J. D. and A. Hibbert. 1963. Moisture and Energy Conditions on a Sloping Soil Mass During Drainage. Journal of Geophysical Research, Volume 68, pp 1081-1087.

Kirkby, M. J. 1978. *Hillslope Hydrology*. Wiley-Interscience, New York, pp 348.

Kirkby, M. J. and R. Chorley. 1967. Throughflow, Overland Flow and Erosion. In: Process Studies in Hillslope Hydrology. M. G. Anderson and T.P. Burt. John Wiley & Sons, England, pp 175.

Lamb, Robert. 1999. Calibration of a Conceptual Rainfall-Runoff Model for Flood Frequency Estimation by Continuous Simulation. Water Resources Research, Volume 35, No. 10, pp 3103-3114.

Loague, Keith. 1988. Impact of Rainfall and Soil Hydraulic Property Information on Runoff Predictions at the Hillslope Scale. Water Resources Research, Volume 24, No. 9, pp 1501-1510.

Maidment, David R. 1993. *Handbook of Hydrology*. McGraw-Hill, Inc. New York, NY.

Milly, P. C. D., and P. S. Eagleson. 1988. Effect of Storm Scale on Surface Runoff Volume. Water Resources Research, Volume 24, No.4, pp 620-624.

Ogden, Fred and Bahram Saghafian. 1997. Green and Ampt Infiltration with Redistribution. Journal of Irrigation and Drainage Engineering, Volume 123, No. 5, pp 386-393.

Ogden, F. and B. Watts. 2000. Saturated Area Formation on Nonconvergent Hillslope Topography with Shallow Soils: A Numerical Investigation. Water Resources Research, Volume 36, No. 7, pp 1795-1804.

O'Loughlin, E. M. 1986. Prediction of Surface Saturation Zones in Natural Catchments by Topographic Analysis. Water Resources Research, Volume 22, No. 5, pp 794-804.

Philip, J. R. 1996. Hillslope Infiltration: Divergent and Convergent Slopes. Water Resources Research, Volume 27, No. 6, pp 1035-1040.

Research Systems. 1999. River Tools 2.0 User's Guide. Research Systems, Interactive Data Language 5.2. (http://www.rsinc.com/rivertools).

Rodriguez-Iturbe, Ignacio and P. S. Eagleson. 1987. Mathematical Model of Rainstorm Events in Space and Time. Water Resources Research, Volume 23, No. 1, pp 180-190.

Salvucci, G. and D. Entekhabi. 1995. Hillslope and Climatic Controls on Hydrologic Fluxes. Water Resources Research, Volume 31, No. 7, pp 1725-1739.

Sepulveda, Nicasio. 1997. Application of Two Direct Runoff Prediction Methods in Puerto Rico. ASCE Journal of Hydrologic Engineering, Volume 2, No.1, pp 10-17.

Simunek, J., M. Sejna, and M. Th. van Genuchten. 1998. The HYDRUS 1D Software Package for Simulating the One-Dimensional Movement of Water, Heat, and Multiple Solutes in Variably-Saturated Media. Version 2.0. US Salinity Laboratory, ARS/USDA. Riverside, California.

Simunek, J., M. Sejna, and M. Th. van Genuchten. 1999. HYDRUS 2D, Simulating Water Flow, Heat, and Solute Transport in Two-Dimensional Variably Saturated Media. Version 2.0. US Salinity Laboratory, ARS/USDA. Riverside, California and International Ground Water Modeling Center, IGWMC – TPS 53. Colorado School of Mines, Golden, Colorado.

Singh, V. P. 1997. Effect of Spatial and Temporal Variability in Rainfall and Watershed Characteristics on Stream Flow Hydrograph. Transactions of the ASAE, Volume 31, No. 2, pp 414-420.

Stagnitti, F., J. Parlange, T. S. Steenhuis, M. B. Parlange, and C. W. Rose. 1992. A Mathematical Model of Hillslope and Watershed Discharge. Water Resources Research, Volume 28, No. 8, pp 2111-2122.

Steenhuis, T. S., M. Winchell, J. Rossing, J. A. Zollweg, and M. F. Walter. 1995. SCS Runoff Equation Revisited for Variable-Source Runoff Areas. Journal of Irrigation and Drainage Engineering, Volume 121, No. 3, pp 234-238.

Van Genuchten, M. Th. 1980. A Closed-Form Equation for Predicting the Hydraulic Conductivity of Unsaturated Soils. Soil Science Society American Journal, Volume 44, pp 892-898.

Wigmosta, M., L. Vail, and D. Lettenmaier. 1994. A Distributed Hydrology-Vegetation Model for Complex Terrain. Water Resources Research, Volume 30, No. 6, pp 1665-1679.

Woolhiser, D. A., and D. C. Goodrich. 1988. Effect of Storm Rainfall Intensity Patterns on Surface Runoff. Journal of Hydrology, Volume 102, pp 335-354.

APPENDICES

Appendix A. Subroutine *Rainfall_Minute*

```
'Program:    Discretization of Rainfall data every minute using
'                Linear Interpolation and average
'Form name:  frmrainfall-minute
'Programmer: Tatiana X. Hernandez.
'Date:       June 30  , 1999.  Last Modified: May 27, 2000
'Purpose:  This program is design to convert the continuous rainfall data in
'          rainfall with a 1 minute resolution.  The program reads date, time, and
'          time to tip in seconds from a text file(.csv) and calculates the intensity
'          of rain every minute.  It interpolates when the data is missing and
'          average when there is more than one point in a minute.
'          It creates an output file (.txt)

Option Explicit
Dim T(50000) As Single           'cumulative time in minute
Dim Ttip(50000) As Single        'time from last tip in seconds
Dim datedata(50000) As String    'date for each tip
Dim timedata(50000) As String    'time for each tip
Dim n As Integer                 'total number of records
```

```
Private Sub cmdinputfile_Click()
'Input a file using a dialog box.  Read values of time to tip, date and time from a text file
and calculate cumulative time in minutes.
Dim i As Integer    'counter for time to tip
Dim c As Integer    'counter for time to tip when they are longer than 5 minutes
Dim filenum As Integer

filenum = FreeFile
Dialogfile.Filter = "all files(*.*)|*.*|comma delimited files(*.csv)|*.csv|text
files(*.txt)|*.txt|"
Dialogfile.FilterIndex = 2
Dialogfile.Action = 1
Dialogfile.CancelError = True
Open Dialogfile.filename For Input As filenum

i = 0
'Calculate cumulative time in minutes
While Not EOF(1)
   i = i + 1
   Input #filenum, datedata(i), timedata(i), Ttip(i)
Wend
Close #filenum
n = i
```

Appendix A. (Continued)

```
'i=1 is the heading or comment line with column's names at the begining of file
For i = 2 To n
  T(1) = 0
  'when there are no tips in a 5 minutes period or more, it skips them
  'and use intensity for that period equal to intensity of next period
  If Ttip(i) / 60 > 5 And Ttip(i + 1) / 60 < 5 Then
    T(i) = Ttip(i + 1) / 60
   ElseIf Ttip(i) / 60 > 5 And Ttip(i + 1) / 60 > 5 Then
    c = i
    Do Until Ttip(i) / 60 <= 5
      i = i + 1
    Loop
    T(c) = Ttip(i) / 60
    i = c
   Else
    T(i) = Ttip(i) / 60 + T(i - 1)
  End If
Next i
cmdcalculate.SetFocus
End Sub
```

```
Private Sub cmdcalculate_Click()
'Interpolate to find the cumulative depth every minute and intensity in in/min

Dim i As Integer            'index for each tip
Dim j As Integer            'index for time every minute
Dim intold As Single        'intensity for period before
Dim Wmin As Single          'cumulative depth of rain in inches
Dim Wminold As Single       'cumulative depth of rain for period before
Dim Wminnew As Single       'cumulative depth of rain for period after
Dim intensity As Single     'intensity in in/min
Dim Jmin As Integer         'time minute to minute for new value
Dim secondata As Integer    'seconds for new value
Dim minutedata As Integer   'minutes for new value
Dim hourdata As Integer     'hours for new value
Dim timedatamin As String   'date and time for new value
Dim filename As String      'file name for input file

Call output_file
frmrainfall_minute.MousePointer = 11
cmdexit.SetFocus
j = 1;  i = 1
Wminnew = 0
```

Appendix A. (Continued)

```
Wminold = 0
intensity = 0
Jmin = 0

Do While i < n - 1
Do While i < n - 1
   i = i + 1
   Wminold = Wminold + 0.01
   Do While Abs(((Day(datedata(i + 1)) * 1440 + Hour(timedata(i + 1)) * 60 +
Minute(timedata(i + 1)) + Second(timedata(i + 1)) / 60) - (Day(datedata(i)) * 1440 +
Hour(timedata(i)) * 60 + Minute(timedata(i)) + Second(timedata(i)) / 60))) < 5
      'Interpolate when it has to create more than 1 value
      Do While j >= T(i) And j < T(i + 1)
         intold = Wmin
         Wmin = Wminold + 0.01 / (T(i + 1) - T(i)) * (j - T(i))
         intensity = (Wmin - intold)
         Jmin = j
         secondata = Int((Jmin - T(i)) * 60 + 0.5) + Second(timedata(i))
         minutedata = Minute(timedata(i))
         hourdata = Hour(timedata(i))
         timedatamin = DateValue(datedata(i)) + TimeSerial(hourdata, minutedata,
secondata)
         Write #1, timedatamin, Jmin, intensity * 60, Wmin
         j = j + 1
      Loop
      If j >= T(i + 1) Then
            Exit Do
       'linear regresion to insert values
       ElseIf j < T(i) Then
         Wminold = Wmin
         intensity = 0.01 / T(i)
         Wmin = Wminold + 0.01 / T(i)
         Jmin = j
         secondata = Second(timedata(i)) - Int((T(i) - Jmin) * 60 + 0.5)
         minutedata = Minute(timedata(i))
         hourdata = Hour(timedata(i))
         timedatamin = DateValue(datedata(i)) + TimeSerial(hourdata, minutedata,
secondata)
         Write #1, timedatamin, Jmin, intensity * 60, Wmin
         j = j + 1
      End If
   Wminold = 0.01
   Loop
```

Appendix A. (Continued)

```
   If Abs(((Day(datedata(i + 1)) * 1440 + Hour(timedata(i + 1)) * 60 + Minute(timedata(i
+ 1)) + Second(timedata(i + 1)) / 60) - (Day(datedata(i)) * 1440 + Hour(timedata(i)) * 60
+ Minute(timedata(i)) + Second(timedata(i)) / 60))) >= 5 Then
    If T(i) = T(i + 1) Then
      If T(i) = 0 Then
        Exit Do
       ElseIf T(i) <= 1 Then
        Wminold = 0
        Wmin = 0
        j = 1
        Exit Do
       ElseIf T(i) > 1 Then
        Do While j <= T(i)
        Wminold = Wmin
        intensity = 0.01 / T(i)
        Wmin = Wminold + 0.01 / T(i)
        Jmin = j
        secondata = Second(timedata(i)) - Int((T(i) - Jmin) * 60 + 0.5)
        minutedata = Minute(timedata(i))
        hourdata = Hour(timedata(i))
        timedatamin = DateValue(datedata(i)) + TimeSerial(hourdata, minutedata,
secondata)
        Write #1, timedatamin, Jmin, intensity * 60, Wmin
        j = j + 1
        Loop
        intensity = 0.01 - Wmin
        Wmin = 0.01
        Jmin = j
        timedatamin = DateValue(datedata(i)) + TimeSerial(hourdata, minutedata + 1,
secondata)
      End If
     'when time to tip is < 1 min, distribute depth over the minute
     ElseIf j > T(i) Then
      If T(i) > 1 Then
        intensity = Wminold - Wmin
        Wmin = Wminold
        Jmin = j
        secondata = Int((Jmin - T(i)) * 60 + 0.5) + Second(timedata(i))
        minutedata = Minute(timedata(i))
        hourdata = Hour(timedata(i))
        timedatamin = DateValue(datedata(i)) + TimeSerial(hourdata, minutedata,
secondata)
       Else
```

Appendix A. (Continued)

```
                Wminold = 0
                Wmin = 0
                j = 1
                Exit Do
            End If
          ElseIf j < T(i) Then
            Exit Do
        End If
        Write #1, timedatamin, Jmin, intensity * 60, Wmin
        Wminold = 0
        Wmin = 0
        j = 1
    End If
Loop
Loop
Close #1
frmrainfall_minute.MousePointer = 0
cmdexit.SetFocus
End Sub
```

```
Sub output_file()
'This sub creates an output file (.txt) using a dialog box and copy
'date and time, time(min), intensities(in/hr), cummulative depth of rain(in)

Dialogfile.Filter = "all files(*.*)|*.*|text files(*.txt)|*.txt|comma delimited files(*.csv)|*.csv|"
Dialogfile.FilterIndex = 3
Dialogfile.ShowSave
Dialogfile.CancelError = True
Open Dialogfile.filename For Append As #1
Write #1, "Date_and_Time", "Time(min)", "intensity(in/hr)", "cummulative_depth(in)"
End Sub
```

```
Private Sub cmdexit_Click()
End
End Sub
```

Appendix B. Subroutine *Event_Minute*

```
'Program:    Separation of storms in Convective and Frontal
'Form name:  frmevent-minute
'Programmer: Tatiana X. Hernandez.
'Created:    July 30  , 1999.  Last Modified: May 26, 2000
'Purpose:    This program is design to separate storms and
'            calculate the duration and total depth of each storm.
'            It used an inter-event period of 1hr for convective storms
'            and 8 hours for frontal storms.  The program reads date
'            and time, time, intensity, and cummulative depth
'            from a text file and calculates total depth of storm
'            and duration of storms.  It creates a .txt output file

Option Explicit
Dim datetimedata(50000) As String   'date and time each minute
Dim duration(50000) As Single       'duration of storm in minutes
Dim depth(50000) As Single          'depth of storm in inches
Dim intensity(50000) As Single      'intensity every minute (in/hr)
Dim n As Integer                    'total number of records
Dim tstorm As Single                'variable to identify type of storm
```

```
Private Sub cmdinputfile_Click()

Dim i As Integer            'counter
Dim typestorm As String     'variable to identify type of storm
Dim c As String             'convective type storm
Dim f As String             'frontal type storm

'Input a file using a dialog box
dialogfile.Filter = "all files(*.*)|*.*|comma delimited files(*.csv)|*.csv|text files(*.txt)|*.txt|"
dialogfile.FilterIndex = 2
dialogfile.ShowOpen
dialogfile.CancelError = True
Open dialogfile.FileName For Input As #1

'Distinguish between convective and frontal type of storm
typestorm = InputBox("Type of storm (c for convective or f for frontal)", "Type of storm", "c")
If typestorm = "c" Or typestorm = "C" Then tstorm = 60  'One hour dry inter-event
If typestorm = "f" Or typestorm = "F" Then tstorm = 480 'Eight hours dry inter-event
```

Appendix B. (Continued)

```
'Read values of date and time, time, intensity and cummulative depth from a text file
i = 0
While Not EOF(1)
   i = i + 1
   Input #1, datetimedata(i), duration(i), intensity(i), depth(i)
Wend
Close #1
datetimedata(i + 1) = 0
n = i
cmdcalculate.SetFocus
End Sub
```

```
Private Sub cmdcalculate_Click()
'calculate cummulative depth of rain and duration for each storm

Dim i As Integer            'index for each tip
Dim j As Integer            'index for time every minute
Dim deltat As Single        'difference in time (minutes)
Dim olduration As Single    'cumulative duration of each storm
Dim oldepth As Single       'cumulative depth of each storm
Dim startstorm As String    'date and time and which the storm starts

Call output_file
frmevent_minute.MousePointer = 11
cmdexit.SetFocus

olduration = 0
oldepth = 0
'i=1 is the heading with the variable names
startstorm = datetimedata(2)
For i = 2 To n
deltat = ((Day(datetimedata(i + 1)) * 1440 + Hour(datetimedata(i + 1)) * 60 +
Minute(datetimedata(i + 1)) + Second(datetimedata(i + 1)) / 60) - (Day(datetimedata(i)) *
1440 + Hour(datetimedata(i)) * 60 + Minute(datetimedata(i)) + Second(datetimedata(i)) /
60))
If Abs(deltat) <= tstorm And duration(i) = 1 Then
   Do
      Write #3, datetimedata(i), duration(i), intensity(i), depth(i), "", ""
      i = i + 1
      If i >= n Then Exit Do
   Loop While duration(i + 1) <> 1
   oldepth = oldepth + depth(i)
```

Appendix B. (Continued)

```
   olduration = ((Day(datetimedata(i)) * 1440 + Hour(datetimedata(i)) * 60 + Minute(datetimedata(i)) + Second(datetimedata(i)) / 60) - (Day(startstorm) * 1440 + Hour(startstorm) * 60 + Minute(startstorm) + Second(startstorm) / 60)) + 1
   i = i - 1
  ElseIf Abs(deltat) <= tstorm And duration(i) <> 1 Then
   Write #3, datetimedata(i), duration(i), intensity(i), depth(i), "", ""
   olduration = ((Day(datetimedata(i + 1)) * 1440 + Hour(datetimedata(i + 1)) * 60 + Minute(datetimedata(i + 1)) + Second(datetimedata(i + 1)) / 60) - (Day(startstorm) * 1440 + Hour(startstorm) * 60 + Minute(startstorm) + Second(startstorm) / 60)) + 1
  Else
   If duration(i) = 1 Then
     startstorm = datetimedata(i + 1)
    Else
     Write #3, datetimedata(i), duration(i), intensity(i), depth(i), olduration / 60, oldepth
     startstorm = datetimedata(i + 1)
     olduration = 0
     oldepth = 0
   End If
End If
Next i
Close #3
frmevent_minute.MousePointer = 0
cmdexit.SetFocus
End Sub
```

```
Sub output_file()
'This sub creates an output file using a dialog box and copy
'the date and time, time(min), intensities(in/hr), cummulative depth(in), total duration(hr), and total depht(in) of storm

dialogfile.Filter = "all files(*.*)|*.*|text files(*.txt)|*.txt|comma delimited files(*.csv)|*.csv|"
dialogfile.FilterIndex = 3
dialogfile.ShowSave
dialogfile.CancelError = True
Open dialogfile.FileName For Append As #3
Write #3, "date and time", "Time(min)", "Intensity(in/hr)", "Depth(in)", "Total_duration_of_storm(hr)", "Total_depth_of_storm(in)"
End Sub
```

```
Private Sub cmdexit_Click()
End
End Sub
```

Appendix C. Output File from the *Event_Minute* Subroutine

Table 13. Sample of output file obtained using the *event_minute* subroutine

Date and time	*Time (min)*	*Intensity (in/hr)*	*Depth (in)*	*Total duration of storm(hr)*	*Total depth of storm(in)*
9/3/1998 4:22:16 PM	1	3.35596	0.05593		
9/3/1998 4:22:49 PM	2	0.24404	0.06000		
9/3/1998 4:33:26 PM	1	0.23415	0.00390		
9/3/1998 4:34:26 PM	2	0.23415	0.00780		
9/3/1998 4:35:26 PM	3	0.13171	0.01000		
9/3/1998 5:10:26 PM	1	0.23415	0.00390		
9/3/1998 5:11:26 PM	2	0.23415	0.00780		
9/3/1998 5:12:26 PM	3	0.23415	0.01171		
9/3/1998 5:13:26 PM	4	0.23415	0.01561		
9/3/1998 5:14:26 PM	5	0.23415	0.01951		
9/3/1998 5:15:53 PM	6	0.02927	0.02000	0.910	0.09
9/3/1998 9:25:50 PM	1	0.14388	0.00240		
9/3/1998 9:26:50 PM	2	0.14388	0.00480		
9/3/1998 9:27:50 PM	3	0.14388	0.00719		
9/3/1998 9:28:50 PM	4	0.14388	0.00959		
9/3/1998 9:29:50 PM	5	0.14388	0.01199		
9/3/1998 9:30:50 PM	6	0.14388	0.01439		
9/3/1998 9:31:50 PM	7	0.14388	0.01679		
9/3/1998 9:32:50 PM	8	0.14388	0.01918		
9/3/1998 9:34:11 PM	9	0.95590	0.03512		
9/3/1998 9:35:17 PM	10	1.84484	0.06586		
9/3/1998 9:36:09 PM	11	2.52603	0.10796		
9/3/1998 9:37:03 PM	12	3.27978	0.16263		
9/3/1998 9:38:02 PM	13	3.64796	0.22343		
9/3/1998 9:39:02 PM	14	4.08619	0.29153		
9/3/1998 9:40:04 PM	15	1.16778	0.31099		
9/3/1998 9:41:20 PM	16	0.96482	0.32707		
9/3/1998 9:42:05 PM	17	1.50248	0.35211		
9/3/1998 9:43:11 PM	18	1.35361	0.37467		
9/3/1998 9:43:47 PM	19	0.89941	0.38966		
9/3/1998 9:44:58 PM	20	0.02010	0.39000	0.336	0.39
9/3/1998 11:51:33 PM	1	0.41176	0.00686		
9/3/1998 11:52:33 PM	2	0.41176	0.01373		
9/3/1998 11:53:05 PM	3	0.39842	0.02037		
9/3/1998 11:54:05 PM	4	0.25605	0.02463		
9/3/1998 11:55:05 PM	5	0.25605	0.02890		
9/3/1998 11:55:45 PM	6	0.06597	0.03000		
9/4/1998 12:09:13 AM	1	1.69098	0.02818		
9/4/1998 12:09:45 AM	2	1.06258	0.04589		
9/4/1998 12:11:28 AM	3	0.36505	0.05198		
9/4/1998 12:12:28 AM	4	0.25148	0.05617		
9/4/1998 12:13:05 AM	5	0.38249	0.06254		
9/4/1998 12:13:45 AM	6	0.44741	0.07000	0.3866699	0.1
9/4/1998 10:37:04 AM	1	1.39737	0.02329		
9/4/1998 10:38:06 AM	2	1.72140	0.05198		
9/4/1998 10:39:10 AM	3	1.29374	0.07354		
9/4/1998 10:40:16 AM	4	1.34253	0.09592		
9/4/1998 10:41:26 AM	5	1.37308	0.11880		
9/4/1998 10:42:15 AM	6	0.90172	0.13383		
9/4/1998 10:43:36 AM	7	0.76376	0.14656		
9/4/1998 10:43:41 AM	8	0.47901	0.15454		
9/4/1998 10:45:11 AM	9	0.32739	0.16000		
9/4/1998 11:16:52 AM	1	0.53191	0.00887		
9/4/1998 11:17:52 AM	2	0.06809	0.01000	0.6966634	0.17

Appendix D. Florida Soil Survey for Myakka Fine Sand

SOIL CHARACTERIZATION LABORATORY, IFAS, UNIVERSITY OF FLORIDA

MYAKKA FINE SAND, S53-16-(1-6)
AERIC HAPLAQUODS, SANDY, SILICEOUS, HYPERTHERMIC — DATE SAMPLED 01/25/83
POLK COUNTY, FLORIDA

				PARTICLE SIZE DISTRIBUTION (% < 2 MM)												
				SAND FRACTIONS					TOTAL							
				VC	C	M	F	VF	SAND	SILT	CLAY	TEXTURE	PH			TOTAL
	DEPTH	HORIZON	LAB	2.0-	1.0-	0.5-	0.25-	0.10-	2.0-	0.05-	<	CLASS	H2O	CACL2	KCL	PHOS
NO	(CM)		NO	1.0	0.5	0.25	0.10	0.05	0.05	0.002	0.002		(1:1)	(1:2)	(1:1)	(ppm)
1	0- 18	Ap	5620	0.0	1.1	33.2	54.3	8.9	97.5	2.2	0.3	FS	4.5	3.8	3.8	
2	18- 64	E	5621	0.0	1.3	32.5	55.1	9.3	98.2	1.2	0.6	FS	4.8	4.2	4.1	
3	64- 76	Bh1	5622	0.0	1.0	30.1	53.6	8.2	92.9	2.7	4.4	FS	4.4	4.1	4.0	
4	76- 91	Bh2	5623	0.0	1.1	29.2	53.9	8.7	92.9	2.5	4.6	FS	4.5	4.3	4.2	
5	91-150	C	5624	0.0	1.1	25.5	58.0	10.7	95.3	2.3	2.4	FS	4.6	4.4	4.4	
6	150-203	C	5625	0.0	1.2	27.6	55.9	9.3	94.0	2.9	3.1	FS	4.9	4.4	4.5	

	ORG	KCL EXTR	NH4OAC EXTR				TOTAL	EXTR	CEC	BASE	PYRO EXTR			CIT-DITH EXTR	
	C	AL	CA	MG	NA	K	BASES	ACIDITY	(SUM)	SAT	C	FE	AL	FE	AL
NO	(%)	----------	----------	(MEQ/100G)	----------					(%)	----	(%)	----		
1	1.34	0.00	1.28	0.18	0.04	0.03	1.53	5.47	7.00	22					
2	0.10	0.00	0.05	0.01	0.01	0.00	0.07	0.67	0.74	9					
3	1.94	2.92	0.42	0.02	0.03	0.01	0.48	20.43	20.91	2	1.18	0.01	0.33	0.05	0.16
4	0.91	1.25	0.09	0.01	0.03	0.01	0.14	13.39	13.53	1	0.61	0.01	0.26	0.07	0.11
5	0.32	0.46	0.04	0.01	0.02	0.00	0.07	5.05	5.12	1					
6	0.41	0.62	0.09	0.02	0.03	0.01	0.15	6.81	6.96	2					

	SAT	WATER CONTENT			WATER CONTENT								AVAIL	BULK	ELEC
	HYDR	1/10	1/3	15									H2O	DENSITY	COND
	COND	BAR	BAR	BAR	3.5CM	20CM	30CM	45CM	60CM	80CM	150CM	200CM			
NO	(CM/HR)	---	(WEIGHT %)	---	----	----	----	(VOLUME %)	----	----	----	----	(CM/CM)	(G/CC)	(MMHO/CM)
1	38.8	8.8	5.9	2.0	38.0	32.2	28.3	21.4	16.9	14.3	11.0	9.9	0.10	1.44	0.04
2	28.0	4.0	2.8	0.2	37.0	34.2	27.4	16.0	10.7	7.7	4.8	4.5	0.06	1.53	0.01
3	12.8	19.0	15.6	4.2	42.8	37.6	35.9	32.6	30.0	27.6	24.2	23.1	0.20	1.38	0.03
4	9.0	11.0	8.5	2.5	36.1	33.3	31.6	25.4	21.0	18.3	15.1	14.4	0.13	1.52	0.01
5	11.2	8.3	6.0	1.3	37.6	35.8	30.3	23.1	18.3	14.9	11.5	10.7	0.11	1.58	0.01
6	9.5	7.7	5.4	1.2	34.7	33.2	31.5	22.6	18.0	14.3	10.6	9.8	0.10	1.60	0.02

	CLAY MINERALOGY											ENGINEERING TEST DATA (FLORIDA DEPARTMENT OF TRANSPORTATION)										
												MAXIMUM		MECHANICAL ANALYSIS (MM)								
												DRY	OPT	<	<	<	<	<	<	<	AASHO	CACO3
	MT	CH	VR	MI	IN	KK	GI	QZ	CL	FD	DL	DENSITY	MOIST	2.0	.42	.074	.05	.02	.005	.002	CLASS	EQUIV
NO	----	----	----	(% < 0.002 MM)	----	----	----	----	----	----	----	(LBS/CU FT)	(%)	----	----	----	(%)	----	----	----		(%)
1	29					12		59														
2												103.3	12.9	100	97	4	3				A-3	
3	14				31	26		29														
4																						
5												111.4	11.5	100	97	8	5	3	2	2	A-3	
6	29					22		49				111.4	11.5	100	97	8	5	3	2	2	A-3	

Figure 38. Sample copy of actual soil hydraulic parameters for Myakka fine sand (Carlisle et al., 1989)

Appendix E. HYDRUS 1D Graphs for Temporal Variability of Rainfall

∗ Frontal Storm

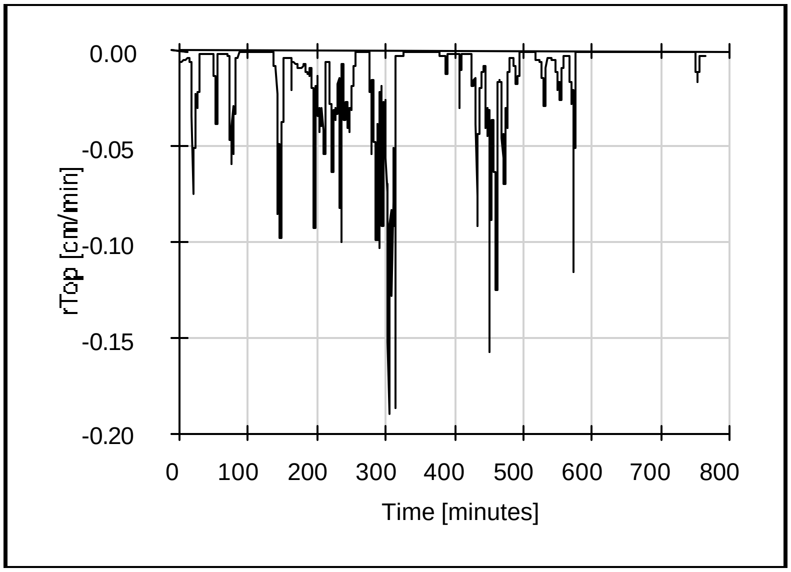

Figure 39. Rainfall rate vs time

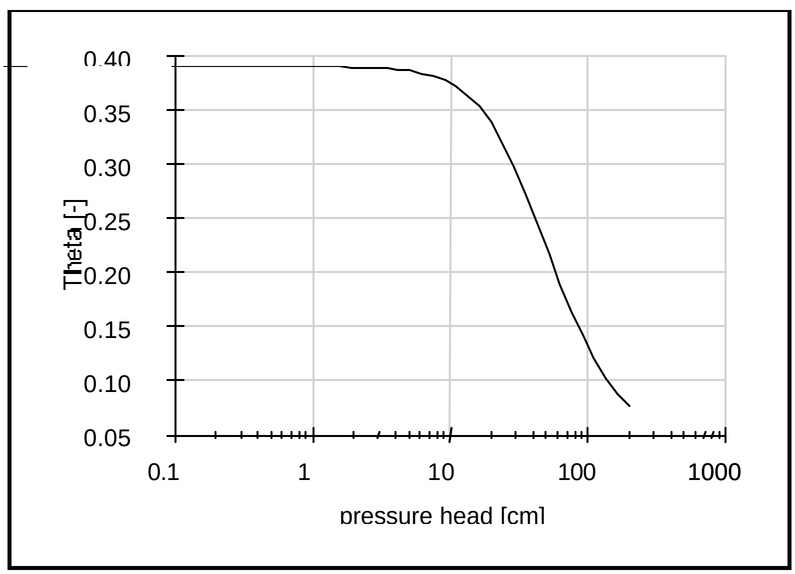

Figure 40. Water retention curve

Appendix E. (Continued)

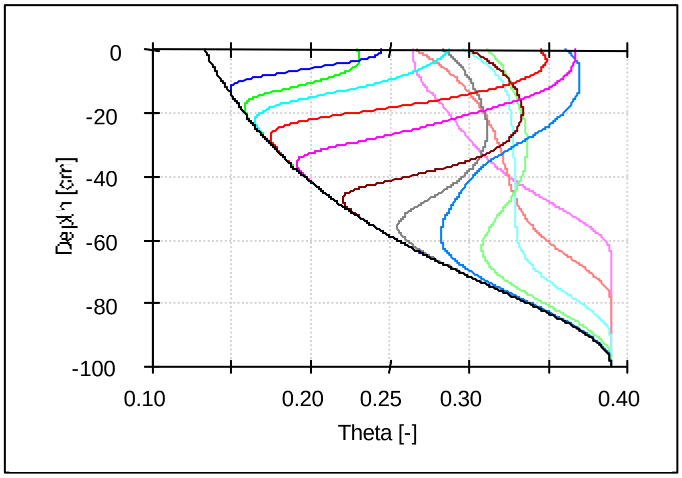

Figure 41. Water content vs depth (1 meter)

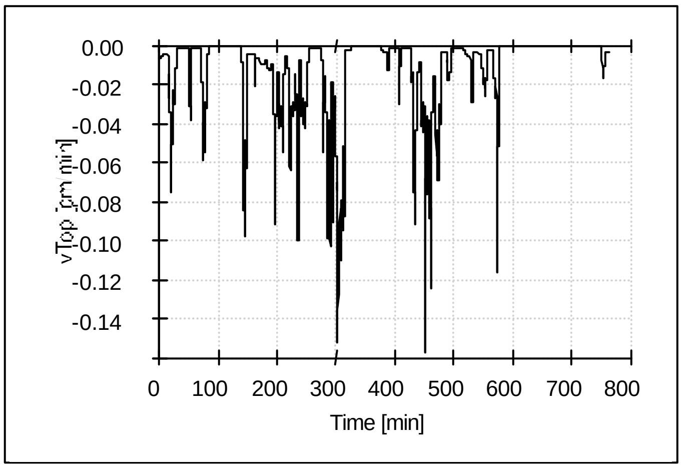

Figure 42. Infiltration rate vs time (1 meter)

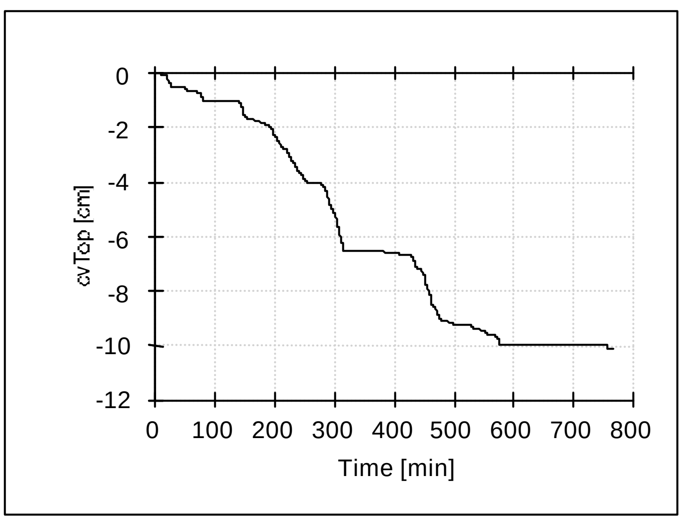

Figure 43. Cumulative infiltration depth vs time (1 meter)

Appendix E. (Continued)

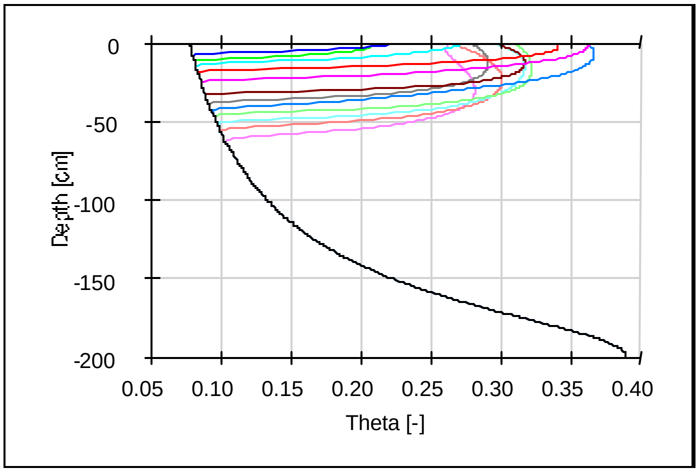

Figure 44. Water content vs depth (2 meters)

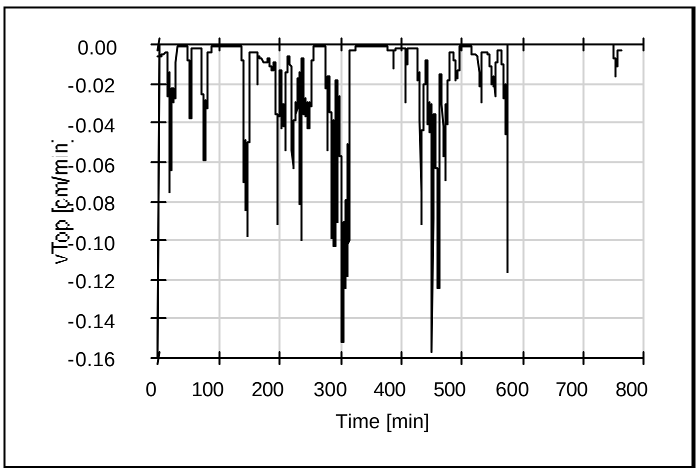

Figure 45. Infiltration rate vs time (2 meters)

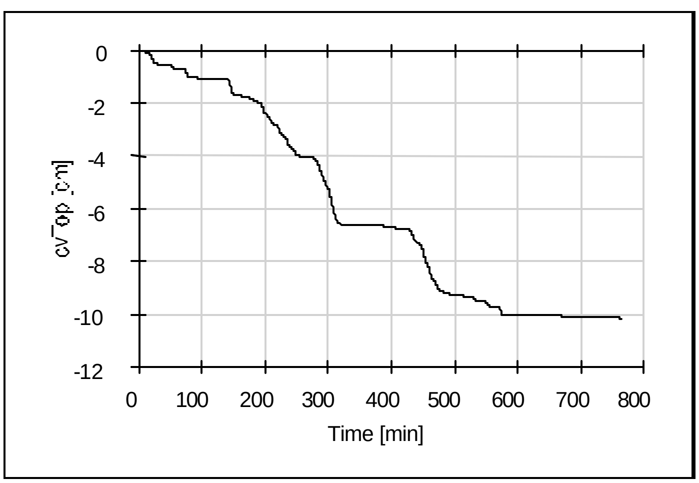

Figure 46. Cumulative infiltration depth vs time (2 meters)

Appendix E. (Continued)

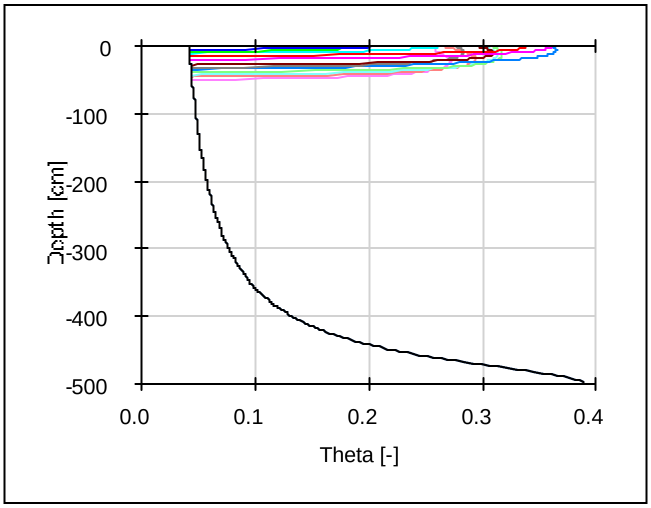

Figure 47. Water content vs depth (5 meters)

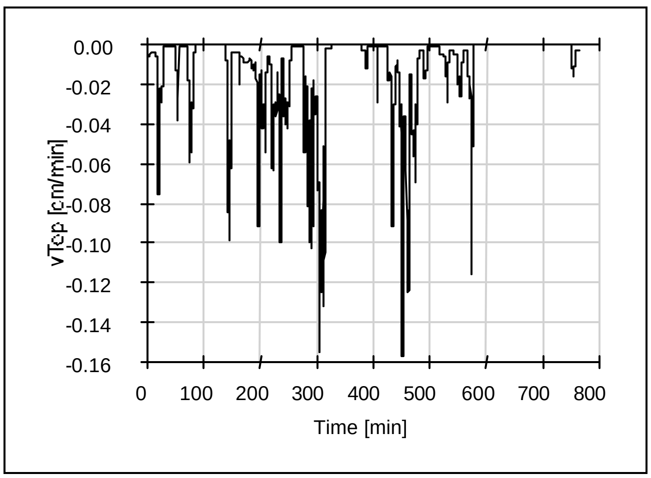

Figure 48. Infiltration rate vs time (5 meters)

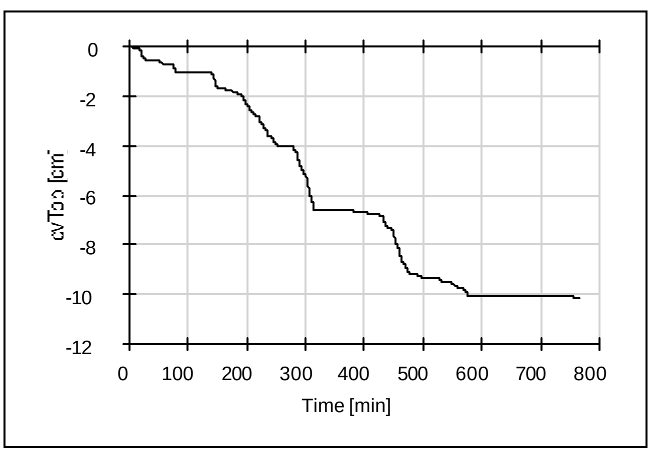

Figure 49. Cumulative infiltration depth vs time (5 meters)

* **Convective Storm**

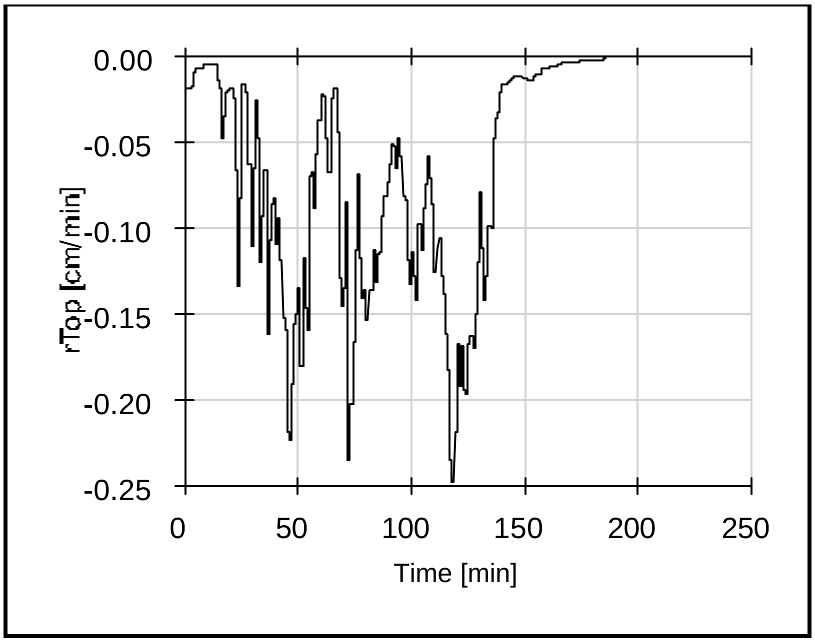

Figure 50. Rainfall rate for comnvective storm

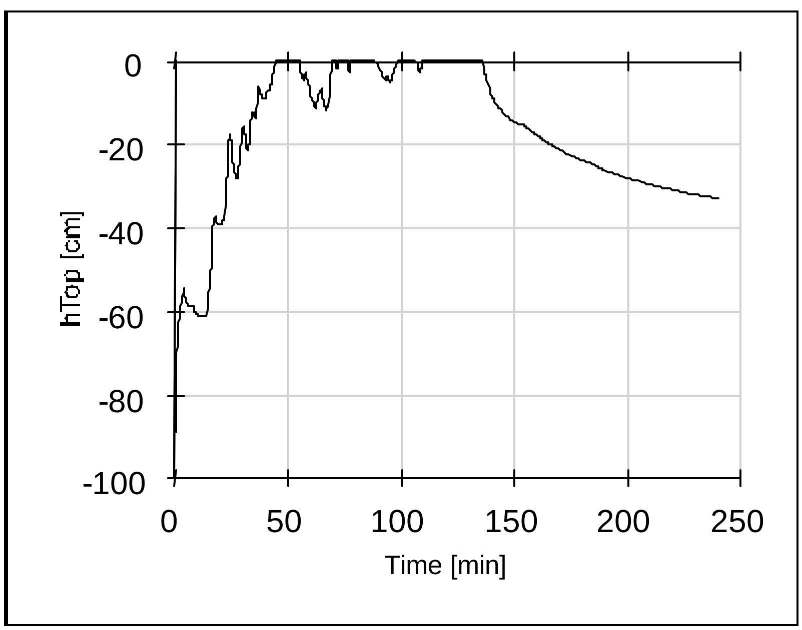

Figure 51. Pressure head at the surface (1 meter)

Appendix E. (Continued)

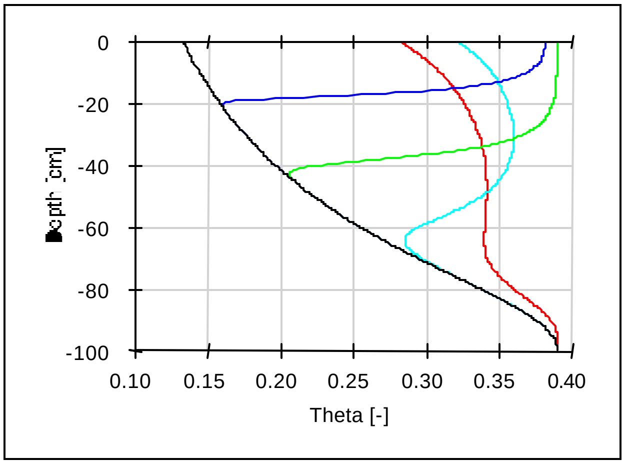

Figure 52. Water content vs depth (1 meter)

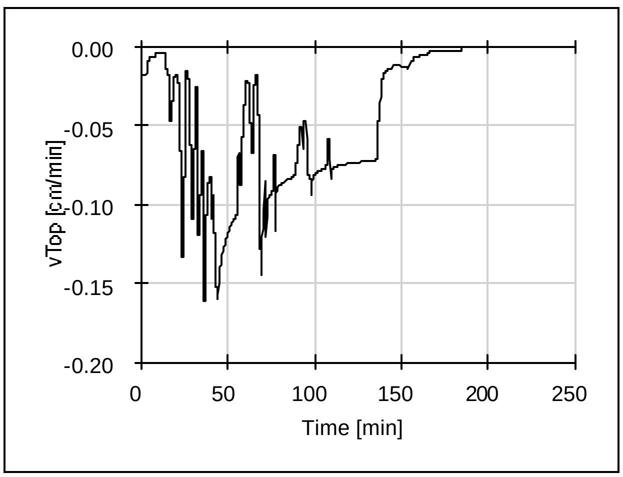

Figure 53. Infiltration rate vs time (1 meter)

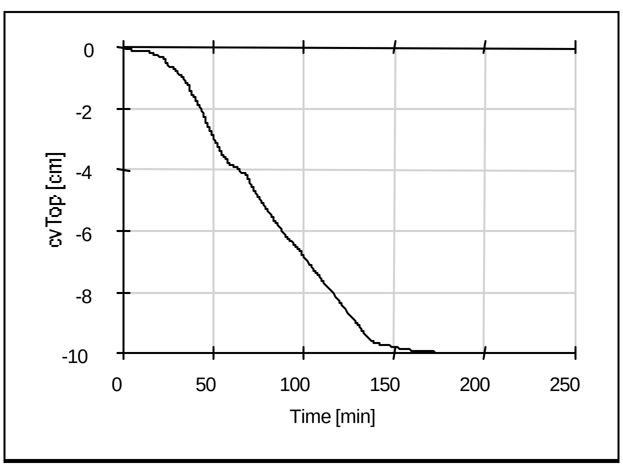

Figure 54. Cumulative infiltration depth vs time (1 meter)

Appendix E. (Continued)

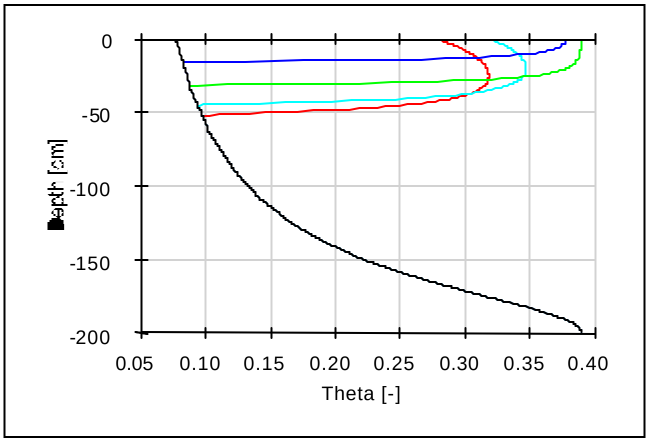

Figure 55. Water content vs depth (2 meters)

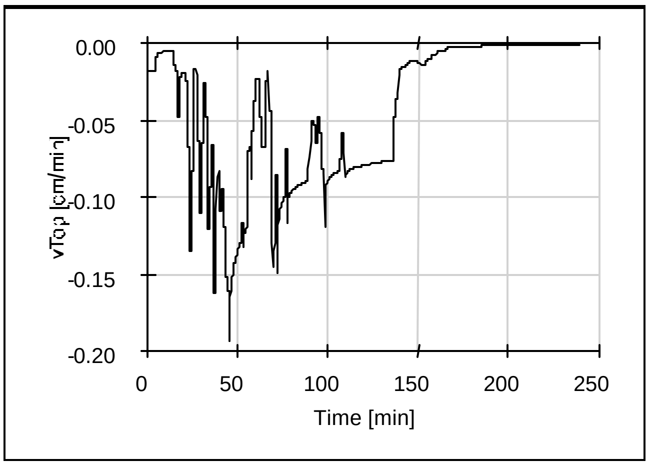

Figure 56. Infiltration rate vs time (2 meters)

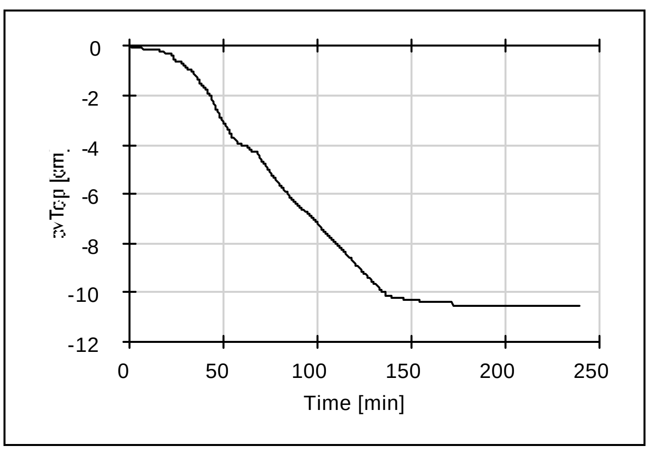

Figure 57. Cumulative infiltration depth vs time (2 meters)

Appendix E. (Continued)

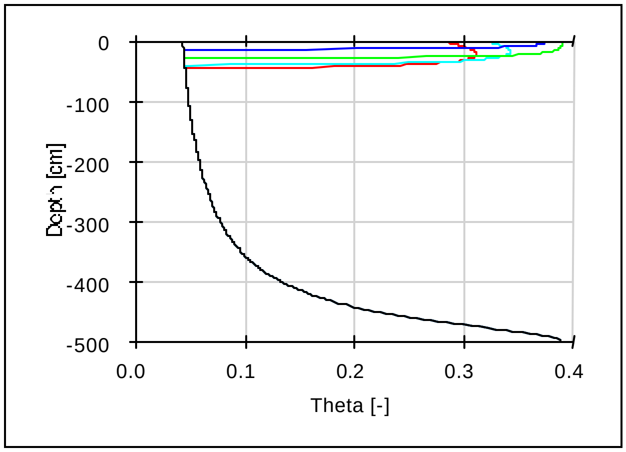

Figure 58. Water content vs depth (5 meters)

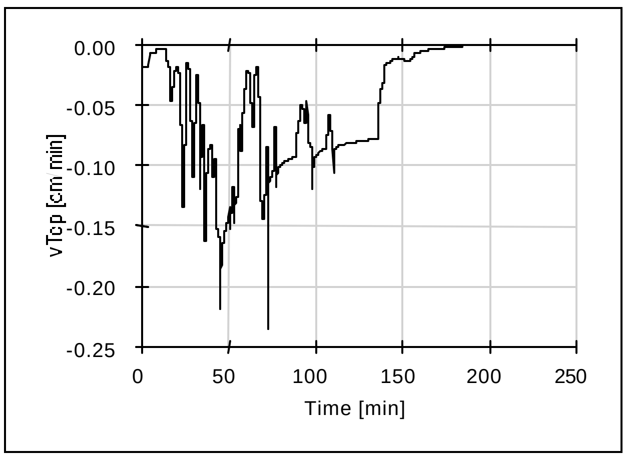

Figure 59. Infiltration rate vs time (5 meters)

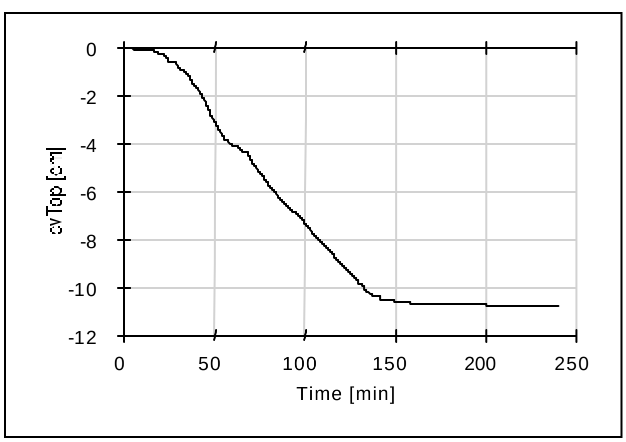

Figure 60. Cumulative infiltration depth vs time (5 meters)

Appendix F. HYDRUS 2D Graphs for Reference Simulation

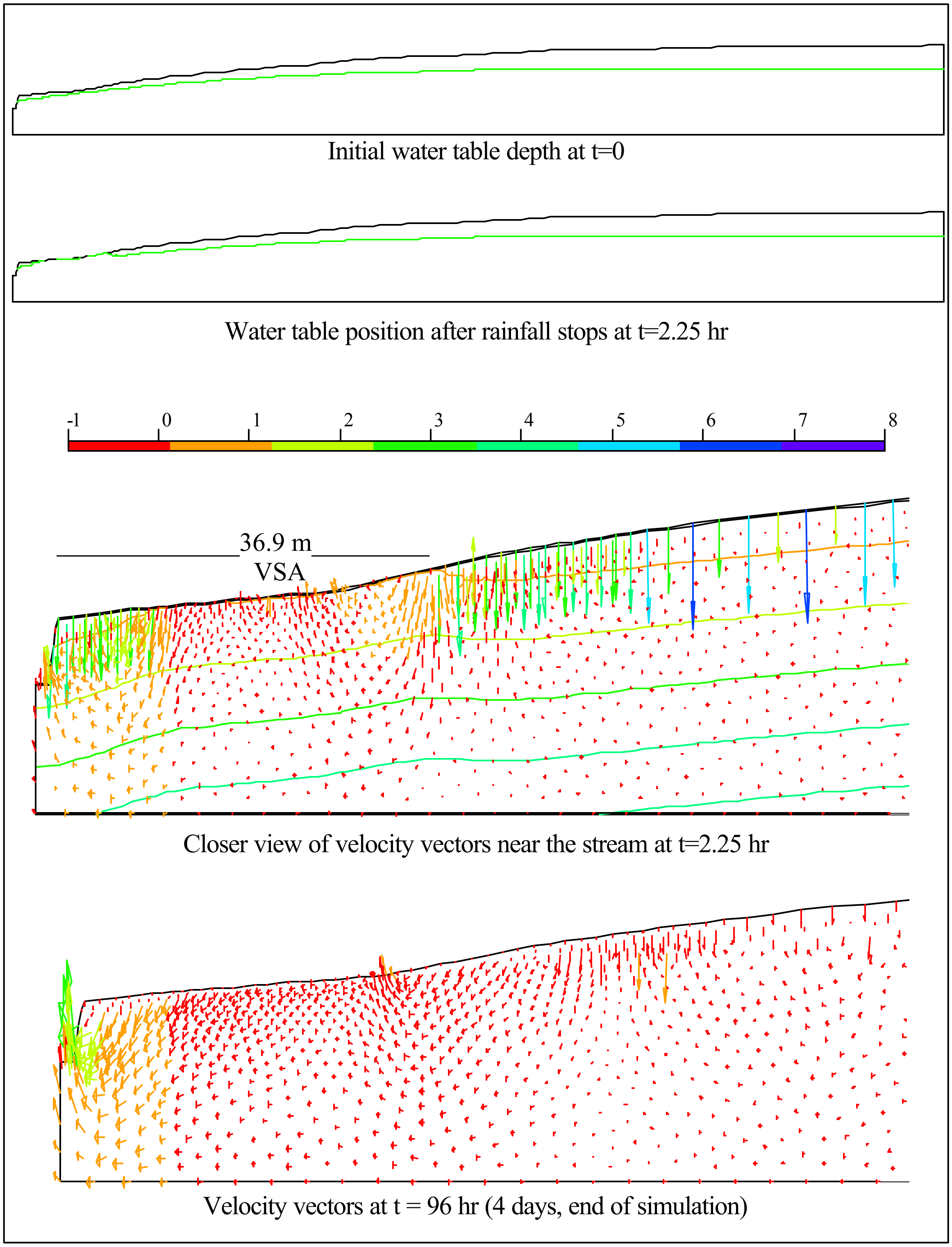

Initial water table depth at t=0

Water table position after rainfall stops at t=2.25 hr

Closer view of velocity vectors near the stream at t=2.25 hr

Velocity vectors at t = 96 hr (4 days, end of simulation)

Figure 61. Profiles of reference simulations from HYDRUS 2D

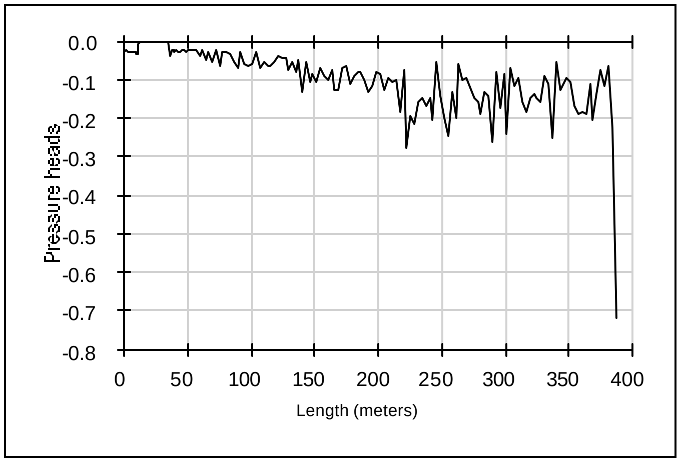

Figure 62. Pressure heads at the surface boundary

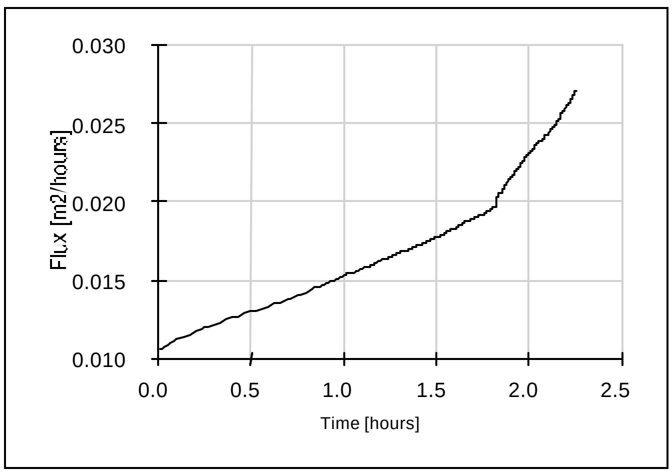

Figure 63. Subsurface storm flux during rainfall

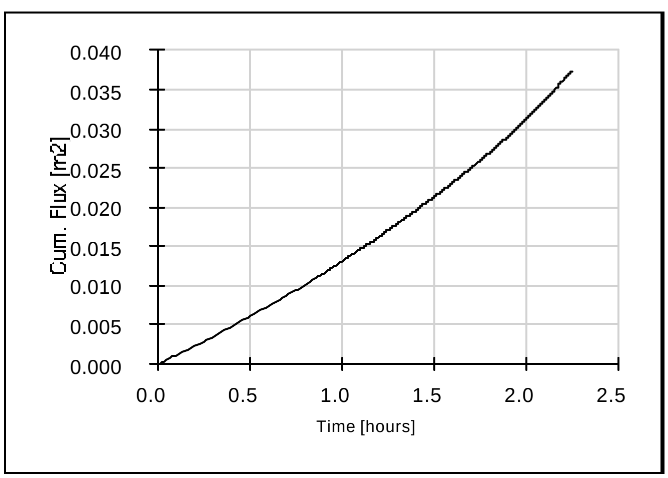

Figure 64. Cumulative subsurface storm flow during rainfall

Appendix F. (Continued)

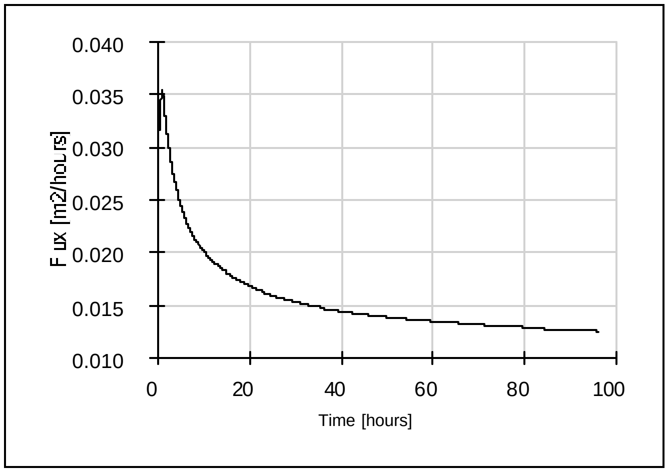

Figure 65. Subsurface flux after rainfall

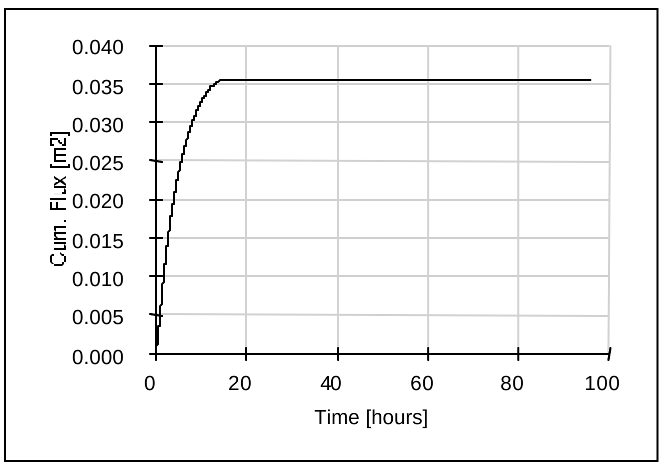

Figure 66. Cumulative seepage flux after rainfall

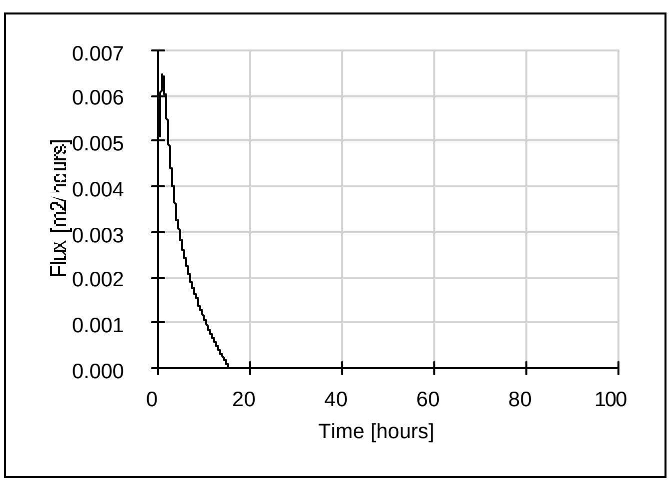

Figure 67. Seepage flux after rainfall

Appendix G. Water Retention Curves for Actual Soil Data and Fitter Parameters

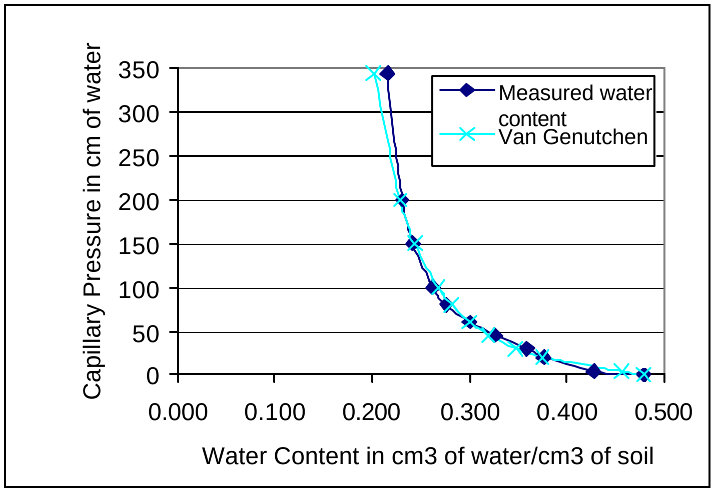

Figure 68. Fitter van Genuchten parameters for Myakka fine sand

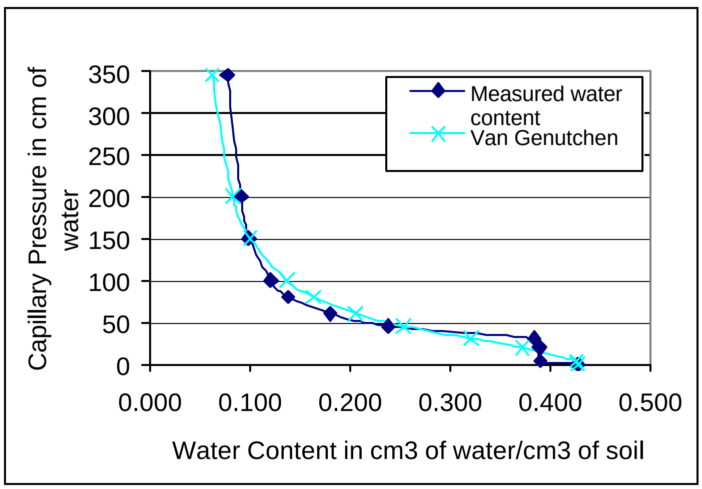

Figure 69. Fitter van Genuchten parameters for Mulat fine sand

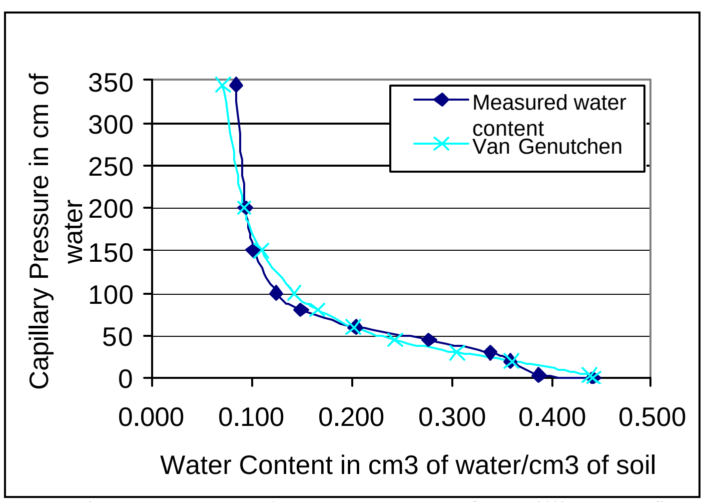

Figure 70. Fitter van Genuchten parameters for Millhopper fine sand

Appendix H. Hyetographs for Convective and Frontal Storms

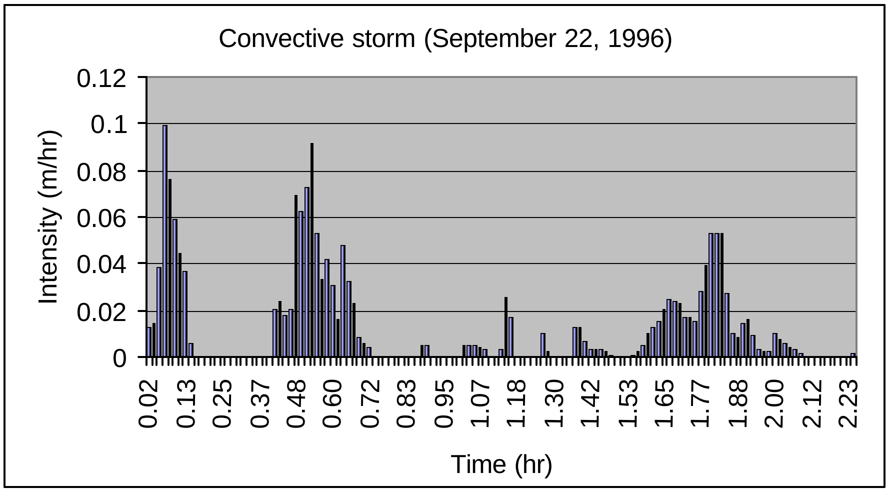

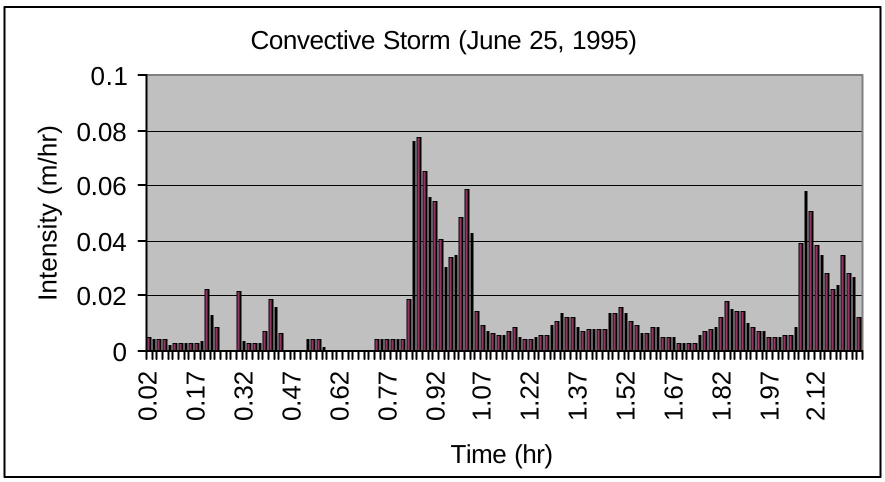

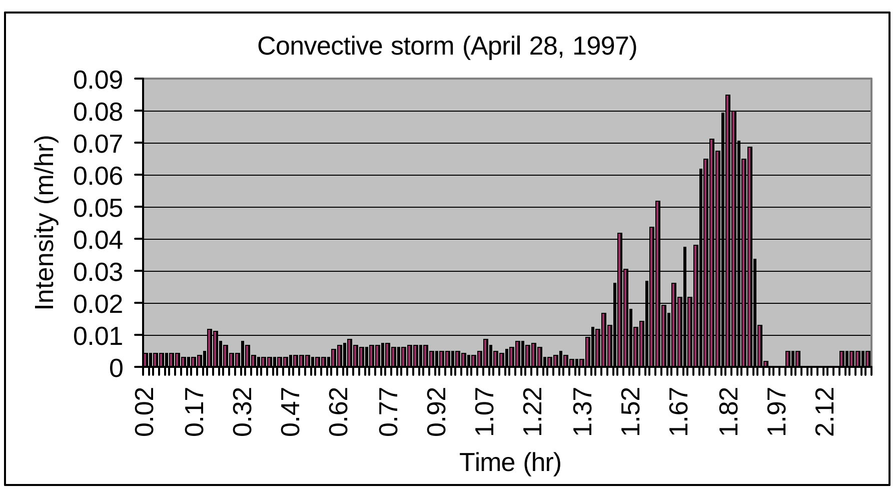

Figure 71. Convective storms used for sensitivity analysis

Appendix H. (Continued)

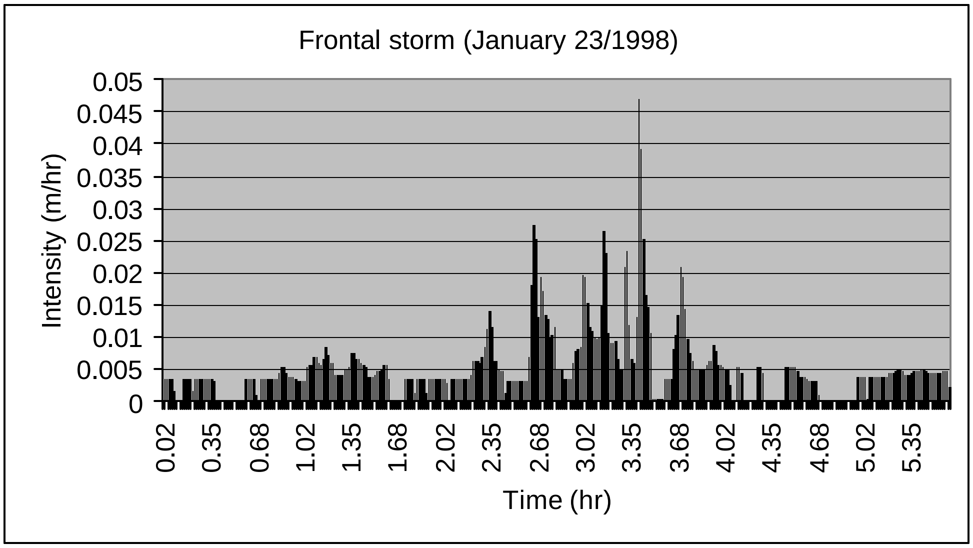

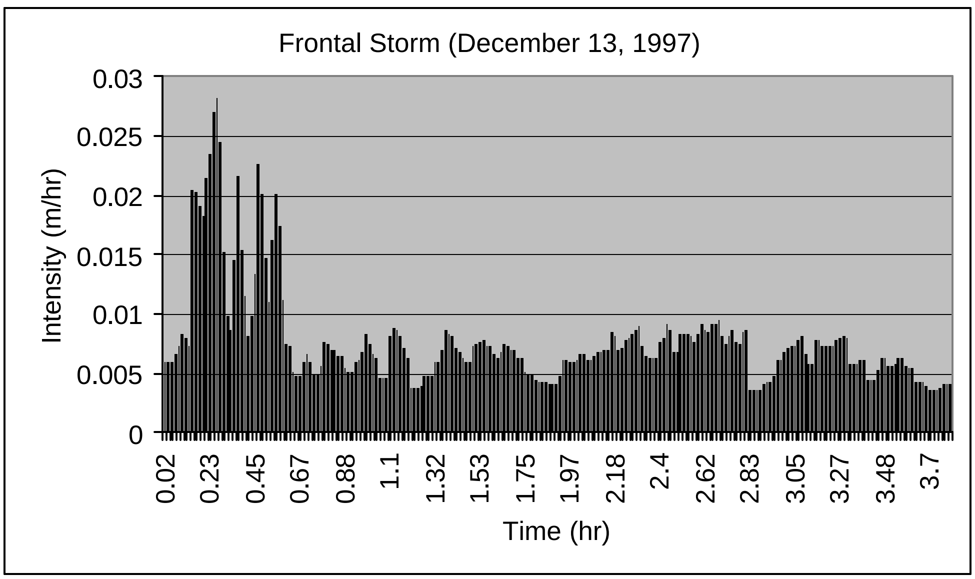

Figure 72. Frontal storms used for sensitivity analysis

Appendix I. Initial Water Table Level

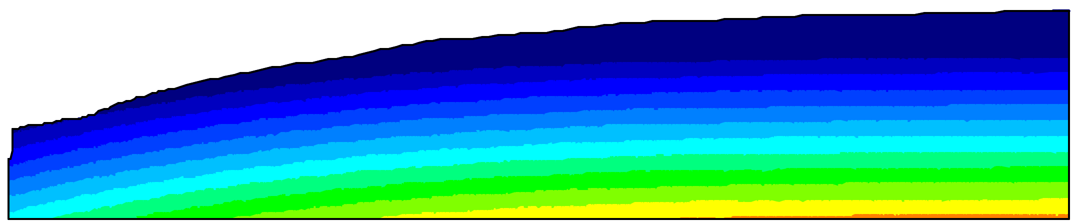

Curved initial water table depth for reference simulation

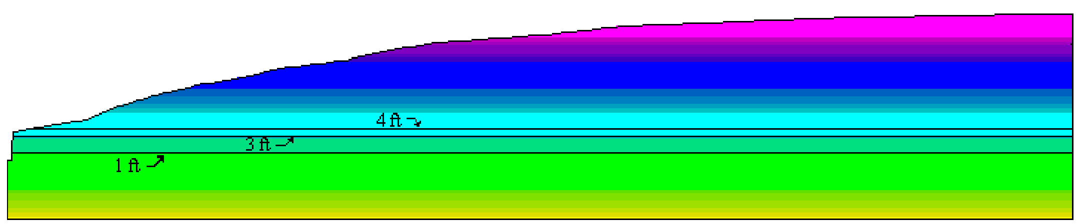

Initial water table depth at 1 ft, 3 ft, and 4 ft

Figure 73. Initial water table level for sensitivity analysis

Appendix J. Graphic Results for Soils Sensitivity Analysis

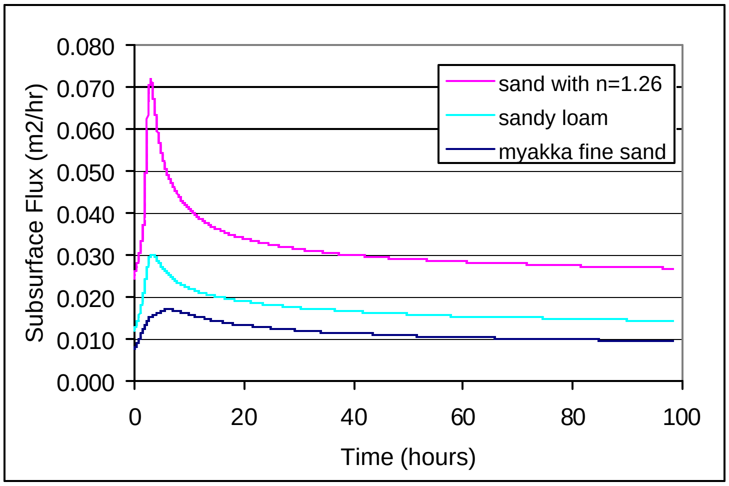

Figure 74. Subsurface fluxes for 3 soil types

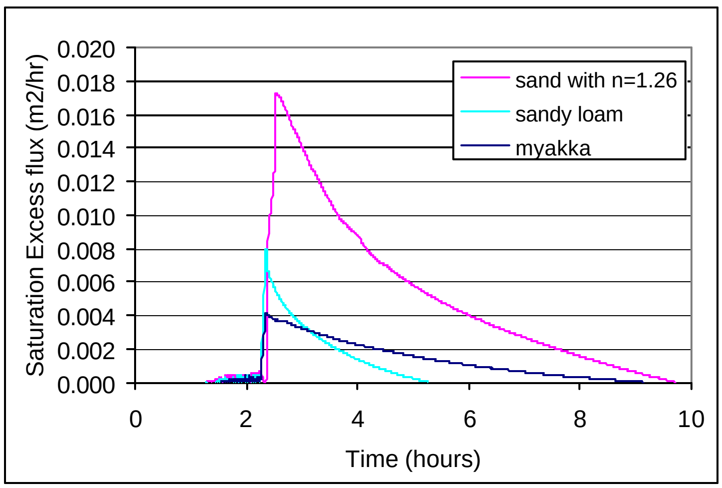

Figure 75. Saturation excess fluxes for 3 soil types

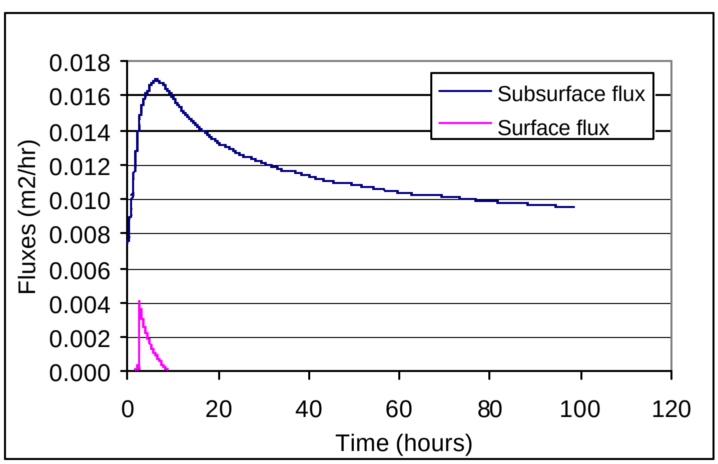

Figure 76. Comparison of fluxes for Miakka fine sand

Appendix K. Graphic Results for Rainfall Sensitivity Analysis

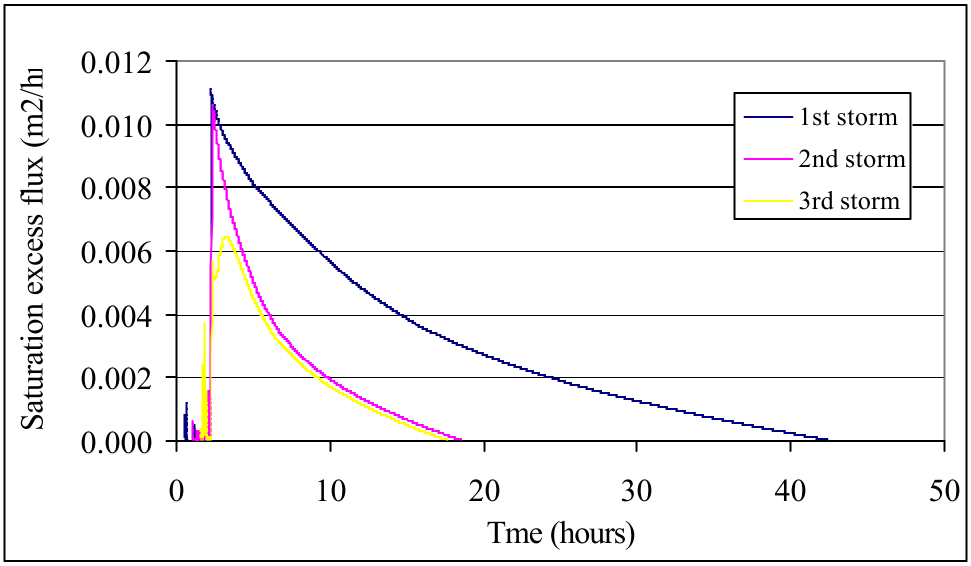

Figure 77. Saturation excess fluxes for convective storms

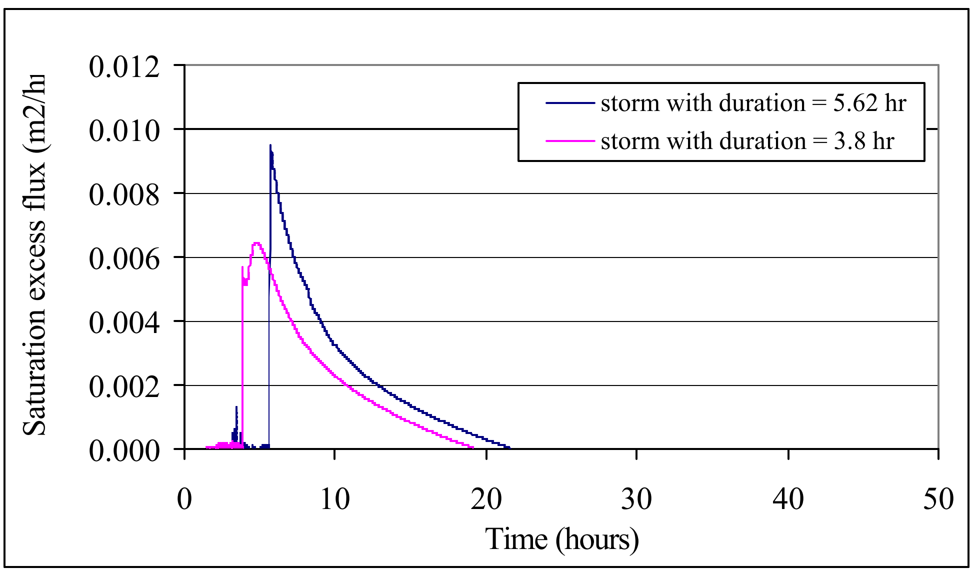

Figure 78. Saturation excess fluxes for frontal storms

Appendix K. (Continued)

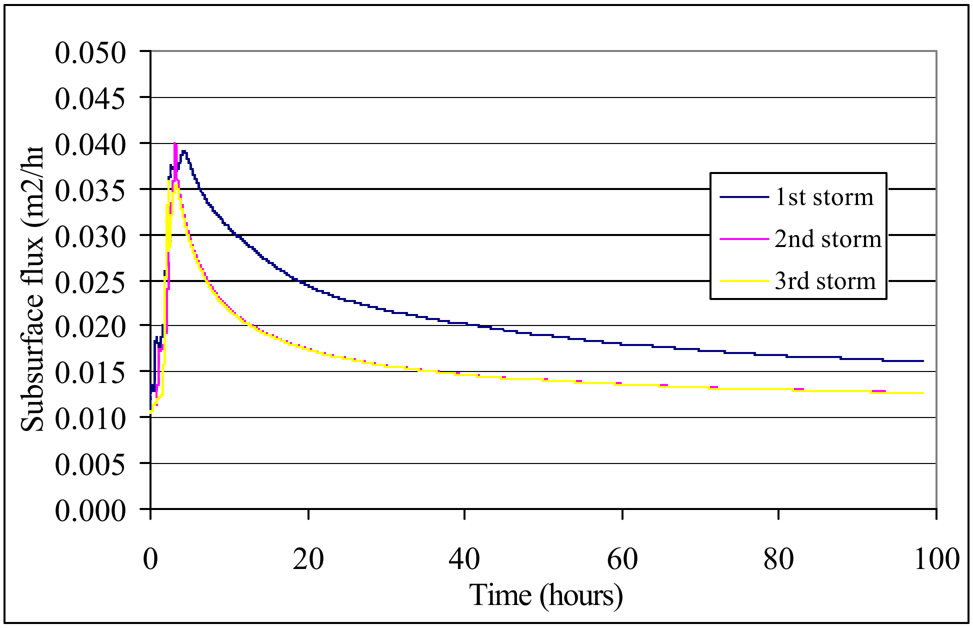

Figure 79. Subsurface fluxes for convective storms

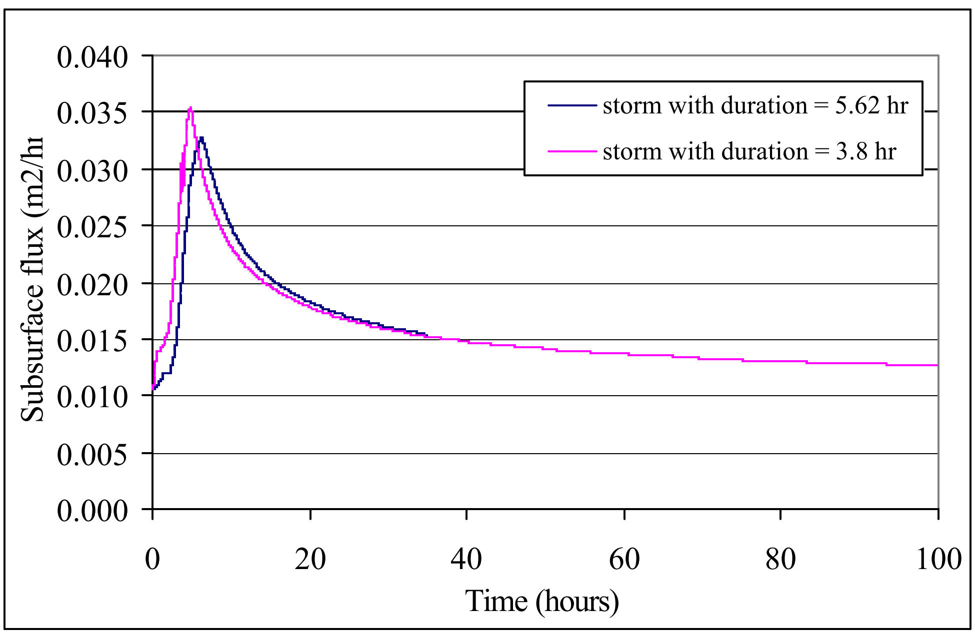

Figure 80. Subsurface fluxes for frontal storms

Appendix L. Graphic Results for Water Table Depths

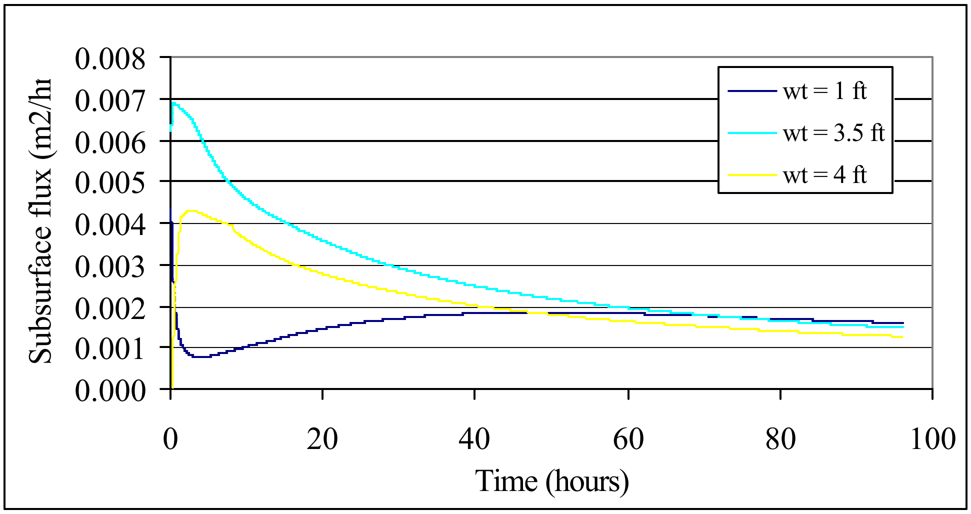

Figure 81. Subsurface flux after rainfall stops

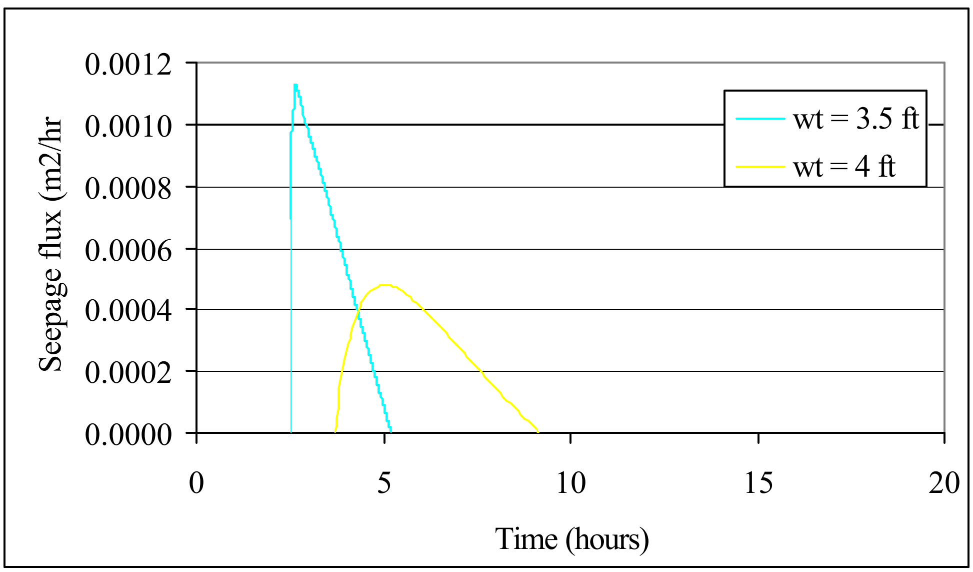

Figure 82. Seepage flux after rainfall stops

Appendix M. Graphic Results for Slope Sensitivity

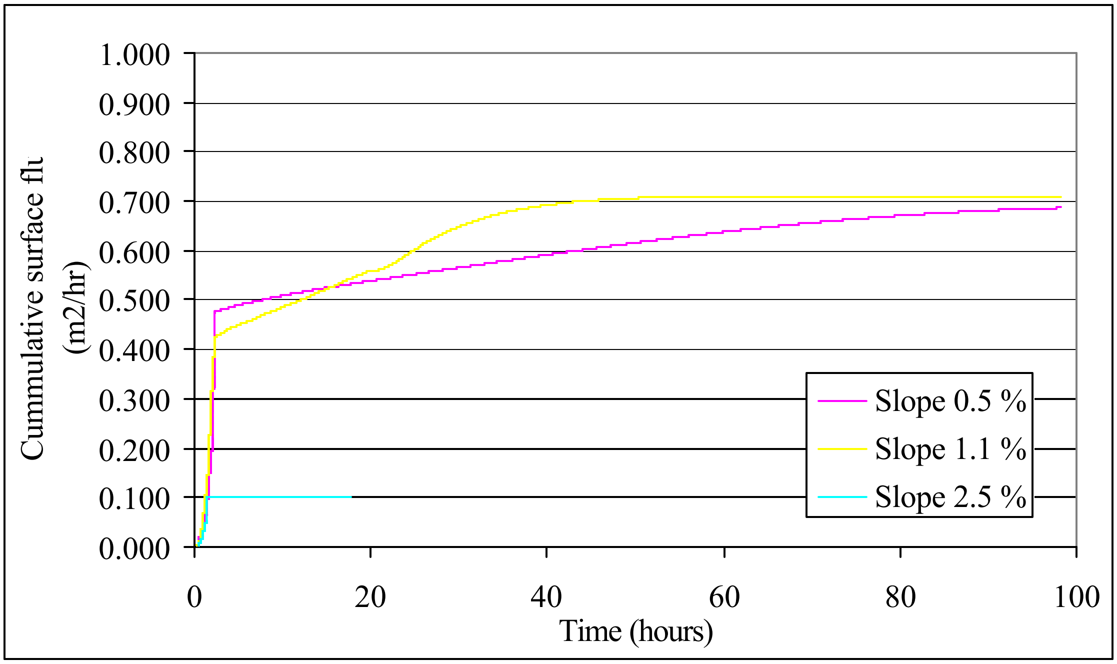

Figure 83. Cumulative surface flux for different slopes

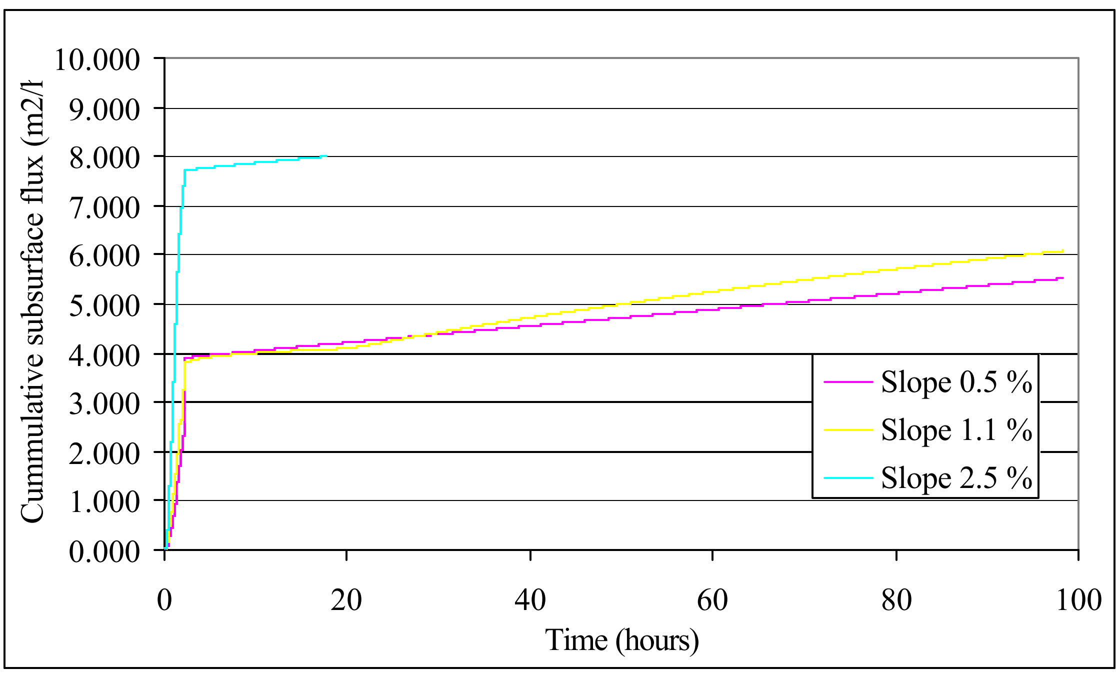

Figure 84. Cumulative subsurface flux

Appendix N. VSA Extent for Concave Curvature

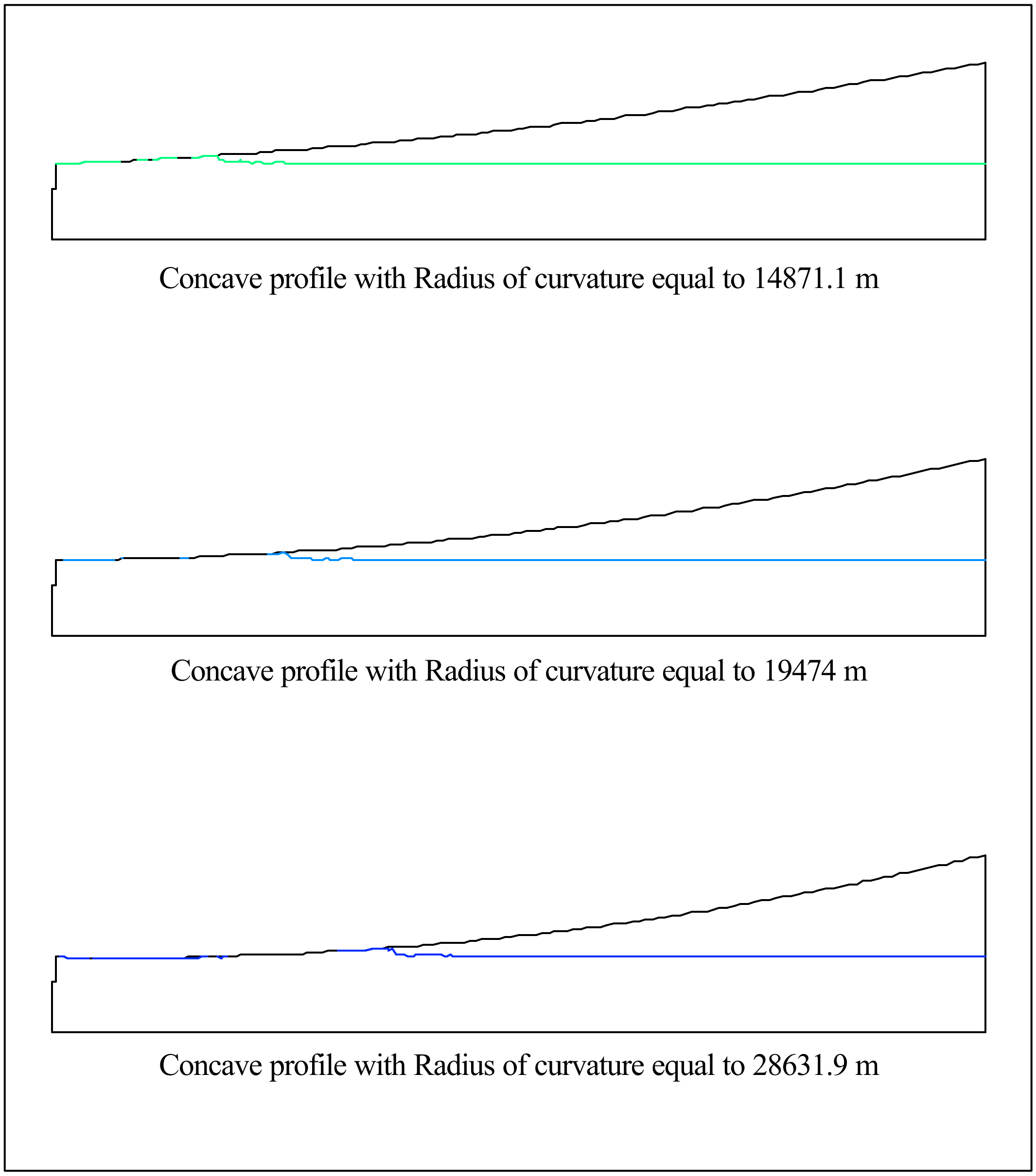

Concave profile with Radius of curvature equal to 14871.1 m

Concave profile with Radius of curvature equal to 19474 m

Concave profile with Radius of curvature equal to 28631.9 m

Figure 85. Extent of VSA after rainfall for concave profiles